THESIS FOR THE DEGREE OF DOCTOR OF PHILOSOPHY

Development of GPCR-based yeast biosensors towards biomedical applications

ANDREA CLAUSEN LIND

Department of Life Sciences

CHALMERS UNIVERSITY OF TECHNOLOGY

Gothenburg, Sweden 2025

Development of GPCR-based yeast biosensors towards biomedical applications

ANDREA CLAUSEN LIND

ISBN 978-91-8103-217-8

Acknowledgements, dedications, and similar personal statements in this thesis, reflect the author's own views.

Doktorsavhandlingar vid Chalmers tekniska högskola
Ny serie nr 5675
ISSN 0346-718X

Department of Life Sciences
Chalmers University of Technology
SE-412 96 Gothenburg
Sweden
Telephone + 46 (0)31-772 1000

Cover:
"Yeast, GPCRs, and GPCR structures towards ligand binding and YBB development."

Printed by Chalmers Digitaltryck
Gothenburg, Sweden 2025

Developing GPCR-based yeast biosensors towards biomedical applications

Andrea Clausen Lind
Department of Life Sciences, Chalmers University of Technology

Abstract

Biosensors, i.e. systems utilizing biological components such as antibodies or enzymes for sensing, have broad applicability in research, industry, and healthcare. Over the past three decades, the yeast *Saccharomyces cerevisiae* has emerged as a biosensor platform, often utilizing the cells´ internal signaling pathways for signal transduction and the transcriptional machinery for production of measurable outputs. G-protein coupled receptor (GPCR)-based yeast biosensors are prominent examples of this, leveraging the yeast mating pathway for signal transduction upon binding of a ligand to the GPCR at the yeast cell surface. These yeast-based biosensors (YBBs) have facilitated the deorphanization of human GPCRs, identification of GPCR-specific designer drugs, and the development of point-of-care (POC) YBBs applicable outside laboratory settings. In this thesis, I present our efforts to further advance GPCR-based YBBs towards biomedical applications and expand the available toolkit for their development.

In the first project, YBB outputs were evaluated as these affect the ease-of-use, time-of-detection, and sensitivity of a sensor. Specifically, two colorimetric outputs - prodeoxyviolacein and deoxyviolacein - were benchmarked against the previously established lycopene across different conditions, thereby broadening the range of available colorimetric outputs.

In the second and third project, we focused on the investigation of key residues in fungal GPCRs. These receptors have shown potential both as therapeutic targets for treatment of fungal infection and as YBB sensing elements for detection of fungal infection. To this end, an untargeted mutant library of the Ste2 mating receptor from the pathogenic fungus *Candidozyma auris* was screened, identifying amino acid substitutions that improved the sensor sensitivity and response curve metrics. Additionally, a designed mutant library for *S. cerevisiae* Ste2, targeting the orthosteric site, was screened and sequenced. Substitutions generating loss-of-function, constitutive activity, or no change in receptor activation were identified.

Finally, a YBB was constructed and optimized for evaluation of ligands of the human free fatty acid 2 receptor (FFA2R), a GPCR implicated in metabolic and inflammatory disease.

Collectively, the results presented in this thesis advance our understanding of fungal mating GPCR structure-function relationships and expand the repertoire of YBB outputs, contributing towards new possibilities in diagnostic, therapeutic, and screening applications for YBBs.

Keywords: yeast-based biosensor, yeast mating pathway, fungal mating GPCR, mutant library screening, colorimetric output, GPR43

Preface

This thesis serves as a partial fulfillment of the requirements for obtaining the degree of Doctor of Philosophy at the Department of Life Sciences at Chalmers University of Technology. The work was supported by the Joint Programming Initiative on Antimicrobial Resistance (JPIAMR) / The Swedish Research Council (project number 2019-00304) awarded to Prof. Verena Siewers. Most of the work was carried out at the Division of Systems and Synthetic Biology, in close collaboration with the Norwegian research institute SINTEF. The PhD studies were carried out between May 2020 and June 2025 under the supervision of Prof. Verena Siewers and co-supervision of Assoc. Prof. Florian David, with Prof. Ivan Mijakovic as examiner.

Andrea Clausen Lind
June 2025

List of Publications

This thesis is based on the work contained in the following papers, referred to by roman numerals in the text:

I. **Lind, A. C.**, David, F., Siewers, V. (2024) Evaluation and comparison of colorimetric outputs for yeast-based biosensors in laboratory and point-of-care settings. *FEMS Microbiology Letters,* Volume 371, 2024, fnae034. https://doi.org/10.1093/femsle/fnae034

II. **Lind, A. C.**, Dahlman, O., Nguyen, G., David, F., Siewers, V. Evolving the ligand sensitivity of *Candidozyma auris* mating G-protein coupled receptor Ste2 towards biosensor applications.
(Manuscript)

III. **Lind, A. C.**, Nguyen, G., Balzer, S., Aune, I. H., Bartolomeo, F., Dahlman, O., David, F., Siewers, V. Investigation of orthosteric site plasticity in the yeast mating factor receptor Ste2 – screening of a designed mutant library.
(Manuscript)

IV. **Lind, A. C.**, Gomes, D. C., Alcaraz, R. B., Mårtensson, J., Sundqvist, M., Forsman, H., Dahlgren, C., David, F., Siewers, V. (2025) Development of a yeast-based sensor platform for evaluation of ligands recognized by the human Free Fatty Acid 2 Receptor. *FEMS Yeast Research*, Volume 25, 2025, foaf001. https://doi.org/10.1093/femsyr/foaf001

Contribution summary

I. I conceptualized the study with FD and VS, carried out the experimental work, analyzed the data, interpreted the results, and wrote the manuscript. I edited the manuscript together with the other authors.

II. I conceptualized the study with FD and VS, carried out experiments, analyzed the data, interpreted the results, and wrote the manuscript. I edited the manuscript together with the other authors.

III. The library was designed together with GN, SB, FB, FD, and VS. I carried out experimental work related to the library variant screening, analyzed the data, interpreted the results together with VS and FD, and wrote the manuscript. I edited the manuscript together with the other authors.

IV. I conceptualized the study with FD, VS, JM, and HF, carried out the experimental work, analyzed the data, interpreted the results together with the other authors, and wrote the manuscript. I edited the manuscript together with the other authors.

Table of contents

Abbreviations

2AP	2-acetyl-1-pyrroline
AI	artificial intelligence
CFU	colony forming units
CRISPR	clustered regularly interspaced short palindromic repeats
DBD	DNA binding domain
DBTL	design-build-test-learn
DNA	deoxyribonucleic acid
ECL	extracellular loop
epPCR	error prone PCR
FFA2R	free fatty acid 2 receptor
G-protein	guanine nucleotide-binding proteins
Gα	G alpha subunit
Gβ	G beta subunit
GFP	green fluorescent protein
Gγ	G gamma subunit
GPCR	G protein-coupled receptor
ICL	intracellular loop
LOD	limit-of-detection
MFα	mating factor alpha/alpha mating peptide
mRNA	messenger RNA
PCR	polymerase chain reaction
POC	point-of-care
PRD	pheromone responsive domain
RFP	red fluorescent protein
RNA	ribonucleic acid
s.d.	standard deviation
SCFA	short-chain fatty acid
TF	transcription factor
TM	transmembrane helix
TOD	time-of-detection
WT	wild-type
YBB	yeast-based biosensor

“Manuscripts don’t burn.”
- Mikhail Bulgakov, The Master and Margarita

Chapter 1: Background

As humans, we experience every moment though thousands of sensory systems within our body. Here, we may immediately think of "the five senses", including the sense of touch, taste, smell, sight, and hearing. These are all examples of senses that are perceived as an input to our brain and allow us to make conscious decisions in response. But what are we actually sensing and responding to?

The impossibility of life without sensing systems

Each of our conscious senses is orchestrated by a system of interconnected sensor systems with increasing levels of complexity. I want you to imagine that you are passing a bakery on your way home, suddenly stepping into a cloud of freshly baked bread aroma. What you consciously register is the smell of the bread, but what your brain recognizes as bread aroma is actually largely attributed to the presence of 2-acetyl-1-pyrroline (2AP), a product of the Maillard reaction occurring when amino acids and sugars are heated together and browning occurs (1). Here, different levels of signaling systems are at play in our body, enabling us to associate the presence of 2AP with bread. On a molecular level, 2AP binds to an olfactory (smell/taste) receptor on the surface of a neuronal cells, triggering the relay of a signal inside the cell. If we instead looking at a cellular level, the binding of 2AP results in activation of the neuronal cell as a whole. This activation triggers the sending of electrochemical signals between neurons in complex neuronal firing patterns, specific to 2AP, and by extension allows us to consciously register the aroma of bread. Taking this one step further, the presence of bread aroma may trigger additional neuronal firing pattens in response, perhaps resulting in a feeling of hunger and increased production of saliva in response (2). Looking over this chain of sensing events, we may ask ourselves: which part qualifies as the sensor mechanism?

A sensor is defined as a device which detects or measures a physical or chemical property and records, indicates, or otherwise responds to it. As such, with a liberal view on how a device is defined, the receptor can be said to be the sensor on a molecular level, and the neuronal cell the sensor on a cellular level. On an even larger scale, the body becomes one giant sensor – with multiple distinct inputs and responses, such as eating in response to the feeling of hunger induced by the aroma of baked bread.

In the end, we are only conscious of a small portion of the sensing systems that are constantly active within our bodies, coordinating the function of these. In fact, not only humans or animals, but all lifeforms are highly dependent on sensing systems to function. While reflecting on this, it occurred to me that sensing systems can be seen as integral to life itself, and that each of the seven pillars of life are in some way or other intertwined with sensory systems. The pillars, outlined by Koshland in 2002 (**Figure 1**), describe a theoretical set of characteristics separating a living organism, such as a bacterial cell or an insect, from a non-living entity, such as a virus or prion (3). Here, I made an attempt to demonstrate how these are interlinked with the presence of sensory systems in living organisms.

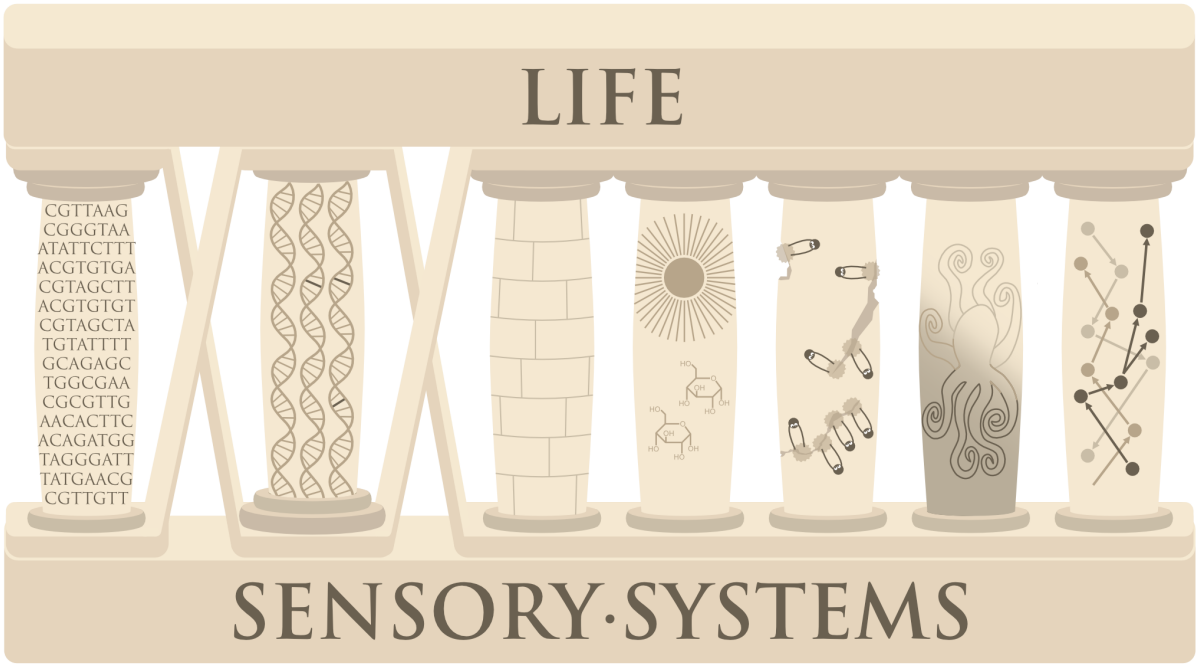

Figure 1. Illustration of the seven pillars of life. In order from left to right, the pillars illustrate Program, Improvisation, Compartmentalization, Energy, Regeneration, Adaptability, and Seclusion as defined by Koshland in 2002 (3). The second pillar is upside down, due to Improvisation – evolution – enabling the development of novel sensing systems via life and not the other way around.

PROGRAM: Throughout the lifespan of a living organism, it has to navigate the how and when of growth, reproduction, and adaptation to environmental changes. Every living being carries within it a program, detailing the life of that organism down to the molecular level, encoded within its DNA (3). The genes therein describe the "how" of how to execute diverse actions within the cell, but what determines the "when"? In many ways, the regulation of gene expression in cells is akin to an enormous orchestra, where the instruments are the genes, the musicians - playing the genes to determine if these are active or silent - are transcription factors, and the conductor is made up of the entirety of the internal and external cues available to the cell (4). These cues are found in chemical gradients, in the presence and absence of specific molecules, and in mechanical variations in the surrounding environment, allowing cells to navigate the myriads of possible gene expression constellations though time and space (5). Take embryogenesis, the development of the embryo, as an example of the precise and intricate tuning of these regulatory systems. Embryogenesis begins with a single fertilized egg cell, a zygote, having the potential of becoming any cell in the body, and progresses in development of a multicellular embryo with multiple organ types and layers of organization (6). This process occurs through a sequence of carefully planned steps of cellular division and differentiation, in which each cell develops a distinct identity depending on its uniquely defined position within the embryo (7). This is only possible through the ability of the cell to detect the many mechanical and chemical cues present, and to implement changes in the activation patten of genes in response. As such, the "when" of the program encoded in the DNA of an organism is

determined by the external and internal cues available to the organism, and by extension their ability to sense and respond to these.

IMPROVISATION: The ability of a species to improvise new solutions for survival through changes in its program, in other words evolution, is determinantal to its ability to adapt to changes in the environment long term. This is at its core a stochastic process, in which the sporadic occurrence of mutations in DNA sometimes results in gain of function or improved adaptation to a given environment. Providing an advantage in survival for the organism, it is likely that the mutation will be passed down in subsequent generations, possibly ending up in a larger part of the population simply by the increased likelihood of survival in the present environment (8). In contrast with the other pillars, improvisation cannot be said to be immediately dependent on sensing systems. Instead, the development of highly specialized sensor systems in living organisms can be said to depend on the improvisation resulting in the evolution of these. An example of species evolution towards an improved adaptation in an changing environment can be found in mosquitoes, where the *Aedes* and *Anopheles* species have evolved a preference for humans as a source of blood in recent millennia through the evolution of highly tuned human odor perception (9). While this indeed provides an advantage in regions with growing human communities, this is also an excellent example of how improvisation is environment specific – as these mosquitoes have lost the nuanced perception of odor allowing them to recognize a wide array of vertebrate food sources (9). Here, both the initially broad and the presently specialized odor perception of the *Aedes* and *Anopheles* species developed through improvisation, fueled by the current availability of food sources.

COMPARTMENTALIZATION: All living organisms are confined to a limited volume, with an intracellular compartment separated from their surroundings (3). This separation enables the maintenance of a stable internal state throughout changing external environments, creating an internal microenvironment optimized for the persistence of the processes within (10). This separation is a classic example of a distinct compartment within eukaryotic cells is found in the lysosome, an organelle specialized in the degradation and recycling of cell components, recycling these into new building blocks (11,12). Separated from the rest of the cell by a lipid bilayer, a defining characteristic of the lysosome is the acidic internal state (pH 4.5-5), as compared to the otherwise neutral pH within the majority of the human cell (pH ~7)(11,12). This acidic environment is ideal for the function of hydrolases, enabling the degradation of biological macromolecules including proteins, lipids, carbohydrates and nucleic acids, but would have been determinantal to other cellular processes. Here, sensory systems play a major part in the communication past the barriers of individual compartments, and in maintaining the specific environments therein (13). As such, the signaling past compartment walls are key to maintaining the cell as a whole, allowing for orchestration of the many parallel processes therein.

ENERGY: Life requires energy to maintain itself, whether it be through movement of chemicals and proteins to maintain the internal state, or to fuel to the metabolism of the cell.

As such, living organisms must be able to extract, store, and utilize energy from external sources, making them dependent on the availability of these. In this case, sensing systems are vital for the cell to be able to sense and adapt the energy metabolism to the specific external energy sources available. As a yeast researcher, I have to use the example of respiro-fermentative growth in yeast, active in the presence of excess external glucose (the primary carbon source) and oxygen (14). Here, the simultaneous activation of respiratory and fermentative energy metabolism pathways results in the production and accumulation of external ethanol as a byproduct of growth. When the glucose is depleted however, the yeast switches to using ethanol as an energy source instead. To navigate between the pathways active in the utilization of the different carbon sources, complex sensing systems are applied, allowing the yeast to optimize the efficiency of its energy metabolism (14).

REGENERATION: The ability of a living organism to continuously repair and renew its components enables its lifespan to be longer than the lifespan of the individual components themselves (3). The process of regeneration is constantly ongoing within living organisms, as damage naturally accumulates over time. Components such as the DNA, proteins, and cell membrane are constantly monitored through an array of sensing mechanisms, allowing the cell to respond to the presence of any faulty components in order to prevent and repair damage. These processes are vital for the continuous function of the cell and the body as a whole. An example of this is found in the tumor suppressor protein p53, the most frequently mutated protein in human cancers (15). Responding to presence of mutated or damaged DNA in healthy human cells, p53 activates signaling pathways towards cell death – apoptosis, resulting in the suppression of any possible tumor activity having been introduced by the present mutations and allows for a new and healthy cell to replace the damaged one. Similar systems exist for maintenance within cells themselves, such as intracellular detection of misfolded proteins and the transport of these to the lysosome for recycling into new protein building blocks (16). The reliance of these regenerative cell functions on the initial detection of underlying issues again underscores the key role of sensor systems for the continued prevalence of life.

ADAPTABILITY: In contrast with improvisation, adaptability refers to the ability of a living organism to rapidly adapt to changes in its environment, instead of the continued evolution over several generations. We might notice this in our own body, such as in the gain of muscle in response to repeated exertion (17), making our bodies less prone to damage as a result of overexertion, or in tanning of the skin in response to UV exposure to protect it from burn (18). While these processes are both encoded in our program, the DNA, they do not happen spontaneously and require a trigger, and input, to be activated (18). Sensing this trigger, the cells alter the expression profile of key genes in order to adapt, benefitting the longevity of the system as a whole.

SECLUSION: According to the final criterion of life, seclusion, living organisms must be able to manage parallel internal pathways while preventing undesired overlap of these. To this end, highly specific enzymes and carrier proteins have developed over time, recognizing distinct targets among thousands and thousands of molecules within the cell (19). Thinking back at the

criteria for a sensor, “detection” and “response” are key terms which also happen to form the basis of enzymatic function. Selective toward distinct target molecules, enzymes are able to detect these by binding, and in response to binding, catalyze a biochemical reaction to produce distinct products. As such, also this criterion is directly dependent on sensory systems within living organisms.

As exemplified above, one cannot separate sensing systems from life, as sensing systems themselves can be said to make up part of the foundation of its existence. For us bioengineers, the diverse biological sensory systems found in nature today make up a smorgasbord of possibilities to harness for biosensor applications. We have applied them in pregnancy tests (antibody-based) (20), diagnostic tests (antibody- or PCR-based) (21), and glucose sensors (enzymatic) (22) to name a few. With the present rise of artificial intelligence (AI), we are further able to advance past the simple copy-paste of already existing biological sensing systems (23,24). Applying these algorithms in protein design, we can tune specific protein characteristics or even develop of *de novo* proteins with a desired function, such as improved thermostability or tailored substrate specificity (25–29). As artificial intelligence (AI) models are dependent on vast amounts of preexisting data for training, however, we cannot forget that even these algorithms owe their function to the plethora of proteins already existing in nature today, and ultimately to the evolution of life.

Synthetic biology: What it is and its use in biosensor development

My research resides within the field of synthetic biology, where we utilize the current understanding of biological systems and their components to develop living biological systems composed entirely or to some part of “unnatural” components (30). These components can be unnatural in the sense that they simply do not belong in that specific system (heterologous), having been moved from one organism to another, or even in that they themselves do not exist in nature (artificial), such as proteins predicted by AI models.

While the concept of synthetic biology was coined in 1980 (31), used to describe bacteria which had been genetically engineered by recombinant DNA technologies, the first application of synthetic biology preceded this event by eight years (32). Since then, the applicability has increased due to the drastically reduced cost of DNA synthesis (33) and sequencing (34), combined with the advancement of technologies used for genetic engineering (35), structural biology (36), and protein engineering (**Figure 2**) (37). Hence, we are now able to alter the genomes of most organisms that can be grown in the lab at a reasonable cost, while having access to vast databanks of genetic information from varying organisms. As a result, synthetic biology is applied within a wide array of biotechnological disciplines today, including but not limited to, metabolic engineering (38), biosensor development (39), and fundamental research (40).

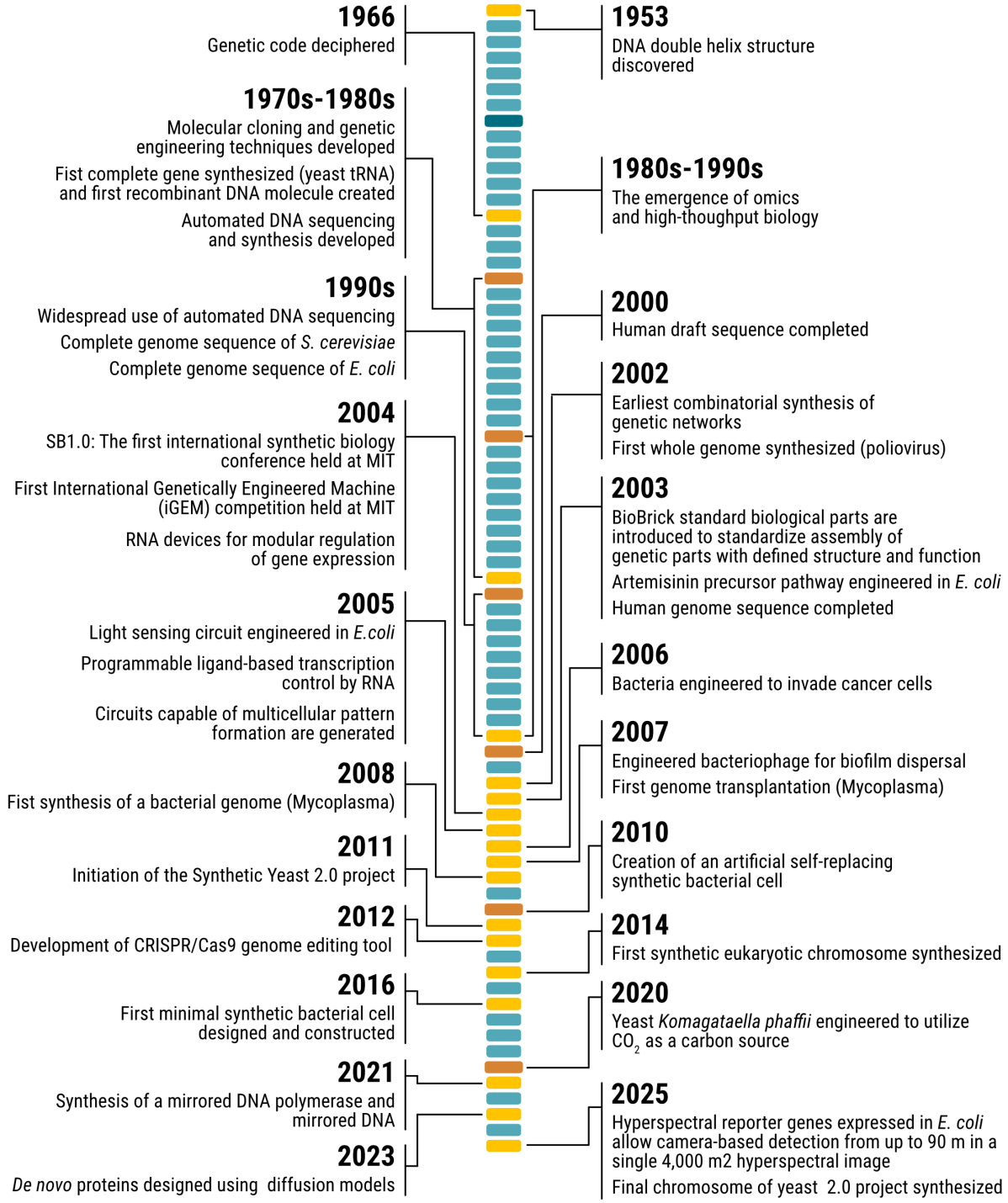

Figure 2. Timeline of key events for the emergence of synthetic biology. Adapted from the timeline presented in "Synthetic biology in Australia: An outlook to 2030" (CC BY-NC 4.0 license) from 2018 (41), adding selected events of the past seven years (32,42–69). Unless otherwise specified, yeast refers to *S. cerevisiae.*

Genes and regulation of gene expression

In order to implement an engineered biological system, we engineer the DNA. As such, we should briefly consider how biological systems are encoded and regulated in the genome to

better understand the concept of synthetic biology. The DNA present in each living cell contains both genes and diverse regulatory mechanisms that modulate when and if a gene is to be active (4). Traditionally, genes refer to coding genes, regions of the genome that contain blueprints for proteins (**Figure 3A**), while non-coding genes that encode regulatory RNA molecules are prevalent as well (70,71). When a coding gene is active, RNA polymerases in the cell "transcribe" it into a blueprint copy in the form of an mRNA molecule, which is transported to a ribosome, by which it is "translated" into a functional protein (4). This is how all proteins are constructed within cells, with the proteins themselves making up the complex machinery that enables the cell to persist, including the machinery for transcription and translation of genes.

Each organism contains thousands of protein-coding genes, varying in number depending on the complexity of the organism. As an example, the estimated number of protein-coding genes in humans amounts to ~20,000 (71) while the protein-coding genes in baker's yeast, *Saccharomyces cerevisiae*, amount to ~5,500 (72). However, the total number of proteins encoded by these genes are not needed at all times, and as such, gene expression is subject to complex regulatory systems that determine when and to what degree a gene should be expressed (73).

Design-Build-Test-Learn in synthetic biology

In synthetic biology, the different regulatory components for gene expression and the genes themselves are viewed as modular parts, parts that can be pieced together to allow for precise tuning of gene expression. The regulatory elements include both those present in the genome such as promoters and terminators, as well as regulatory proteins such as transcription factors, that regulate when the transcription machinery is recruited to a promoter (**Figure 3B**)(73). The individual parts are assembled into "devices", a collection of parts that create a desired function, which are frequently compared to electric circuits in that these can be constructed with switches and oscillators (74). The cell that hosts the device is defined as a "chassis" (74). In the development of engineered biological systems, we rely on an iterative cycle of design-test-build-learn for successful implementation of an envisioned result (DBTL; **Figure 3C**). We design a system towards a specific outcome based on our present or inferred knowledge, implement it, and evaluate it to learn whether further adjustments are needed. Take the production of the red pigment lycopene, a commercially and medically important compound, in the yeast *S. cerevisiae* as an example (39,75). Lycopene is not naturally produced in this yeast; however, it can be derived from farnesyl diphosphate, an intermediate compound in the yeast metabolism, by the expression of genes of enzymes CrtE, CrtB, and CrtI from other organisms (heterologous) which catalyze reactions towards the production of the compound (**Figure 3D**). In a work by Chen and colleagues in 2016, the yield of lycopene production was increased 22-fold through iterative engineering cycles towards increasing the amount of precursor, identification of CrtB enzyme candidates with higher efficiency, and lastly engineering of the regulatory network of the strain (75). Within the field of synthetic biology, and perhaps within science as a whole, this process extends past that of an individual project,

as we constantly learn from and build on the knowledge of those who came before us in an iterative process towards advancement of diverse research fields.

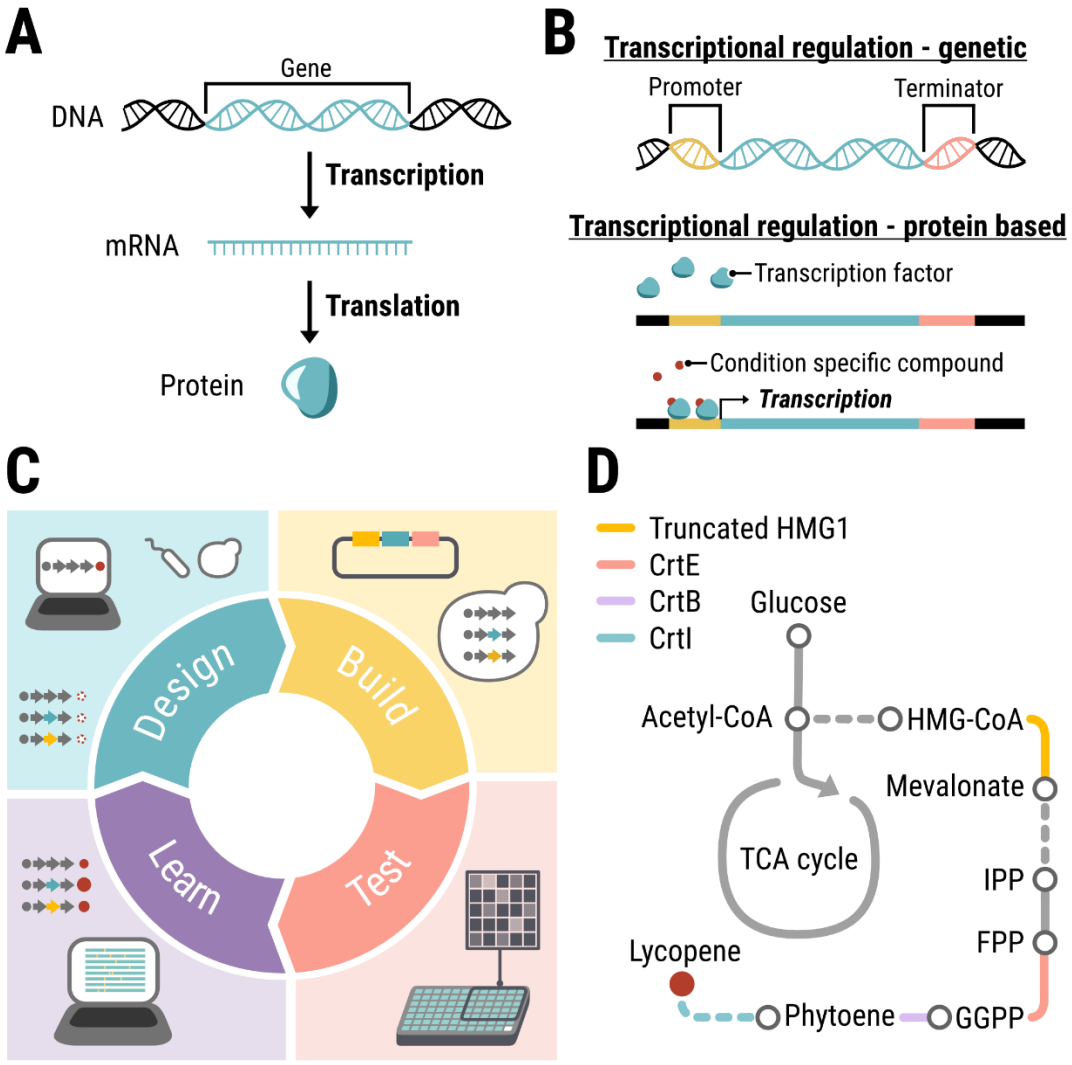

Figure 3. **A synthetic biology overview.** (A) Coding genes are transcribed to make mRNA, and the mRNA is translated to make a protein (B). Genetic- and protein-based regulation determines when and to what extent a gene is expressed. (C) The iterative Design-Build-Test-Learn cycle of synthetic biology. *Design* includes chassis selection, planning of pathway (device) constructions, and modelling. *Build* includes implementation of the devices in the chassis. *Test* includes evaluation, and *Learn* the insights gained from evaluation. (D) The lycopene production pathway derived from yeast metabolism, where grey lines signify inherent parts of the yeast metabolism and colored lines signify engineered or heterologous steps. Engineering includes both altering of endogenous enzymes, such as truncation of *HMG1*, and introduction of heterologous enzymes CrtE, CrtB, and CrtI (75).

A general introduction to biosensors

Biosensors developed via synthetic biology in yeast are the general focus of this thesis. However, before diving deeper into how these are developed, it is necessary to define and discuss what biosensors are and the important metrics considered in their design. A biosensor

is generally described as a device that detects a chemical or biological analyte via a biological sensing component, generating an output signal proportional to the analyte concentration in response (76). Classic examples include pregnancy tests, relying on antibodies for detection of human chorionic gonadotropin (hCG) present in the urine of pregnant women, and glucose sensors, relying on the glucose oxidase (GOx) enzyme for measurement of the glucose present in blood – both commercially available biosensors that are applied in point-of-use settings (76).

In the case of biosensors developed in yeast, or other microbial hosts, via synthetic biology the organism makes up a chassis for implementation of the sensing device. Upon detection of the analyte of interest, the transduction of the signal is intracellular and results in a transcriptional response with a measurable output, such as production of a colorimetric pigment within the cell. Here, synthetic biology has been applied to encode the sensor system entirely in the DNA of a living organism, allowing for diverse opportunities for diagnostic and analytical sensor applications.

Sensor metrics: In sensor development

Knowing what a biosensor is, we can think about the metrics that are important in biosensor design. These depend largely on the target application of a biosensor, for instance if the aim is application as a diagnostic tool in hospital settings, as a tool for point-of-care (POC) detection, or for patients to use at home. The metrics can be divided into two groups, namely those related to sensor design and those related to sensor performance. Initially looking into metrics affected by sensor design, these include:

- **Ease-of-use**, i.e. whether a sensor can be applied by anyone in any place or if the application requires trained personnel and special equipment (77). As such, the ease-of-use affects the possibility of distribution outside a hospital setting.
- **Cost** and **scalability**, i.e. the cost of production and distribution of a sensor, as well as the scalability of production and application (78,79). These are important to consider for the possibility of going beyond the simple development of a proof-of-concept sensor design, greatly affecting the possible application areas.
- **Shelf-life** and **storage requirements**, i.e. how long and in which conditions a sensor can be stored, which also has major effects on the applicability (80). For example, if storage at fridge temperatures is required it negatively affects the applicability in remote locations, and if the shelf life is short, it limits the possibility of production scale up.

While some of these are easily quantifiable, such as cost, others are more diffuse, such as the ease-of-use of a sensor. Instead looking into the metrics of sensor performance, most are determined via the sensor response curve, i.e. the output intensity (E) in relation to the concentration of the target analyte as determined by the variable slope sigmoidal equation (**Figure 4**) (81).

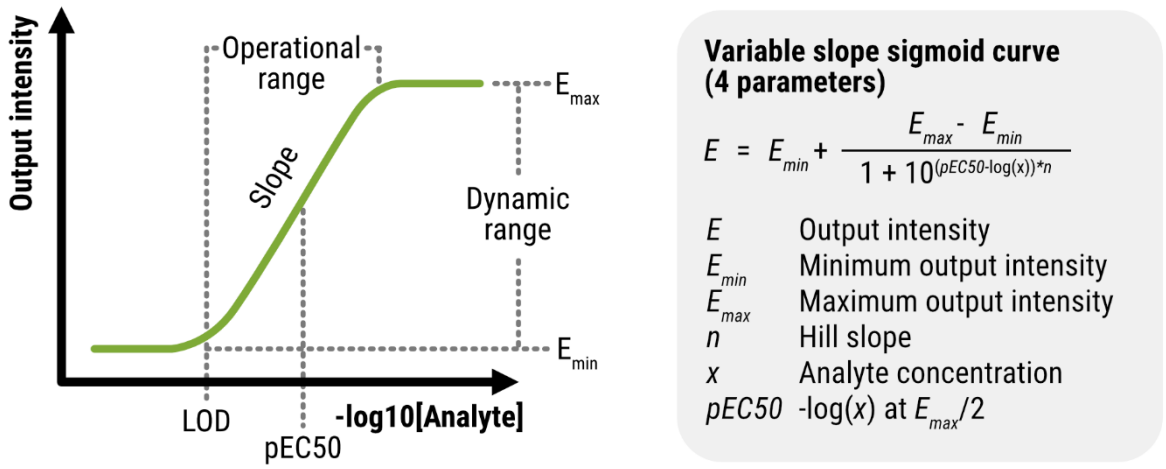

Figure 4. The response curve for a given sensor, determined by fitting a variable slope sigmoid curve to measurement data (81). Based on this curve, the response parameters (described in the text) can be determined. Slope, Hill slope; LOD, limit-of-detection.

- **Limit-of-detection (LOD)**, i.e. the lowest concentration at which the analyte can be reliably detected (82), with the required LOD being defined by the availability of the target analyte in a sample.
- **E_{min}**, i.e. the baseline output in the absence of analyte, determined at the minimal curve asymptote (81).
- **E_{max}**, i.e. the maximum output upon induction at high analyte concentrations, determined at the upper curve asymptote (81).
- **pEC50**, i.e. the negative logarithm of the analyte concentration at 50 % of E_{max}, indicating the potency of sensor activation for a specific ligand.
- **Operational range**, i.e. the concentration range within which the sensor output intensity is linearly proportional to the analyte concentration. Here, a wide operational range allows for quantitative measurements, while a narrow operational range produces a binary response applicable for simple determination of whether an analyte is present or not, with the range being highly dependent on the Hill slope.
- **Hill slope**, i.e. the steepness of the linear range of a response curve, largely affected by the ligand-binding properties of the receptor. In some cases, only a small amount of analyte needs to bind the receptor in order to trigger a maximum response – i.e. a digital response – while in other cases, the response is proportional to the concentration – i.e. linear (83).
- **Dynamic range**, i.e. the range from the LOD to saturation for the output (82). Often, a wide dynamic range is desired as this allows for clear determination of sensor activation.
- **Reproducibility and robustness**, i.e. the consistency of sensor readings over multiple instances, devices, users, and varying environmental conditions (82). These metrics are essential for the clinical applicability of a sensor, as they affect the possibility of result interpretation.

- **Selectivity**, i.e. the ability of a sensor to correctly distinguish the target analyte from other compounds (82). For correct diagnosis, a high selectivity is key, preventing misidentification of other compounds as the target analyte.
- **Time-of-detection**, i.e. the time needed for a diagnostic to reach a stable output after exposure to the analyte. As a general rule, a short TOD allows for rapid diagnosis and an appropriate medical response (84).

These metrics form the basis of sensor performance, but the requirements for a satisfactory performance varies widely depending on the target application. For example, if the aim is to use a sensor as a point-of-care diagnostic, we are likely to want a digital response and therefore a steep slope, while a gentle slope is desired when quantification is needed.

Sensor metrics: In clinical diagnostics

The metrics of sensor performance in turn affect the ability of said sensor to correctly classify patients in clinical diagnosis. Sensor selectivity, robustness, and reproducibility tie into the diagnostic metric of **specificity** while the sensor LOD ties into the diagnostic metric of **sensitivity,** used to determine sensors applicability in healthcare settings.

To better understand what the sensitivity and specificity of a diagnostic test refers to, we first need to understand the possible outcomes of diagnosis (85). These include four categories, namely;

- *True positive*: The patient has the disease and test is positive.
- *False positive*: The patient does not have the disease and the test is positive.
- *True negative*: The patient does not have the disease and the test is negative.
- *False negative*: The patient does have the disease and the test is negative.

Ideally, a test would have no false positives and no false negatives, but such is seldom the case. Instead, tests are often developed with a trade-off between the two. For applicability in clinical settings, the accurate detection of true positives (sensitivity; Equation 1) is often prioritized over the correct identification of true negatives (specificity; Equation 2), as it is important not to miss early detection in the case of disease.

$$\text{Sensitivity} = \frac{\text{True positives}}{\text{True positives} + \text{False negatives}} \qquad (1)$$

$$\text{Specificity} = \frac{\text{True negatives}}{\text{True negatives} + \text{False positives}} \qquad (2)$$

Here, we should also consider that while it may seem reasonable to prioritize high sensitivity over high specificity, enabling detection of as many true positives as possible, this is only the case within limits. Low diagnostic specificity results in overdiagnosis, incorrectly classifying healthy patients as sick. In some applications, such as surveillance of viral spread where a positive diagnosis does not necessarily result in further medical care, an incorrect positive

diagnosis does not have a big impact. However, in the case of diagnostic development towards detection of a life-threatening disease, or a disease in which follow-up evaluations are invasive, a lower specificity becomes an issue. This is further amplified in the case of population-wide screenings, where the sheer number of tests will result in a high number of false positives even if the diagnostic specificity is high. Say for example that a diagnostic test has 99 % specificity, meaning that out of 100 tests one will result in a false positive result. Applying this test to the entirety of Sweden's population of 10.6 million people, we would end up with 106,000 false positive misclassifications. This is why many diagnostic screenings are applied only for risk groups, such as parts of the population over a certain age and those with predisposition towards a specific disease, or when there is cause for concern. Breast cancer screening is a common example of this, where excessive screening in young women is known to result in overdiagnosis (86). In this case, a positive diagnosis (even if false) in the initial screen can result in invasive testing, unnecessary use of cancer treatments, a mental burden for the patient, and waste of resources for the healthcare system (86).

Having established these core metrics – both for biosensor design and clinical diagnostics – the next question is how to engineer a biosensor platform that can effectively meet these demands. Here, the choice of platform organism is essential, as it will affect the cost of production, the shelf-life, and robustness in diverse conditions. Further considering the development of the sensor via synthetic biology, the availability of tools for genetic engineering and how well-characterized an organism is further affects the possibilities of tuning the sensor response metrics after implementation. In this thesis, I work with the yeast *S. cerevisiae*, one of the most well-studied yeasts in terms of both genetics and physiology, in biosensor development towards improvement of several of the sensor performance metrics outlined above.

Why utilize yeast as a biosensor chassis?

The yeast I am referring to here, *S. cerevisiae*, is also known as baker's yeast or budding yeast, and is sequenced (51), and a host for bioproduction of diverse commercially relevant products (87). As a result of its frequent and long-term application in research, *S. cerevisiae* is one of the most familiar to most via food due to its essential efforts in the production of fluffy bread. Less frequently known, however, is that *S. cerevisiae* has also had a side gig in academia, being one of the oldest model organisms used to study human disease (88), the first eukaryote of which the genome was well-studied microbes for which an array of standardized tools and protocols have been developed for efficient genetic engineering of the yeast genome (89).

While this in itself makes *S. cerevisiae* an attractive host for implementation of synthetic biological systems, one should further take into account the suitability of a given microbe as a host for the specific sensor (or other) implementation intended. Here, suitability refers to whether the desired system is straightforward to implement in the host organism or whether there are better microbial platform alternatives. This depends both on the intended sensor design in relation to the inherent properties of the microbe, such as whether the analyte of

interest is produced/degraded by the host or whether the biological sensing component can be produced by it, and the tools available for implementation.

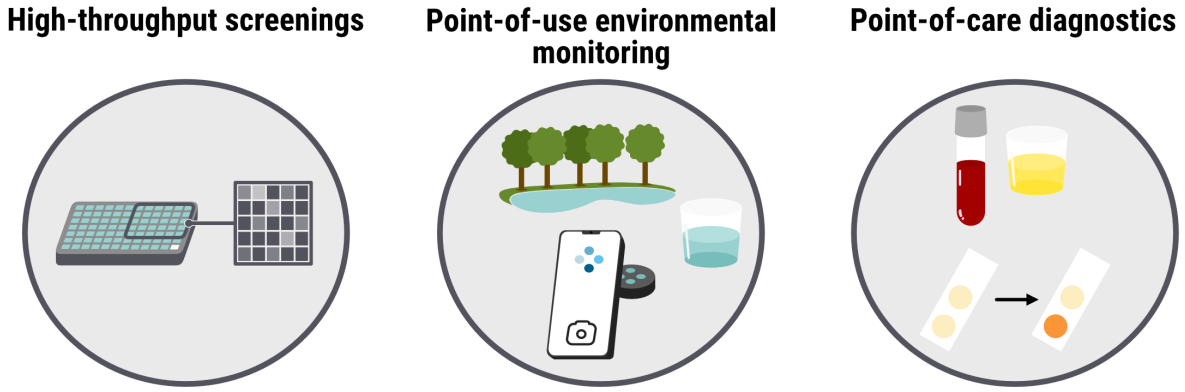

Figure 5. Examples of application areas for yeast biosensors. Yeast has been applied in high-throughput screening studies for detection of ligands and protein activity (90), developed towards point-of-use applications (91), such as for detection of pesticides in water with bioluminescence as an output (92), and towards application in point-of-use diagnostics using production of colored compounds as an output (39).

Today, yeast-based biosensors (YBBs) have been developed towards applications in industrial settings, pharmacological research, and bioengineering applications (93–95). In my case, I have worked specifically with YBBs using G protein-coupled receptors (GPCRs) as a biological sensing component, as these are relevant in biomedical applications (39,40,96). These receptor proteins are present at the surface of a cell, enabling sensing of an extracellular analyte, and are only found in organisms of the eukaryotic domain, such as fungi (including yeast) and mammals. In fact, yeast has long been applied as a model for the study of GPCR activation and signaling via the yeast mating pathway, and has been developed as a well-established GPCR-based biosensor platform in turn (19,83,97,98), making it an appropriate sensor host.

The yeast mating pathway as platform for sensor development

To better understand the yeast mating pathway and its applicability towards the study of GPCR activation, we should have a brief initial look into the mating system of yeast found in nature as opposed to the yeast strains applied in research. In nature, *S. cerevisiae* is likely to be diploid, i.e. carrying a double set of chromosomes (99). In extreme environmental conditions, such as starvation, diploid cells split into four haploid spores, each with a single set of chromosomes and with two possible mating types (**a** or **α**) (100). While both haploid and diploid cells are able to reproduce asexually via budding, where a small bud emerges from the mother cell and separates into a new cell once it has reached a certain size, haploid cells of opposite mating types are also able to mate to make a new diploid cell (101). This process is activated by the binding of a small mating peptide, mating factor **a** or **α**, produced by the opposite mating type yeast, to the corresponding mating GPCR, Ste3 or Ste2, respectively (19). To enable efficient mating, haploid cells found in nature are able to switch mating type after budding, enabling mating with nearby cells that were previously of the same mating type (99,102).

In most commonly deployed *S. cerevisiae* strains used in research however, the cells are unable to switch mating type, while retaining the majority of the mating machinery (99,103). These haploid strains have a fixed mating type **a** or **α** (103), and have been preferred for research and genetic engineering purposes due to increased ease of genetic engineering and genetic stability of strains. As a result, the mating machinery of these strains remains inactive unless the mating pheromone of the opposite mating type yeast is added to the culture, making it possible to study the GPCR-mediated activation of the mating pathway in the absence of mating (83). Today, the mating pathway of *S. cerevisiae* is characterized to the point of modularization – enabling precise tuning of pathway activation (83). Several applications have been demonstrated for GPCR-based YBBs (**Figure 5**), such as in point-of-use screening of high-value compounds (91), point-of-care detection of infectious, i.e. pathogenic, microbes (39), and deorphanization of human GPCRs for which the binding agent was previously unknown (40,90).

Signaling through the yeast mating pathway

Before diving into the details of the yeast mating pathway signaling, I want to start by quickly commenting on what a signaling pathway generally refers to in biological systems. "Signaling" in this case refers to the transfer of information from one part of the cell, where an input is detected, to another part of the cell, capable of producing a biological response in turn (**Figure 7A-C**)(104). In biological systems, this transfer of information often occurs via a sequence of protein interactions or signaling molecules detected by proteins within the cell (104). But how, then, are proteins able to communicate information, and how do they know to which other protein the signal should be relayed among the thousands of proteins present within the cell? It is fascinating really, that the answer to both these questions lies in the highly specific protein structures found in biological systems. This means that each protein is only able to interact with a highly specific set of proteins or signaling molecules in a specific order, resulting in complex but defined signaling networks that sometimes overlap between pathways. The signal itself is relayed via the triggering of structural changes in the proteins involved, such as addition of a phosphate group in specific protein sites (i.e. phosphorylation), the release of a protein from a protein complex (consisting of multiple proteins), or via binding of second messengers (small signaling molecules)(104–106). So, with this in mind we can now have a look at the yeast mating pathway as it exists in wild-type haploid yeast, focusing on the central mating pathway components often considered in biosensor design.

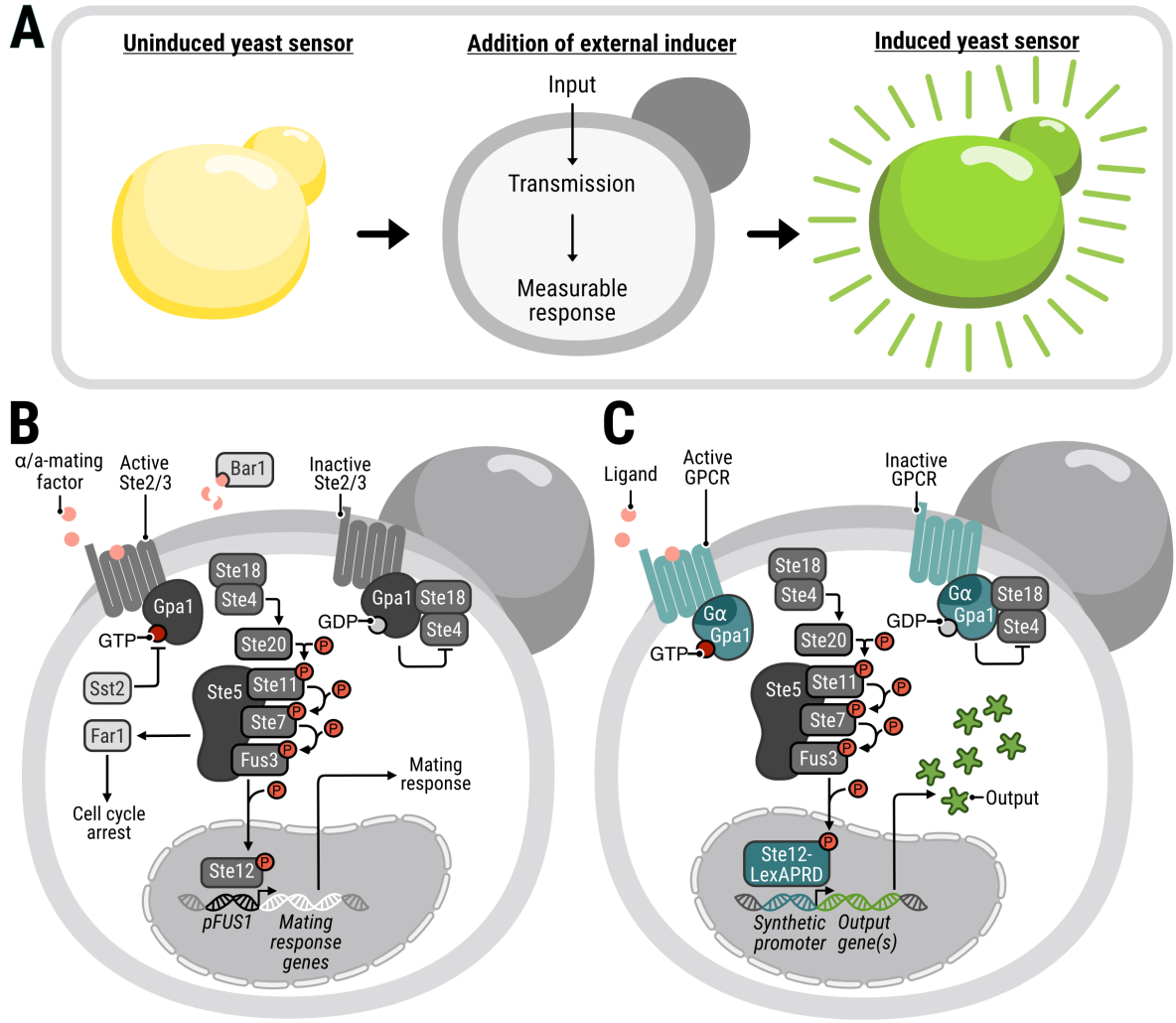

Figure 6. Yeast sensor cell design and mating pathway engineering. The figure shows a simplified overview of a yeast sensor function, and an overview of the central yeast mating pathway components prior to and after engineering towards biosensor applications. (A) In the development of yeast-based biosensors, the yeast itself serves as the device. It is able to detect a target analyte (ligand), transmission of an intracellular signal, and production of a measurable output, such as fluorescence. In the yeast mating pathway (B & C), the cell detects an extracellular analyte, which activates intracellular signaling resulting in a transcriptional response and the production of a measurable output. (B) In wild-type yeast, the α/a-mating factor binds the mating GPCR, Ste2/Ste3, stimulating the exchange of GDP for GTP in Gpa1. This results in the activation of Gpa1 and the subsequent release and activation of the Ste4-Ste18 G protein complex. Ste4-Ste18 in turn recruits Ste20, the first protein in the mitogen activated protein kinase (MAPK) cascade including Ste11, Ste7, and Fus3, all bound to protein scaffold Ste5. Next, Fus3 activates Ste12, which binds promoter *pFUS1* and initiates transcription of mating related genes alongside other transcription factors of the yeast mating response. Several feedback-regulatory mechanisms are present in the yeast, including inhibition of Gpa1 activation by Sst2 and degradation of the α mating factor by Bar1. Additionally, Far1 is activated by the pathway, inducing cell cycle arrest in preparation for mating. (C) For sensor applications of yeast, the mating pathway has been streamlined and modularized to allow for a tunable response. Modifications include removal of feedback-inhibition and induced cell-cycle arrest by deletion of Sst2, Far1, and Bar1. Additionally, expression levels of central pathway proteins affecting the pathway output (shown in blue) can be tuned, including the

GPCR, Gpa1, the transcription factor (TF), and the pathway response genes (shown in green). In some cases, the TF Ste12 and promoter *pFUS1* are replaced by synthetic alternatives, to allow for stricter control of the output response. P, phosphate; TF, transcription factor; GDP, guanosine diphosphate; GTP, guanosine triphosphate.

As previously mentioned, the yeast mating pathway is activated upon binding of a mating pheromone (α/a mating factor) to the corresponding mating GPCRs (Ste2/Ste3), causing a conformational change in the receptor (**Figure 6B**). Common for all GPCRs is that these receptors bind G proteins inside the cell and mediate their activation by acting as guanine-nucleotide exchange factors (107). In the case of Ste2 and Ste3, the receptors bind the heterotrimeric G protein complex Gpa1-Ste4-Ste18 (Gαβγ) and mediate the exchange of Gpa1-bound GDP to GTP, activating Gpa1 and causing subsequent dissociation of Gβγ (Ste4-Ste18) (19,107). The Gβγ heterodimer in turn mediates the phosphorylation of Ste11 by Ste20, with Ste11 being the first protein in the mitogen activated protein kinase (MAPK) cascade (19). Ste11 further phosphorylates Ste7, which phosphorylates Fus3, with all three proteins being bound to the sane scaffold protein, Ste5, for proximity (19). Lastly, Fus3 phosphorylates transcription factors involved in the yeast mating response, such as transcription factor Ste12, which results in the activation of the mating response.

As is the case for most biological systems, the yeast mating pathway activation is subject to regulatory mechanisms within the cell, with major feedback-inhibition including accelerated Gpa1 inactivation by Sst2 (108), and degradation of the α mating factor by Bar1(19). Other pathway components relevant to consider for biosensor applications of yeast are Far1, responsible for the induction of cell-cycle arrest in cells prior to mating (109), and the mating pheromone genes of the respective mating type yeast, including *MFA1*, *MFA2*, *MF(alpha)1*, and *MF(alpha)2* (110).

Engineering the yeast mating pathway towards biosensor applications

Over the past three decades, the yeast mating pathway has been extensively studied and engineered towards biosensor applications. Early studies relied on placing desired output genes under the *pFUS1* promoter, deleting *FAR1* to avoid cell-cycle, and deleting *SST2* and *BAR1* to avoid feedback regulation (40,111). Here, output genes refer to those encoding quantifiable proteins of choice, such as fluorescent proteins or proteins catalyzing the production of a colorimetric compound (93). As the degree of GPCR activation directly correlates with the expression level of output genes under the *pFUS1* promoter, the degree of GPCR activation can be inferred from the level of output gene expression (Figure 6**C**)(83).

As previously mentioned, the yeast mating pathway has been applied towards the deorphanization and study of human GPCRs (40,90), allowing for the evaluation of these in a biological system void of the feedback-regulation present in their native host. In these cases, the genes of Ste2/Ste3 are often deleted to avoid interference in pathway activation (40). Furthermore, engineering efforts have improved the coupling between heterologous GPCRs and the yeast pathway by modifying Gpa1 – specifically, by replacing the five C-terminal

amino acids of Gpa1 with those of the appropriate heterologous Gα subunit (112). This modification has not only elucidated specific GPCR-Gα interactions in human cells but has also broadened the range of GPCRs that can be functionally evaluated in yeast (112).

While the key components of the yeast mating pathway have been gradually unveiled over the past three decades, it is only in recent years that the modularization of the pathway has been truly explored. Shaw and colleagues (83) streamlined the pathway of a-type yeast by deletion of genes encoding proteins involved in feedback regulation and cell-cycle arrest (*SST2*, *BAR1*, *FAR1*), elimination of possible interference from other GPCRs and G proteins (*STE3*, *GPR1*, *GPA2*), and deletion of genes encoding the yeast mating peptides (*MAF1*, *MFA2*, *MF(alpha)1*, *MF(alpha)2*). Next, the authors deleted the genes of central pathway components and reintroduced these with promoters of varying strengths, identifying expression levels of Gα, GPCR, and reporter genes as key in the tuning of pathway response characteristics – including LOD, baseline activity, operational rang, and dynamic range (**Figure 7**).

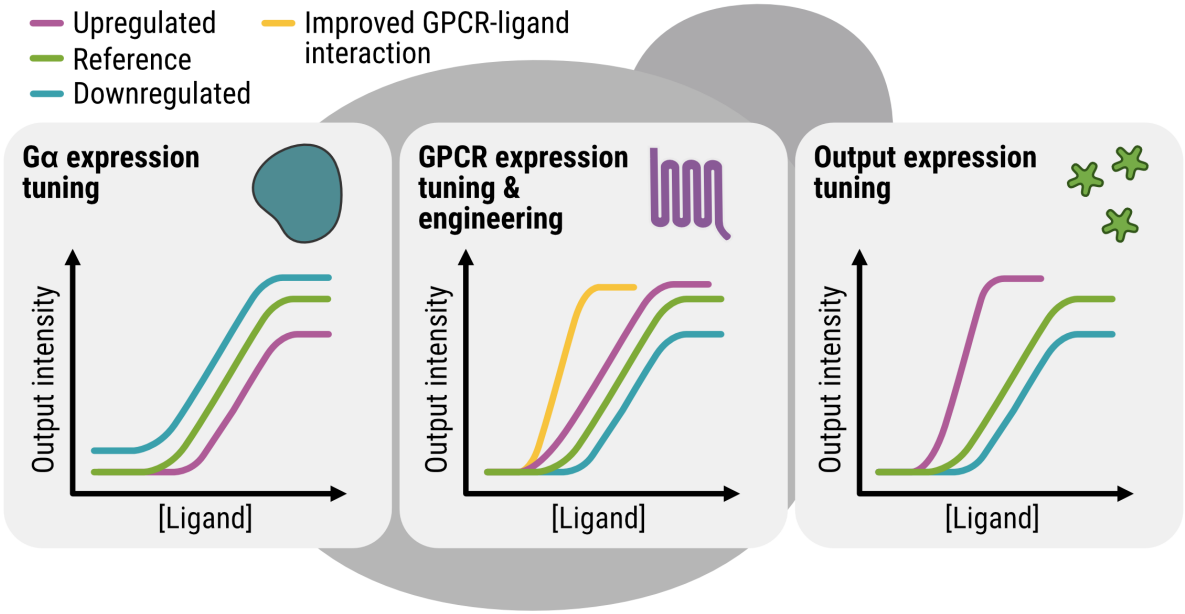

Figure 7. General overview of major tunable components of the streamlined yeast mating pathway. Here, Gα expression tuning affects the baseline expression level and can limit the dynamic range, operational range, and LOD. Meanwhile, GPCR expression tuning affects the LOD and response intensity, and the GPCR ligand interaction affects the Hill slope, sensitivity, operational range and dynamic range. Lastly, output tuning affects the dynamic range, operational range, and Hill slope.

To further refine this system, and to completely decouple mating pathway signaling from the mating response genes managed by Ste12, this TF was replaced with a synthetic alternative. By including the pheromone responsive domain (PRD) of Ste12 (amino acid 216-688) and replacing the DNA binding domain (DBD) with the full length bacterial LexA repressor, the authors produced a pheromone responsive TF unable to bind the mating response genes (**Figure 7**). Moreover, a corresponding synthetic promoter was constructed, containing six LexA operator sequences (*LexO*) upstream of a *LEU2p* core promoter, allowing for strong

expression of the response genes, and resulting in an increased dynamic range of the sensor (**Figure 7**).

In this thesis, I mainly employ the streamlined yeast mating pathway, as developed in the aforementioned studies, as a chassis for constructing GPCR-based biosensors in yeast. By leveraging the modular and tunable nature of this system, my work aims to evaluate and optimize sensor performance for diverse applications.

The relevance of G-protein coupled receptors (GPCRs)

Why the interest in GPCRs specifically? GPCRs are highly conserved throughout the eukaryotic kingdom, regulating vital biological functions in response to diverse external stimuli such as photons, ions, lipids, and peptides (113). In humans, GPCRs make up the largest family of membrane proteins (113). To date, approximately 34 % of the US Food and Drug Administration (FDA)-approved drugs target GPCRs (113), underscoring the importance of continued research towards elucidation of GPCR involvement in the development and progression of disease. Moreover, the diversity within these receptors in terms of the type of ligand recognized, their applicability for sensing of external stimuli, and their high sensitivity and selectivity further makes these receptors highly attractive for biosensor applications in yeast (114,115).

So, what does a GPCR look like and how does the receptor activation work? All GPCRs across the eukaryotic domain consist of a bundle of seven transmembrane alpha helixes (TMs), enabling the transduction of a signal across the cell membrane (116). These are connected by intracellular loops (ICL) and extracellular loops (ECL), with the N-terminus of the protein being extracellular and of varying length, and the C-terminus being intracellular. GPCRs are however divided into classes A-F based on structural variations, with human GPCRs being encompassed by classes A-C and F, and fungal GPCRs making up class D (117,118). While the ligand type and the ligand binding pocket varies, the general activation mechanisms of different GPCRs remains the same – with extracellular binding of the ligand causing a structural shift of the TMs, enabling the GPCR to act as a guanine-nucleotide exchange factor for the intracellular Gα.

Based on these aspects, GPCRs stand out as prime candidates for yeast-based biosensor development due to their wide ligand range, high specificity, and ability to detect extracellular analytes directly at the cell surface. By leveraging these properties, we can design biosensors capable of identifying a wide array of compounds, from small molecules to peptides, without the need for transport past the cell membrane. Moreover, understanding the fundamental structure and activation mechanisms of GPCRs provides a strong foundation for engineering strategies towards improved ligand binding that will be discussed in the following sections – strategies applied with the aim to develop GPCRs for precise, robust, and versatile biosensing applications.

Chapter 2: Design of biosensors for biomedical applications

Having established some background on sensor systems, synthetic biology, sensor metrics, the yeast mating pathway, and GPCRs, we are now ready to dive into the research of my PhD. The following chapters will explore three avenues within GPCR-based yeast biosensors (**Figure 8**); (1) evaluating and benchmarking colorimetric yeast outputs (**Paper I**), (2) engineering fungal mating GPCRs towards greater sensitivity via library-based screening approaches (**Paper II & III**), and (3) attempted improvement of sensor metrics of free fatty acid 2 receptor (FFA2R) expressed in yeast (**Paper IV**). In my research on these distinct yet interconnected subjects, I aimed to explore and expand the current toolbox for development of GPCRs towards biomedical applications.

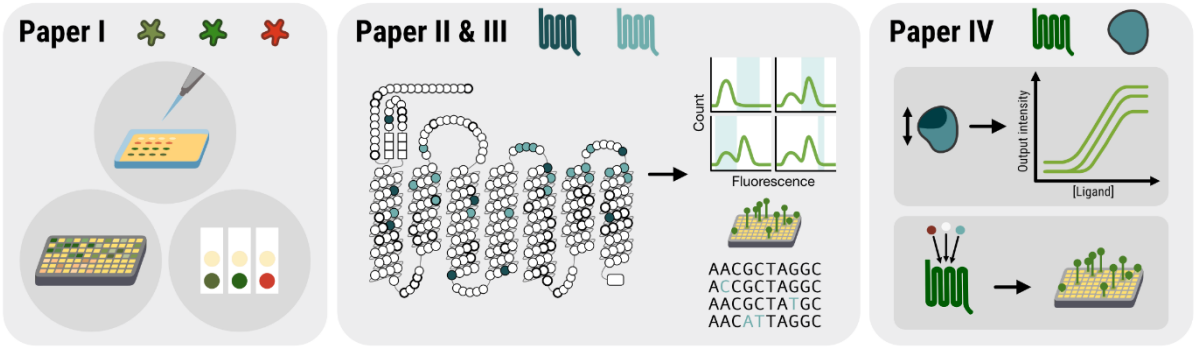

Figure 8. Simplified overview of the contents of Paper I-IV. Paper I focuses on the evaluation and benchmarking of colorimetric outputs on agar plates, in liquid media, and on paper-slips. In Paper II and III, targeted and untargeted mutant GPCR libraries are generated for two fungal mating GPCRs, followed by screening towards identification of variants with improved response curve metrics. In Paper IV, the human FFA2R GPCR was expressed in yeast, the response curve metrics optimized via Gα tuning, and diverse ligands screened in the optimized platform.

Evaluation and benchmarking of colorimetric outputs

Selection of a biosensor output may to some seem like the last step to consider in biosensor design, but it is actually a choice with major impact on sensor applicability in different settings. Further affecting several sensor metrics, such as LOD, dynamic range, and operational range, as well as the ease-of-use of a sensor, the choice of output should in fact be one of the first considerations in yeast biosensor design.

General introduction to yeast biosensor outputs

In yeast, the main categories of outputs include colorimetric, fluorescent, luminescent, and growth-based (119), each with applicability in distinct biosensor settings. Limitations are imposed on each of the different outputs depending on the required equipment, incubation time, and response curve produced, which can be summarized as follows:

Colorimetric outputs, such as lycopene and betalains, are sensitive and allow for detection by the naked eye (39,91). As such, colorimetric outputs are appropriate for point-of-use applications where a binary response is desired, while they can be used for quantitative measurements in lab-based settings (39,40,91). While several of these outputs require a substrate, such as β-galactosidase requiring a cleavable substrate consisting of a colorimetric output and galactose (40,91), this is not always the case (39).

Fluorescent outputs, such as green fluorescent protein (GFP) and red fluorescent protein (RFP) allow for sensitive detection and quantification without the addition of a substrate. While fluorescent outputs make up the most widely applied type of outputs in lab-based screenings, they have limited use outside a laboratory setting due to the need of excitatory light (90,120).

The **luminescent** output produced by luciferase allows for rapid and sensitive detection, but requires the addition of a substrate (91,121). While traditionally limited to lab-based settings, recent work highlights the possibility of point-of-use applications using the camera of a phone with an 3D-printed attachment (91).

Growth-based outputs rely on the production of lacking nutrients or antibiotic resistance in selective conditions, allowing for slow but sensitive detection (115,122). However, this output is largely limited to lab-based settings due to requiring conditions favoring the growth of the organism to function well.

Having outlined the general landscape of yeast biosensor outputs and their respective advantages and limitations, we will move on to the application of biomedical sensors in point-of-use settings. For this application, sensors need to be rapid, sensitive, and user-friendly (39,91,123), making the optimization of the output critical. In the following section the results of **Paper I** are presented, where we focus on the evaluation of two promising colorimetric outputs, prodeoxyviolacein and proviolacein, and benchmarking of these against the already established colorimetric output lycopene for use in both lab-based and point-of-care settings

(39). With these outputs allowing for detection in the absence of an external substrate, they showed potential for applications in both lab-based screenings and for point-of-use detection.

Implementation of prodeoxyviolacein and proviolacein as biosensor outputs

Prodeoxyviolacein (green/brown) and proviolacein (green) are intermediate products of the violacein pathway in *Chromobacterium violaceum*, and have previously shown potential as biosensor outputs in yeast as strong pigments (124–126). However, the performance of these outputs outside of agar plate-based screenings had yet to be evaluated. As such, we set out to evaluate the applicability of prodeoxyviolacein and proviolacein in agar-based screening on different media, in liquid media, and on paper slips in **paper I**. For the purpose of benchmarking, the response metrics of these outputs were compared to the already established colorimetric output lycopene (39).

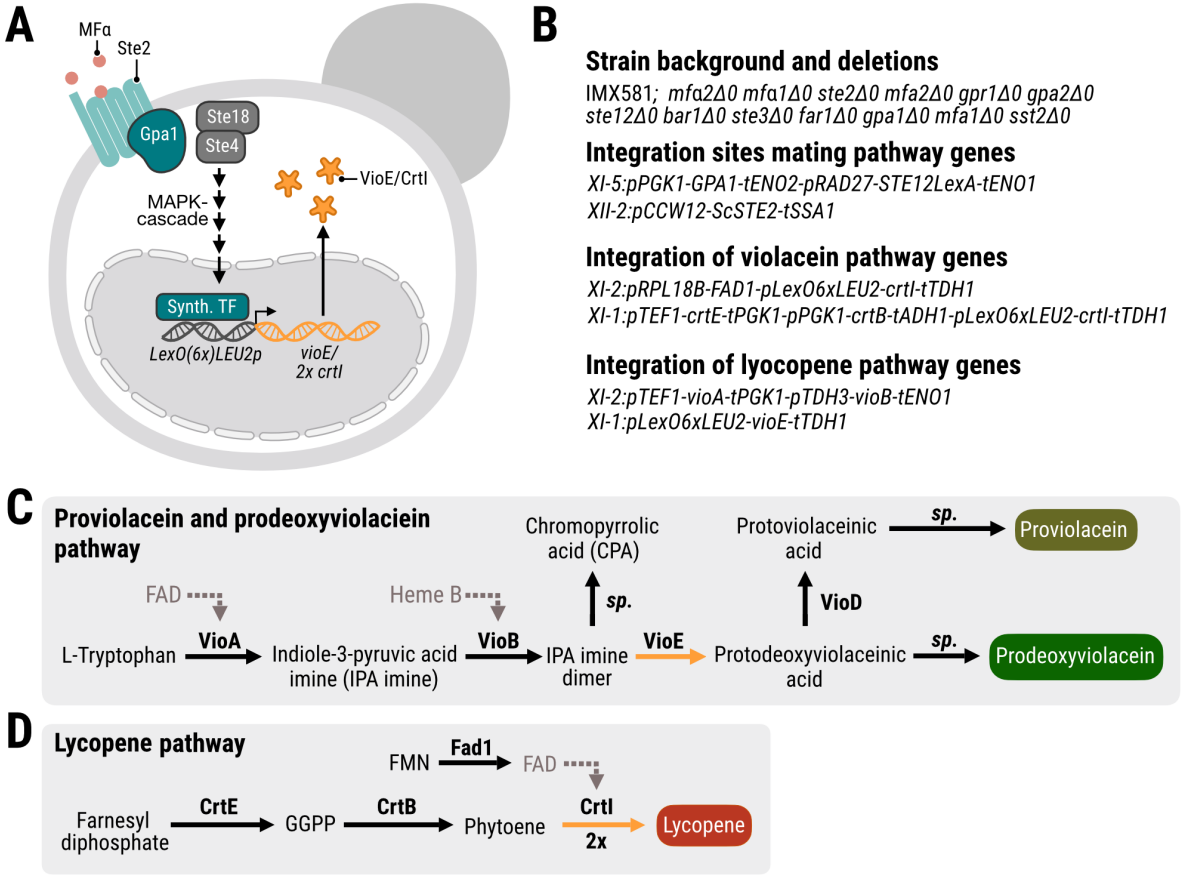

Figure 9. Overview of the platform strain used for the evaluation of the respective outputs. (A) Simplified overview of the streamlined mating pathway and the output genes produced in the colorimetric output strains. (B) Strain background and detailed genetic modifications of strains. (C) Overview of the proviolacein/prodeoxyviolacein pathway and cofactors. Note that oxygen and NADPH requirements of enzymes are displayed in Paper I, Figure 1. (D) Overview of the lycopene pathway and cofactors. MFα, α mating factor; Synth. TF, Synthetic transcription factor; VioA, flavin-dependent L-tryptophan oxidase; VioB, 2-imino-3-(indol-3-yl)propanoate dimerase; VioC, violacein synthase; VioD, protodeoxyviolaceinate monooxygenase; VioE, violacein biosynthesis enzyme; GGPP, geranyl geranyl diphosphate; sp., spontaneous.

As a platform for evaluation of induction of pigment production, a yeast strain with a minimized mating pathway was applied (**Figure 9A**). The strain was constructed largely based on the minimized mating pathway strain (Design 4) by Shaw and colleagues (83), while implemented in a CEN.PK strain background (127) as opposed to the previously used S288C (83). Non-essential pathway genes were deleted, in addition to *STE2*, *GPA1*, and *STE12*, which were re-integrated expressed under the same promoters as used for expression in the Design 4 strain (**Figure 9B)**. Gene expression cassettes were constructed based on the pYTK (128) and pMC (129) plasmid toolkits, allowing for efficient integration in established genomic sites from the EasyClone-MarkerFree toolkit (**Figure 9B)** (130). Note that as a result, the integration sites of mating pathway genes were different than those of the strain developed in a S288C strain background. Genes from the colorimetric output pathway were introduced in genomic locations established in the same paper.

Both prodeoxyviolacein and proviolacein are produced from the precursor L-tryptophan, via the introduction of three, respectively four, genes (**Figure 9C**). These include *vioA*, *vioB*, and *vioE* for prodeoxyviolacein and *vioA*, *vioB*, *vioE* and *vioD* for proviolacein, integrated as single copy genes with strong promoters for expression. As VioE is the first enzyme in the pathway to produce a colorimetric product, the gene was placed under control of the synthetic inducible promoter *LexO(6x)LEU2p*.

The lycopene pathway has been previously optimized for biosensor applications in yeast (39), providing a strong output upon induction of the mating pathway (**Figure 9D**). To this end, the expression of pathway genes *crtE*, *crtB*, and *crtI* from *Erwinia herbicola* were introduced, with two copies of *crtI* expressed under the inducible promoter. Additionally, *FAD1* from *S. cerevisiae*, responsible for the production of the CrtI redox cofactor FAD, was overexpressed (39).

Evaluation of induction in different medium complexities

Depending on the application area of a biosensor, the medium complexity will vary. For example, in bioengineering settings we often work with defined media, while for biosensor applications in healthcare the medium is likely to be undefined. As such, we evaluated the performance of the different outputs on agar plates with increasing medium complexity, in the absence and presence of the inducer (0 μM and 1 μM α mating factor). Three different media were evaluated, including low complexity (synthetic defined medium; SDC), mixed (SDC + 5 % yeast extract peptone medium; SDC + 5 % YPD), and high complexity (YPD; **Figure 10**). As a negative control, an output null strain was applied, lacking any of the colorimetric pathway genes. Moreover, strains lacking the Ste2 receptor were included, in which the mating pathway cannot be activated, to gauge the leakiness of the output production.

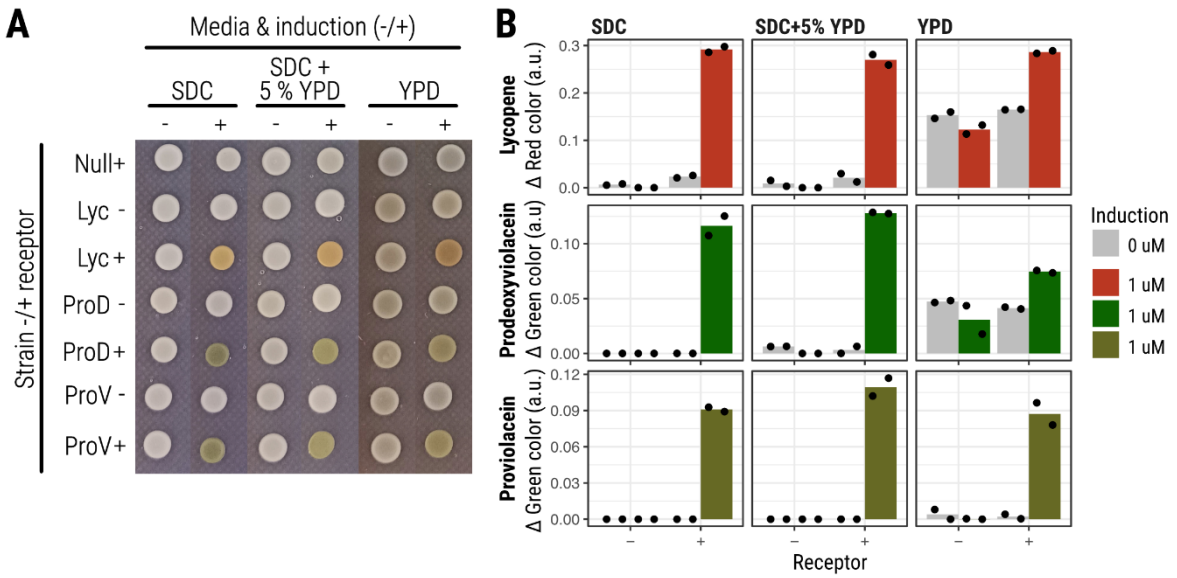

Figure 10. Evaluation of output induction on different medium complexity. (A) Strains were spotted on agar plates with varying medium complexity (see text), with or without 1 µM of the *S. cerevisiae* α mating factor (induction +/-). The null strain does not contain genes for pigment production. (B) Results were investigated after 24 h of incubation, via image-based quantification of outputs relative to the output-null strain on the same plate. The increase in red/green/green-brown pigment was calculated by relative to the uninduced state of the strain. This was done both for strains with and without the Ste2 receptor. Strains were evaluated in duplicates and negative values were set to zero.

We found that that medium complexity indeed affected the outputs, comparing the red and green pigment intensities for the lycopene, prodeoxyviolacein, and deoxyviolacein strains (**Figure 10A-B**). After 24 h of incubation, all three colorimetric outputs were clearly discernible by eye across all tested media (**Figure 10A**), with only slight differences between minimal and mixed-complexity media (**Figure 10B**). Interestingly, in all cases, growth on high complexity medium produced a higher baseline expression for lycopene and prodeoxyviolacein, also present in the proviolacein after an extended incubation (Paper I, Supplementary Figure 2). Upon consideration of that our strain was constructed for minimal basal expression in low complexity media (83), it is possible that the difference in nutrient availability affected the baseline expression of the strains in complex medium. However, the fact that baseline expression was found even in the absence of a receptor was unexpected, as the synthetic transcription factor should not be active in the absence of pathway activation. As such, it is important to consider the target application of the sensor already in the optimization of the mating pathway, to allow for early adjustment and evaluation of pathway components in the appropriate settings.

Interestingly, we further found that induction of strains with the Ste2 receptor affect the growth, especially in low complexity media (**Figure 10A**). This was found both in strains with and without a colorimetric output coupled to the yeast mating pathway, indicating that there are still some unknown or less explored effects of pathway activation with growth-related effects.

Evaluation of induction on paper slips

For application of yeast-based biosensors in point-of-care, the use of yeast dried onto paper-slips has been demonstrated, for which lycopene was previously shown to produce a visible output after 3 h of incubation (39). As such we opted to evaluate the lycopene expressed in our strain together with prodeoxyviolacein and proviolacein in the same setting (**Figure 11**).

We found that lycopene outperformed the prodeoxyviolacein and proviolacein pigments, producing a stronger intensity response (note the difference in axis scaling on the bar plots) and a shorter TOD. While the previously demonstrated TOD of lycopene was exceeded by two hours, one has to consider that the strain backgrounds differ, including the receptor-ligand pair used for pathway induction (39). Moreover, the camera and camera setup can affect the readout, as is often the case in image-based analysis. While output production in liquid was also evaluated, the readout was weak for lycopene and non-detectable for proviolacein and prodeoxyviolacein (see Paper I for details). This is in part caused by equipment availability, as we performed manual measurements as opposed to the continuous surveillance in a plate reader applied previously, introducing noise in the data (39).

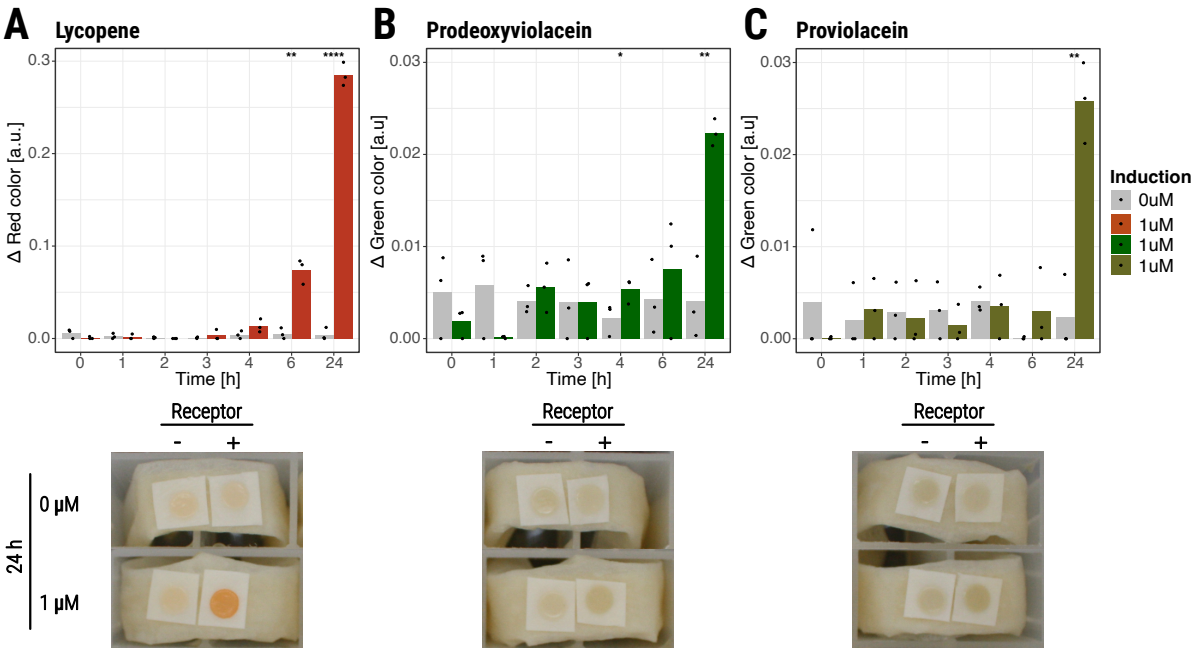

Figure 11. Evaluation of colorimetric output induction on paper slips. Strains were dried onto paper slips and placed on wicking paper dipped in YPD media with or without 1 µM *S. cerevisiae* α mating factor, followed by incubated for 24 h. Photos were taken at indicated timepoints, from which the red/green pigment intensity was evaluated in ImageJ. Bar plots present the pigment intensity of strains for (A) lycopene, (B) prodeoxyviolacein, and (C) proviolacein over time compared to the control without the Ste2 receptor. The lower part of the figure shows pictures collected after 24 h of incubation for the respective outputs. Stars indicate statistical significance as calculated by a one-sided t-test, * p <=0.05, ** p <=0.01, and **** p <=0.0001. Three strain replicates were used, and negative values were set to zero.

What we have learned

In **Paper I**, we investigated proviolacein and prodeoxyviolacein as colorimetric yeast biosensor outputs in liquid, on agar plates, and on paper slips. The pigments were benchmarked against the previously established colorimetric output lycopene, finding that while both proviolacein and prodeoxyviolacein provided comparable detection on agar plates, independent of media complexity, these produced a weaker output on paper slips and were non-detectable in the liquid assay. In general, our study would have benefitted from further optimization of the violacein pathway, such as by tuning expression levels of the violacein pathway genes, engineering of the L-tryptophan metabolism (131), or by increased cofactor availability (39,132), as has been demonstrated extensively for lycopene (39,75). Even so, only few prior examples exist of violacein pathway optimization in *S. cerevisiae* for which titers are reportedly low, but exact titers have not been reported (133–135). However, extensive strain engineering would remove the advantage of pigments derived from the violacein pathway being easy to implement as sensor outputs.

Overlooking the presently developed mating pathway-based yeast biosensors optimized for point-of-use applications, the current timescale of the sensor response cannot be said to be rapid. However, depending on the application area, the present time span of detection is short enough to be viable for application as point-of-care sensors, and may still result in shorter detection time compared to traditional detection methods (39). This is the case both for colorimetric and luminescent outputs, where the best TOD was reported as 2 h and 30 min respectively (91,136). In our study, we did not find response times comparable to these.

In summary, our results underscore both the opportunities and the current limitations of employing proviolacein and prodeoxyviolacein as colorimetric outputs in yeast biosensors. While these pigments proved robust on agar plates, yielding a response comparable to lycopene, their weaker or non-detectable signals in paper-based and liquid assays highlight that further optimization is needed for a broader spectrum of applications. However, engineering the violacein pathway or host metabolism towards this scenario must be balanced against the simplicity of implementation that originally motivated the investigation of these pigments as sensor outputs.

Investigating the structure-function dynamics of fungal mating GPCRs via library-based screening approaches

In this section, we will focus on the sensing aspect of GPCR-based yeast biosensors as evaluated in **Paper II** & **III**. The choice of target molecule (ligand) and the GPCR greatly affects sensor applicability, in terms of sensitivity of detection, selectivity towards the ligand, and response phenotype (digital/linear).

In recent years, the interest in fungal GPCRs (class D) both for detection (39,83,114) and treatment (137) of pathogenic fungal infections (137,138) has increased, as fungal GPCRs have been implicated in fungal virulence and pathogenesis (139,140). These applications are enabled by these receptors being structurally distinct from other classes of GPCRs, and by fungal GPCRs being involved in diverse cellular processes such as nutrient sensing, reproduction, and growth (138). Specifically for fungal mating GPCRs in yeast, belonging to subclass D1 out of 14 possible subclasses, they are linked to the transfer of genes between different clades of fungi upon sexual reproduction, and may therefore aid in the propagation of traits involved in pathogenesis and antimycotic resistance (141). As a result, the fungal mating receptors have been suggested possible targets for antagonistic therapeutics, blocking the binding of the ligand to the receptor (140). Conversely, as mating pathway activation results in cell-cycle arrest and growth inhibition in wild-type yeast, agonistic therapeutics that stimulate receptor activation may also be applicable (140). Other than as targets for therapeutics, fungal mating GPCRs have also been suggested as applicable towards detection of fungal pathogens via yeast based biosensors (39,83,114). Even so, the structure of class D GPCRs remains understudied to date, with the exception of class D1 receptor Ste2 from *S. cerevisiae,* for which the structure and residues interacting with the Gα and ligand have been determined via cryogenic electron microscopy (**Figure 12A-B**) (118,142).

As such, the fungal mating GPCRs are interesting to study in order to elucidate ligand-receptor interactions, structure-function dynamics, and the potential for biosensor applications. Here, we investigate the plasticity and structure-function dynamics of two fungal mating GPCRs via mutagenesis of the receptors, with the aim of identifying mutations resulting in altered or non-altered receptor function, via:

Paper II: Untargeted mutagenesis of Ste2 from fungal pathogen *Candidozyma auris* (*Cau*Ste2) and screening for receptors with a lower LOD.

Paper III: Targeted mutagenesis of the ligand binding (orthosteric) site of Ste2 from *S. cerevisiae* (*Sc*Ste2) in a designed library and screening for functional, constitutively active, and loss-of-function variants.

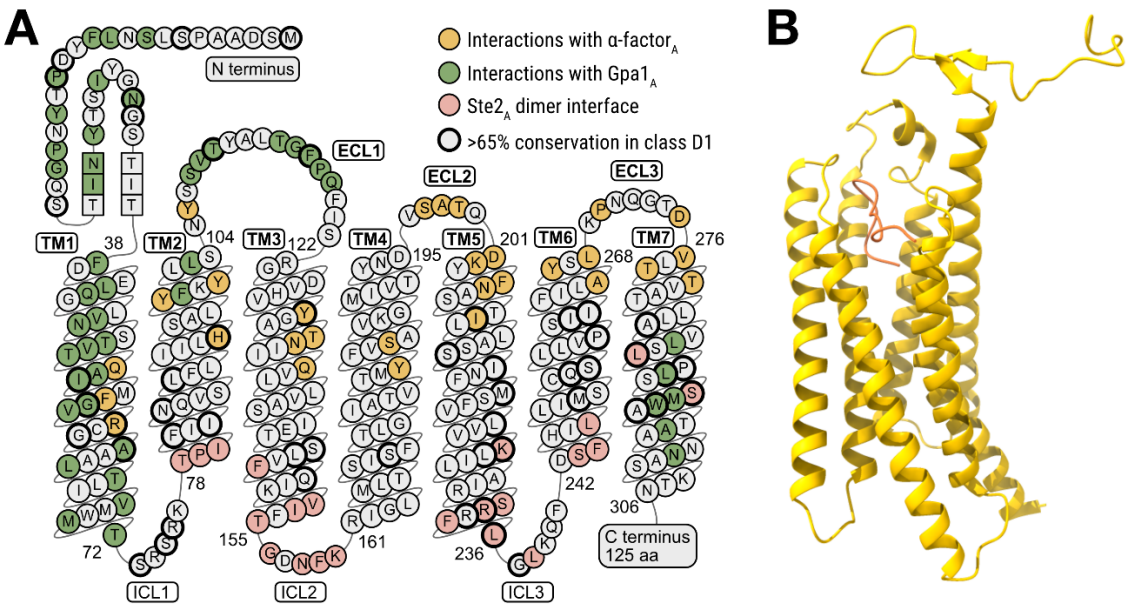

Figure 12. Structure overview of *Sc*Ste2, a class D1 GPCR. (A) Snakeplot including interactions with Gpa1, the α mating factor and the dimer interface between $Ste2_A$ and $Ste2_B$ as determined by cryoEM by Velazhahan and colleagues (118). (B) Cartoon of CryoEM generated protein structure of $Ste2_A$ (yellow) bound to the α mating factor (pink), $Gpa1_A$ (not shown) and $Ste2_B$ (not shown; Protein Data Bank, accession code 7AD3) (118,143).

Construction of screening platform strains

For GPCR-based sensing via the mating pathway in yeast, the GPCR-ligand and the GPCR-Gα binding dynamics have been shown to strongly impact the sensor response metrics, including dynamic range, LOD, operational range, slope, and selectivity (40,114,144). As such, we can apply mutagenesis of the receptor and evaluate mutants via their ability to activate the yeast mating pathway as a way of screening mutant receptor libraries. For this purpose, platform strains were constructed for evaluation of the mutant GPCR libraries, in which the mating pathway activation was benchmarked for the wild-type (WT) *Sc*Ste2 and *Cau*Ste2 receptors and their cognate ligands though induction at increasing concentrations.

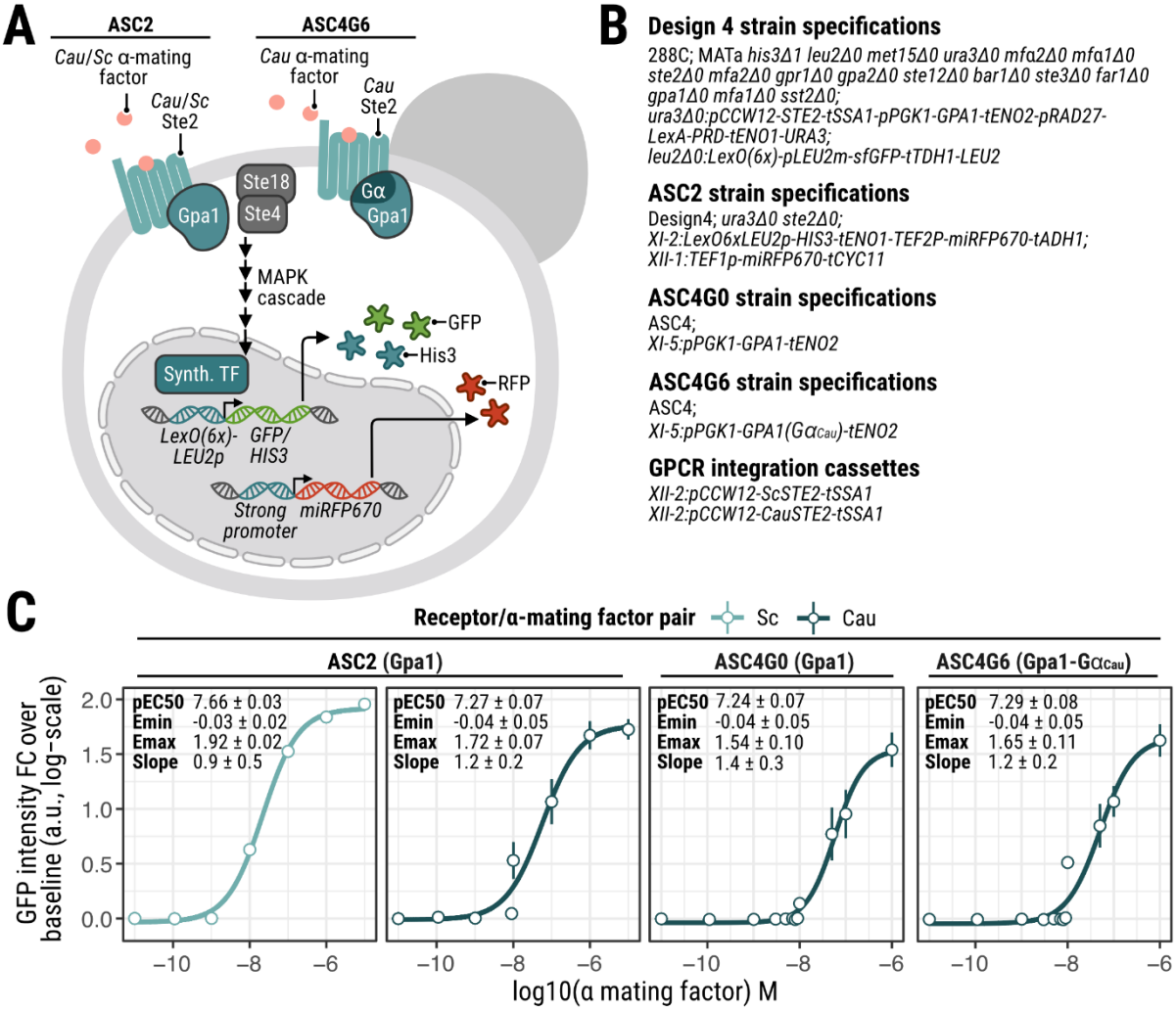

Figure 13. Overview of the screening platform strains. (A) Minimized mating overview with/without a chimeric Gpa1, in which expression levels of key components have been tuned (shown in blue/green) (B) Background and constructed strain specifications. (C) Evaluation of the response-curve of platform strains with genome integrated Ste2 by flow-cytometry, after 3 h incubation with the corresponding α mating factor pair. The GFP intensity is presented as log10 fold-change over baseline for the respective strains, dots display the mean and vertical lines the s.d. of three biological replicates. GFP, green fluorescent protein; RFP, red fluorescent protein; Synth. TF, synthetic transcription factor; Gα, G protein α; E_{min}, the effect at baseline; E_{max} the maximal effect; pEC50, -log10(concentration at 50 % of the maximal effect); Slope, Hill slope.

Two different screening platforms were applied for library screening, the first with the Gα of *S. cerevisiae* (strain ASC2) and the second with a chimeric Gα (strain ASC4G6), in which the five C-terminal amino acids were replaced with that of putative Gpa1 from *C. auris* (**Figure 13A-B**). Both strains were developed from the minimized mating pathway strain (Design 4) produced by Shaw and colleagues, in which *GFP* is present as a reporter gene for fluorescent evaluation of pathway activation (83). To allow for additional growth-based selection, *HIS3* was introduced expressed from the synthetic *LexO(6x)LEU2p* promoter. *ScSTE2* and *URA3*

were deleted to allow for re-introduction of GPCR variants in integration site XII-2 (130) or expressed from plasmids with auxotrophic selection. Lastly, constitutive expression of miRFP670 was introduced to allow selection of viable cells in screenings by fluorescence activated cell sorting (FACS), producing platform strain ASC2. By further deleting *GPA1* and re-introducing a chimeric variant expressed from genomic locus XI-5 (130), platform strain ASC2G6 was produced. These strains were benchmarked with genomic expression of wild-type *ScSTE2* and *CauSTE2*, respectively (**Figure 13C**). As the integration site of genes can affect expression levels, ASC2G6 was evaluated next to a strain with the wild-typ *GPA1* integrated in the same genomic site, ASC2G0.

Upon evaluation by flow cytometry, strain ASC2 was found to produce an LOD of 10 nM both for expression of *ScSTE2* and *CauSTE2* ($p < 0.001$ and $p < 0.05$, one-sided paired t-test), while the pEC50 and max activation was slightly higher for the expression of *ScSTE2* (**Figure 13C**). Instead comparing the expression of *CauSTE2* in strain ASC2G6 to that of a strain ASC2G0, no difference was found between the response curves, while strain ASC2G6 produced a significant increase in response intensity at the LOD of 10 nM compared to ASC2G0 ($p<0.01$, one-sided unpaired *t*-test; **Figure 13C**).

For evaluation of the GPCR libraries, we opted for plasmid-based expression as it allows for higher transformation efficiencies, and thereby screening of a larger number of variants. While plasmid-based expression of *Sc*Ste2 was initially attempted with the same strong promoter *pCCW12* used for genomic expression, this caused a larger portion of the yeast population to lack GFP expression (pAL001, **Figure 14A**). This was likely due to part of the population dropping the plasmid, which has been shown to occur in cultures with auxotrophic selection due to cross-feeding (145), and possibly further amplified by the toxicity or metabolic burden of STE2 overexpression. Instead, the medium-strength promoter *pHHF1* was applied, resulting in a larger portion of the cell population seemingly retaining the plasmid (pAL002, **Figure 14A**). Applying pAL002 for expression of *ScSTE2* in platform strain ASC2, we found that the LOD and pEC50 of the response curve corresponded to that of genomic expression (**Figure 14B**). However, as the activation curve was evaluated based on the mean GFP fluoresce of the population, the dynamic range was decreased due to the portion of inactive cells.

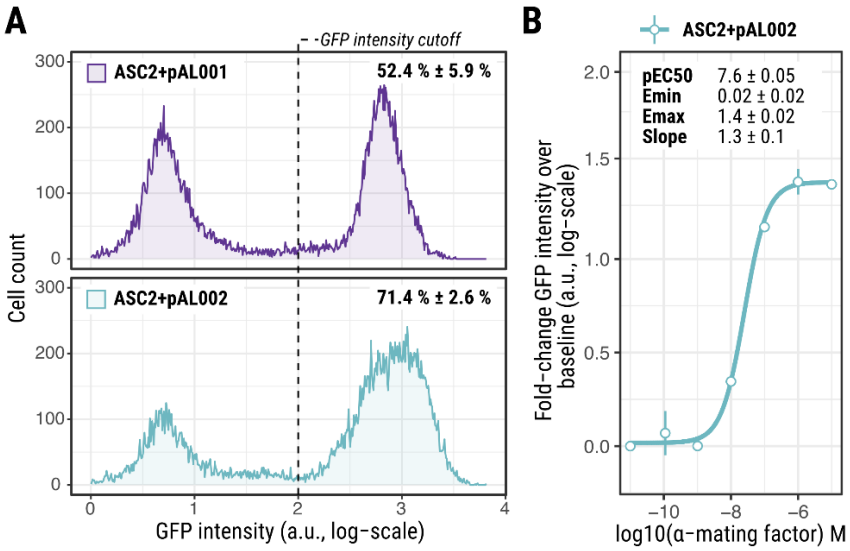

Figure 14. Evaluation of induction in ASC2 with plasmid-based expression of ScSTE2. (A) Plasmid-based expression of *ScSTE2* under strong promoter *CCW12p* (pAL001) and medium strength promoter *HHF1p* (pAL002) respectively was evaluated. Strains were incubated 3 h with 1000 nM *Sc* α mating pheromone and evaluated by flow cytometry to determine the percentage of cells in the population with high GFP intensity, defined by an arbitrary cutoff at a GFP intensity > 2 (dotted line). Density plots display the pooled events of three biological replicates, a total of 15,000 events. (B) Response curve of strain ASC2 with plasmid pAL002 after 3 h of incubation with the *Sc* α mating pheromone, evaluated by flow cytometry. The GFP intensity is presented as log10 fold-change over baseline for the respective strains, dots display the mean and vertical lines the s.d. of three biological replicates. E_{min}, the effect at baseline; E_{max} the maximal effect; pEC50, -log10(concentration at 50 % of the maximal effect); Slope, Hill slope.

Generation and screening of variant GPCRs libraries

With the screening platform strains ready for application in library evaluation, the next step was library construction and screening. The space of possible protein variants for a given protein is huge, considering there are 20 possible amino acids (aa) for each aa position in a protein. In a small protein of 100 aa, there are 1900 possible variant amino acid sequences for investigation of every possible single amino acid substitution (number aa positions multiplied by the number of possible substitutions per position). Further considering that the same amino acid can be encoded by several different codons in the DNA, that the codon can affect the protein expression level, and that not only single but also co-occurring substitutions are of interest, the number of variants increase drastically. To cope with this fact, different strategies for library generation have been devised, ranging from mutagenesis of the whole protein sequence via error prone PCR for evaluation of random protein variants (146), to rational library design based on known protein structures and inferred ligand interactions (147). In my work, I applied two different strategies for library generation and screening depending on the target application, of which details are outlined in **Figure 15** and described in the figure text.

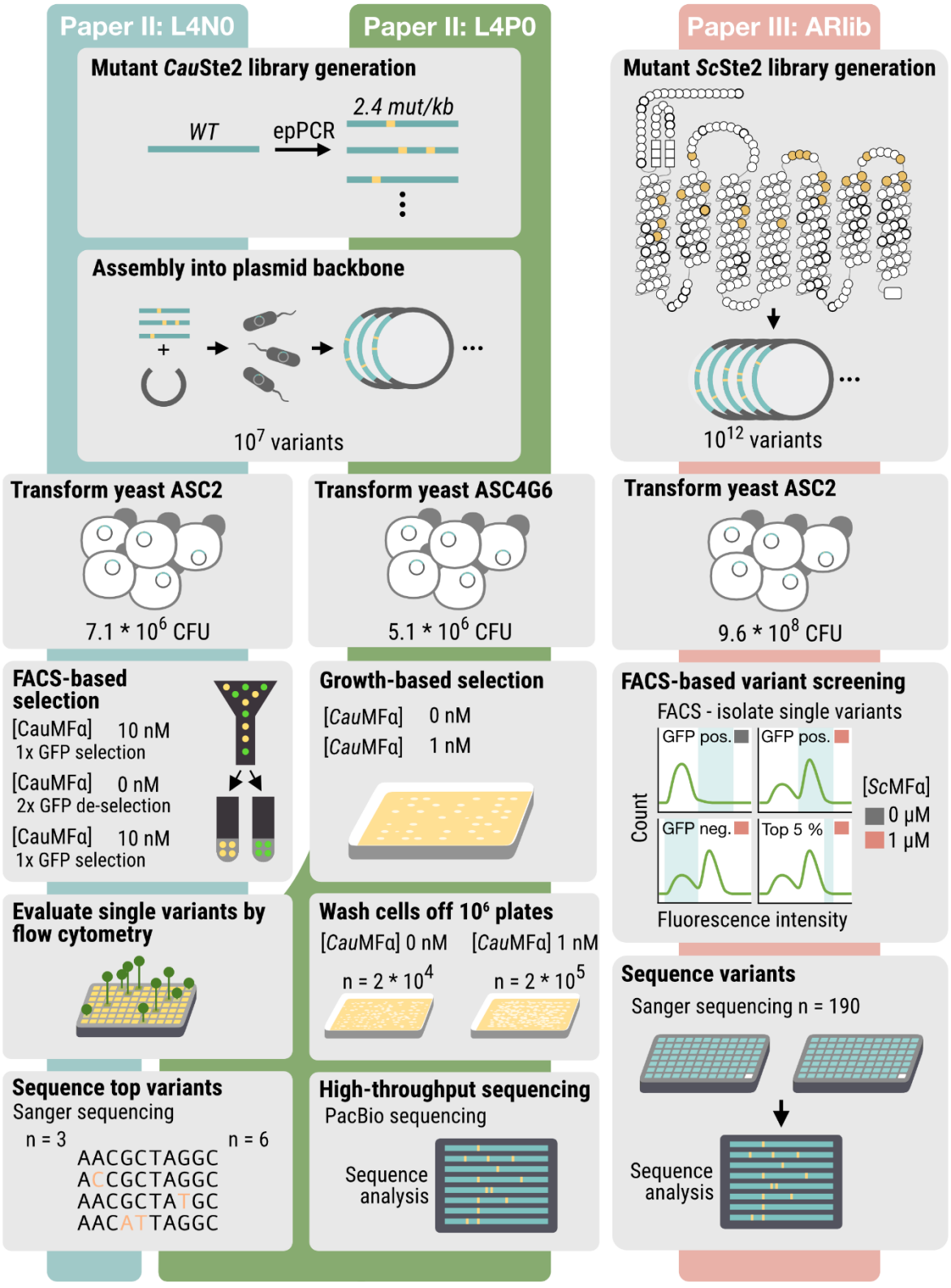

Figure 15. Overview of library generation and screening strategies applied for libraries L4N0, L4P0, and ARlib. Yeast libraries L4N0 and L4P0 (Paper II) were generated from the same plasmid library, produced by error prone PCR (epPCR) of *CauSTE2* and assembly into the pAL002 plasmid backbone.

Library ARlib (Paper III) was designed and ordered as a pre-assembled plasmid library, targeting the orthosteric site of the GPCR with substitutions based on the amino acid distribution in each position among the entirety of known fungal mating GPCRs. Libraries L4N0 and ARlib were evaluated in the ASC2 platform strain and library L4P0 in the ASC4G6 platform strain. For library L4N0, FACS was applied to enrich cells with high GFP fluorescence intensity at 10 nM *Cau* α mating peptide (MFα) in one round of sorting, followed by two rounds of sorting at 0 nM to remove false-positive candidates. Lastly, 96 candidates were sorted out, evaluated by flow cytometry and growth, followed by sequencing of top candidates. For library L4P0, cells were plated with auxotrophic selection and with/without 1 nM *Cau*MFα induction respectively, at different dilutions. Single variants were isolated by pickling large single colonies from diluted induced plates, evaluation of these by flow cytometry, followed by sequencing of top candidates. Moreover, cells were washed off from the plates with high cell densities, barcoded, and PacBio sequenced to generate long reads with high throughput. These were analyzed towards identification of single and cooccurring enriched mutations. Cells were washed off plates with high cell densities from the induced and uninduced plates respectively, which were barcoded separately prior to sequencing. For library ARlib, FACS was applied to sort out 96 candidates from four gating settings, including cells with high GFP fluorescence intensity in absence of induction, cells without fluorescence intensity at 1 μM of *Sc*MFα, cells with high fluorescence intensity at 1 μM of *Sc*MFα, and cells with top 5 % fluorescence intensity at 1 μM *Sc*MFα. In total 190 variants were sequenced, divided between the different sorting conditions. mut, mutation; kb, kilo base pair; n, number; CFU, colony forming units; FACS, fluorescence activated cell sorting; GFP, green fluorescent protein.

Paper II: Untargeted mutagenesis of the *Cau*Ste2 receptor via error prone PCR (epPCR) was employed, generating on average 2.4 mut/kb in the resulting library (**Figure 15**). Library screening was applied with the aim of identifying amino acid positions and substitutions affecting the receptor-ligand interaction and improving the sensor LOD.

Paper III: Rational library design targeting the majority of the orthosteric (ligand binding) site of *Sc*Ste2 was employed, with substitutions defined by the relative amino acid abundance in each position within Class D1 GPCRs (118) (**Figure 15**). Screening was applied with the aim of identifying substitutions in the orthosteric site impacting ligand binding and receptor structure, as well as substitutions that do not affect the receptor function, contributing towards our understanding of Class D1 GPCR plasticity.

Mutating *Candidozyma auris* Ste2 towards improved sensitivity

The fungal pathogen *Candidozyma auris* (*Cau*; formerly *Candida auris*) has unusually high persistence and transmissibility in the clinical environment (148), as well as frequent occurrence of resistance to antimycotics (149). While *C. auris* is predominantly an opportunistic pathogen, infecting those that have increased susceptibility, the mortality related to infection is high (150). As such, *C. auris* is presently on the World Health Organizations (WHOs) critical fungal pathogen priority list (150). Additionally, *C. auris* can be misidentified as other common pathogenic fungi, such as *Candida albicans, Clavispora lusitaniae* (*Candida lusitaniae*), and *Nakaseomyces glabrata* (previously *Candida glabrata*), by traditional diagnostic methods (148,151). While alternative methods for correct identification of *C. auris* have been developed in recent years, such as MALDI-TOF MS and special growth media (148),

these often require prolonged incubation times of 2-10 days and in addition to special equipment (148), thereby limiting applications in point-of-care settings or remote clinical environments. Hence, there is a call for new diagnostic methods and treatments for *C. auris* infection (151).

As previously discussed, the mating GPCRs of fungi have been implicated in fungal virulence, with these receptors being suggested as therapeutic targets (140,152,153). Additionally, fungal GPCRs have shown potential for application in point-of-care biosensors (39). In **Paper II**, we constructed and screened an untargeted mutant *Cau*Ste2 library towards identification of variants producing a lower LOD (**Figure 15**), indicative of an improved ligand or Gα interaction. Using this method, we aimed to contribute towards the understanding of amino acid residues in the receptor with importance for receptor function, while developing the receptor towards the possibility of YBB-based point-of-care detection of *C. auris*. While functional expression of the receptor has previously been demonstrated in *S. cerevisiae* (114), the selectivity of *Cau*Ste2 and the ligand response curve had yet to be evaluated in yeast prior to this work **Figure 13C**.

After library generation by epPCR, the mutagenic library was evaluated in two different platform strains, including ASC2 (library L4N0) and ASC4G6 (library L4P0) **Figure 15**. Library L4N0 was screened by FACS through four rounds of sorting, initially enriching variants with a high GFP fluorescence intensity at the WT LOD of 10 nM *Cau* α mating factor. Here, we noticed enrichment not only of possible candidates, but also of false-positives, cells with a constitutive expression of GFP (Paper II, Figure S3). In fact, approximately 20 % of the total cell population exhibited high levels of GFP expression in the absence of induction. As such, two additional FACS sorting rounds were deployed to isolate cells without GFP expression in the absence of inducer, resulting in a library in which 1.6 % of the population exhibited high levels of GFP expression in the absence of induction, and 6 % of the population exhibited high levels of GFP expression in the presence of induction. From this library, cells were sorted onto non-selective agar plates, yielding 90 candidates. These were evaluated by flow cytometry at 0 and 10 nM induction (Paper II, Figure S4), with the top three candidates being sequenced and integrated into the genome of a fresh platform strain prior to evaluation of the response curve (**Figure 16A**). Note that compared to the response observed in the initially isolated library strains with plasmid-based expression was higher, indicating that either mutations in the platform strain or the change from plasmid-based to genomic expression affected the activation (Paper II, Figure 4).

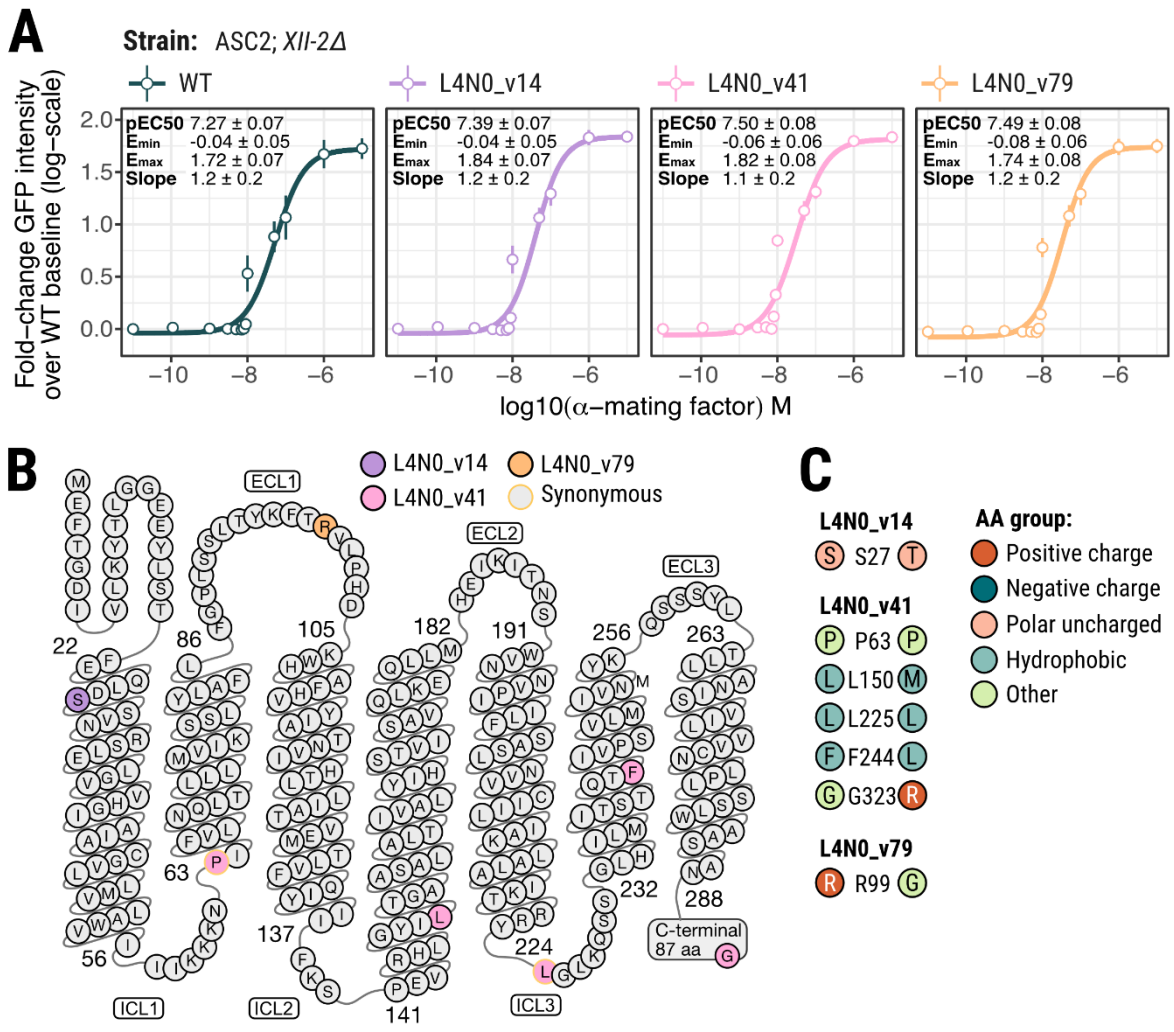

Figure 16. Overview of isolated variants from library L4N0. (A) Response curve of variants as determined by flow-cytometry. The GFP intensity is presented as log10 fold-change over baseline for the respective strains, dots display the mean and vertical lines the s.d. of three biological replicates. (B) Snakeplot of *Cau*Ste2 as predicted by AlphaFold2 (154), with the variant-specific substitutions marked by color. (C) Amino acid substitutions resulting from mutations for each candidate and position are listed, with the amino acid type before and after mutation indicated by color. E_{min}, the effect at baseline; E_{max} the maximal effect; pEC50, -log10(concentration at 50 % of the maximal effect); Slope, Hill slope; AA, amino acid; ECL1-3, extracellular loop 1-3; ICL1-3, intracellular loop 1-3.

Comparing the difference in the response curves of variant strains to that of the WT control, the main improvement was found in the pEC50 of variants L4N0_v41 and L4N0_v79. While the LOD of strains was significantly reduced compared to the WT, the difference was minor (p<0.05, one-sided paired t-test). The biggest reduction in LOD was found in strain L4N0_v41, with significant induction at 8 nM of α mating pheromone. Next, the locations of substitutions in the receptor variants (**Figure 16B-C**) were compared to the locations in the heterologous GPCR *Sc*Ste2, for which the interactions with the α mating factor, Gpa1, and the Ste2 dimer interface have been determined (**Figure 12A**). For L4N0_v14 (S27T), the single substitution

in TM1 may impact dimer formation, while the structural difference between serine end threonine is minor (**Figure 16B-C**). For L4N0_v41 (P63P, L150M, L225L, F244L, G323R) containing three substitutions and two synonymous substitutions, the non-synonymous substitutions are located in TM4, TM6, and the C-terminus of the protein. Of these, the substitution G323R in the C-terminus of the protein is likely to have the biggest structural effect, introducing a large negatively charged residue in place of a small and non-charged residue, possibly affecting the GPCR-Gpa1 interaction. Lastly, L4N0_v79 (R99G) has a single substitution in ECL1, introducing a small non-charged residue in place of a large and negatively charged residue. As ECL1 is known to be part of the *Sc*Ste2 dimer interface, it is possible that these residues have a similar function in *Cau*Ste2, and thereby that the substitution affects dimer formation.

As the improvements found were minor, we opted for another round for library screening, this time applying platform strain ASC4G6 with a chimeric Gpa1-Gα_{Cau} to enable better interaction between the heterologous receptor and the *S. cerevisiae* mating pathway (**Figure 13A**). A different screening approach was applied as well, utilizing auxotrophic selection on agar plates and induction at a lower induction concentration of 1 nM *Cau* mating factor (**Figure 15**). In total, 72 colonies were isolated for further screening. Again, flow-cytometry was applied for initial candidate evaluation, inducing at 0, 1, and 10 nM of ligand (Paper II, Figure S6). Six top candidate receptors were selected, sequenced and further analyzed. The variant receptor genes were then re-cloned into the initial pAL002 plasmid backbone and transformed into the initial ASC4G6 strain, in which response curves were determined (**Figure 17A**). The response curves of variant strains were evaluated alongside the WT control over three 96-well plates. Comparing the controls, there was clear variation in the response curves between plates in terms of pEC50 and slope, in part caused by overfitting to higher concentrations in the case of Plate 2 (**Figure 17A**). Investigating the LOD of the control strains across the plates, a significant induction compared to the uninduced baseline was found at 9 nM, 10 nM, and 7 nM respectively ($p<0.05$, $p<0.001$, and $p<0.05$, one-sided paired t-test) (**Figure 17A**). As such, the response curve and LOD of variants were compared to the control on the same plate. Note however, that this also calls into question the robustness of GPCR-based YBB activation.

Investigating the LOD of isolated variants as compared to the uninduced state, significant induction was found at 1 nM induction for strains L4P0_1, L4P0_19, L4P0_29, and L4P0_67 ($p<0.01$ - 0.05, one-sided paired t-test), and at 3 nM for strains L4P0_19 and L4P0_51 ($p<0.01$ - 0.05, one-sided paired t-test). Among the evaluated strains, all had a higher pEC50 compared to the WT on the same plate, with variants L4P0_45, L4P0_51 and L4P0_67 displaying the biggest improvement. Strains L4P0_45 and L4P0_51 further produced a drastically increased slope with a switch-like activation, however, L4P0_51 also had a higher baseline expression compared to the control in the absence of induction.

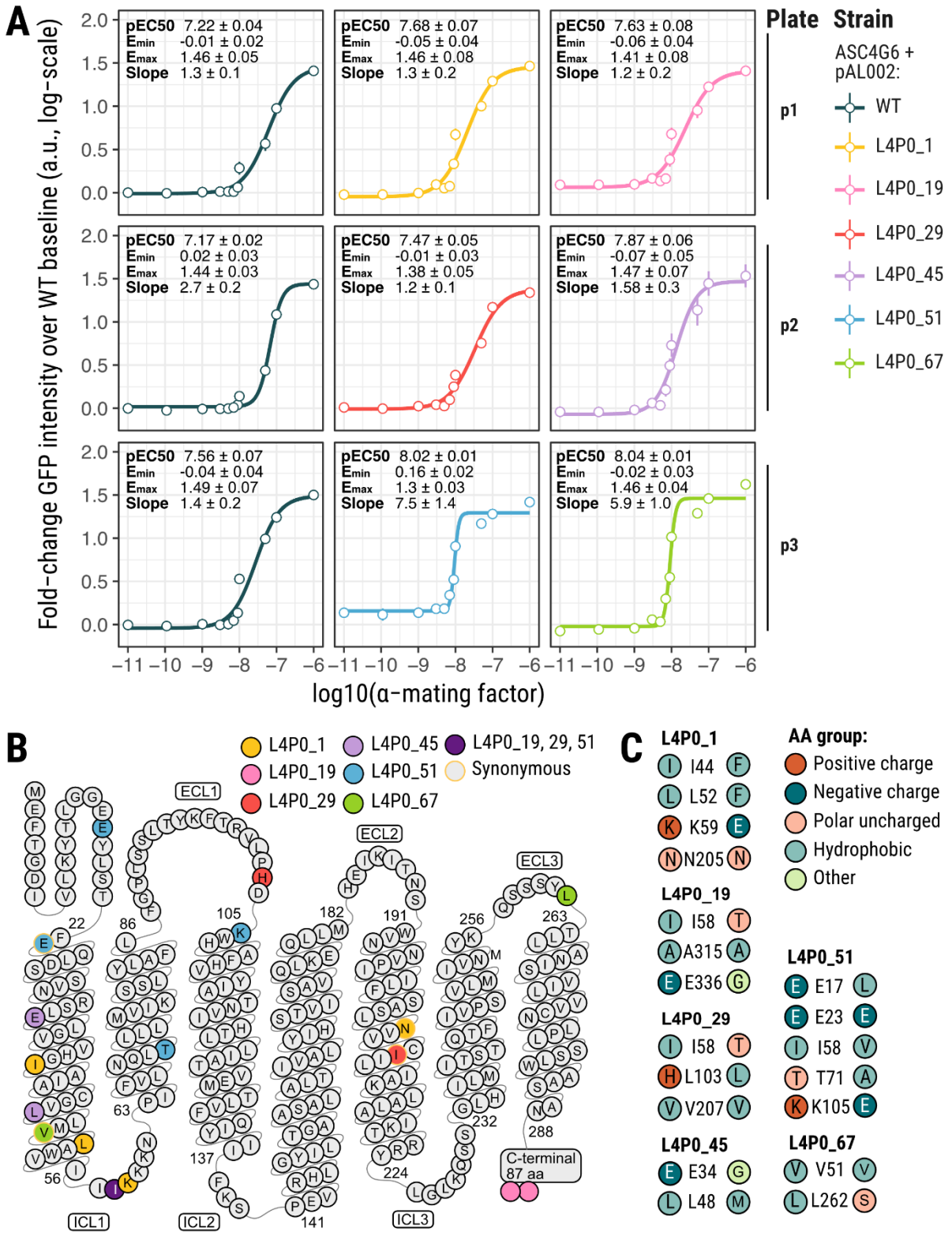

Figure 17. Overview of isolated variants from library L4P0. (A) Response curve of variants as determined by flow-cytometry. The GFP intensity is presented as log10 fold-change over baseline for the respective strains, dots display the mean and vertical lines the s.d. of three biological replicates. (B) Snakeplot of *Cau*Ste2 as predicted by AlphaFold2 (154), with the variant-specific substitutions marked

by color. (C) Amino acid substitutions resulting from mutations for each candidate and position are listed, with the amino acid type before and after mutation indicated by color. p1-p3, plate 1-3; E_{min}, the effect at baseline; E_{max} the maximal effect; pEC50, -log10(concentration at 50 % of the maximal effect); Slope, Hill slope; AA, amino acid; ECL1-3, extracellular loop 1-3; ICL1-3, intracellular loop 1-3.

Further investigating the location and nature of substitutions, we speculated on their effect based on the structure-function of residues in heterologous GPCR *Sc*Ste2 (**Figure 12A**). Firstly, four of the isolated variants (L4P0_1, L4P0_19, L4P0_29, and L4P0_51) were found to have substitutions in intracellular loop 1 (ICL1; **Figure 17B-C**). Two of these substitutions were the same, I58T, introducing a threonine in place of an isoleucine and thereby the possibility of hydrogen-bond formation. The remaining substitutions included I58V in variant L, introducing a minor structural difference in the residue, and K59E, introducing the possibility of salt-bridge formation or hydrogen bonding. While ICL1 is not directly implicated as interacting with the Gpa1 in ScSte2, the nearby intracellular residues of TM2 are (**Figure 12A**). Thereby, it is not improbable that such an interaction is possible for ICL1 of *Cau*Ste2, as ICL1 indeed seems to be of importance for receptor function. However, substitutions in ICL1 never occurred as single substitutions, meaning that the observed effect may result from the co-occurrence of these.

Looking into further non-synonymous substitutions in the individual variants, L4P0_1 (I44F, L52F, K59E, N205N) has two additional mutations in TM1 (**Figure 17B-C**), in locations known to be important for dimer formation in *Sc*Ste2 (**Figure 12A**). Both of these resulted in the introduction of larger aromatic amino acid residues in place of a smaller hydrophobic amino acid and may increase the strength of Van-der-Waals interactions. In L4P0_19 (I58T, A215A, E336G) the remaining substitution is located in the C-terminus, known to be important for Gpa1 coupling, and removes the possibility of ionic or hydrogen bonding. Similarly, the additional substitution in in ECL1 of L4P0_29 (I58T, H103L, V207V) removes the possibility of ionic and hydrogen bonding, and may contribute towards Ste2 dimer formation. In L4P0_45 (E34G, L48M), one of the variants with the biggest improvement in pEC50 and LOD, substitutions were located in positions of TM1 likely to affect dimer formation. The substitutions resulted in introduction of a small, nonpolar, residue in place of the negatively charged glutamic acid, and the larger hydrophobic methionine in place of a leucine. The variant with the highest number of substitutions, L4P0_51 (E17L, E23E, I58V, T71A, K105E), has one mutation in the N-terminus possibly affecting dimer formation though the substitution of a negatively charged residue with a smaller hydrophobic residue, in addition to the previously discussed substitution in ICL1. Remaining substitutions in this variant were found in the areas of TM2 (T71A) and TM3 (K105E) are not likely to interact beyond the receptor. Even so, it is possible that they affect the overall structure and function, as this is the only variant that exhibits a baseline expression over that of the WT control. The final variant, L4P0_67 (V51V, L262S), had a single substitution in a position of ECL3 known to be important for ligand binding in the heterologous receptor *Sc*STE2. With the substitution of the hydrophobic leucine with the polar serine, the possibility of hydrogen bonding is introduced, possibly affecting ligand binding directly. This variant also exhibited the biggest improvement in terms of the response curve and LOD (**Figure 17**).

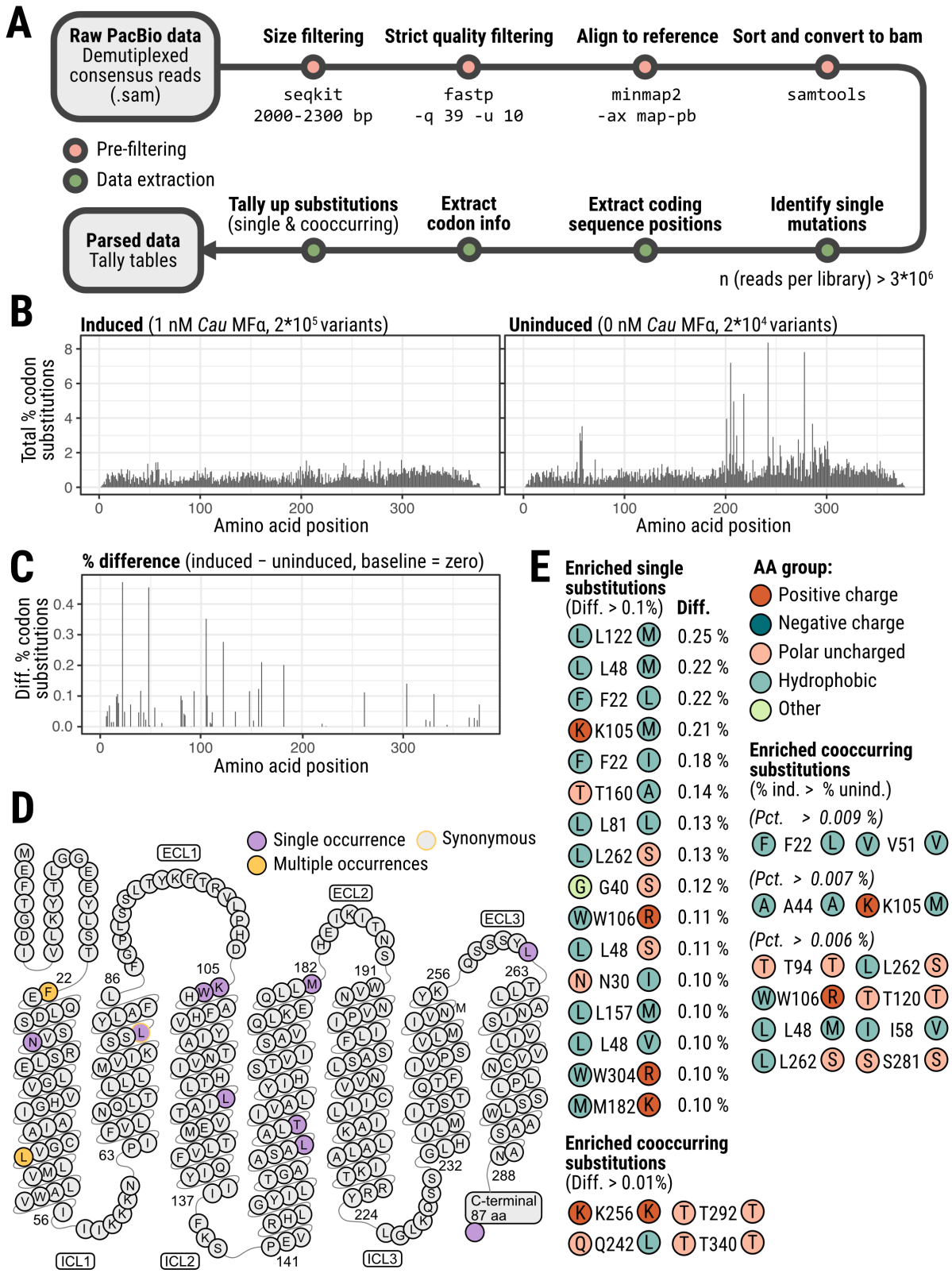

Figure 18. **PacBio sequencing data processing and results**. (A) Processing of reads prior to analysis, including filtering by read quality and size, followed by alignment to the reference *CauSTE2* sequence. Next, information on codon substitutions was extracted from the mutation data, and the counts of single and cooccurring amino acid substitutions tallied, followed by normalization by the total read count in

the respective library. (B) The mutational landscape across the coding sequence was investigated by summing up the percentages of codon substitutions at each position for the respective libraries and plotting these. (C) The difference in the total percentage of codon substitutions between the induced and the uninduced library at each position (% induced - % uninduced, baseline set to zero). The following analysis included enriched positions only (% difference > 0). (D) Positions identified by investigation of enrichment of specific codon substitutions, setting a cutoff at % difference > 0.1 %, marked in color in the *Cau*Ste2 snakeplot. (E) Following up on this analysis, the resulting amino acid substitutions (synonymous and non-synonymous) identified as enriched in the induced *Cau*Ste2 library variants are presented. These include single substitutions enriched in over 0.1 % of all reads, cooccurring substitutions enriched in 0.01 % of all reads, and the top enriched cooccurring substitutions for which at least one of the substitutions is part of the enriched single substitutions. Diff., difference; ECL, extracellular loop; ICL, intracellular loop.

Lastly, the distribution of substitutions resulting in higher sensitivity in *Cau*Ste2 without affecting the baseline activity was investigated. To this end, growth-based selection was applied to isolate L4P0 sub-libraries active in the absence or presence of 1 nM *Cau* α mating respectively (**Figure 15**), followed by extraction and barcoding of the "induced" and "uninduced" sub-libraries. Note here that these libraries differed in size, with the CFU count of the uninduced library being ~20,000 and that of the induced library ~200,000. Next, PacBio sequencing was applied, allowing for sequencing of long-reads with high-throughput, and consequently for the analysis of both single and co-occurring substitutions in reads. This is in contrast with short-read high-throughput sequencing methods such as Illumina, which solely allows for identification of hotspots for single mutations. Tallies of single and cooccurring codon substitutions were extracted after data preprocessing (**Figure 18A**). The substitution profiles across the receptor for the respective libraries was gauged by plotting the total substitution percentage per position (**Figure 18B**), revealing similarities across the baseline of the two libraries. Whether this is due to bias in mutagenesis from library generation, bias of errors from the PacBio sequencing, or due to similar rates of enrichments of these positions in the two libraries is unclear. In contrast to the similar baseline between the two samples, the uninduced library (containing false positive variants) presented enrichment of multiple positions that were not enriched in the induced library (containing all positives). This indicates that the substitution profile of variants exhibiting constitutive activity is distinct, while that of variants with improved sensitivity is varied.

To identify positions enriched in the induced library relative to the uninduced library, the difference in total codon substitutions at each position was investigated (**Figure 18C**), revealing several candidate positions. From these, the enrichment of specific codon substitutions was investigated, and the resulting amino acid substitutions of top candidates (% difference > 0.1) further examined (**Figure 18D-E**). Among these, the already identified and experimentally verified substitution L262S was present in addition to the previously identified substitution L48M, validating the applicability of this screening method. Several substitution hotspots were indicated by the presence of more than one substitution, including TM1, the extracellular region of TM3, and the transmembrane region of TM4. While substitutions in TM1 likely affect the *Cau*Ste2 dimer formation, it is possible that the substitutions found in

TM3 and TM4 either affect the receptor structure or ligand interaction directly, given that the orthosteric site differs from that of heterologous GPCR *Sc*Ste2. Lastly, the enrichment of cooccurring substitutions was investigated. Initially, the same approach as applied for the identification of single enriched substitutions was utilized to investigate the enrichment of any specific substitution pair in the induced library as compared to the control (**Figure 18E**). However, as this yielded limited results, substitutions cooccurring together with the previously identified enriched single substitutions were investigated as well (**Figure 18E**). Here, substitution L262S was present twice, with two different synonymous substitutions. Notably, substitution I58V, which was previously found in variant receptor L4P0_51, was found to cooccur with F22L, one of the top enriched substitutions in the enriched library. Interestingly, several synonymous substitutions cooccurred with the already identified single substitutions, and the previously identified single substitutions did not appear together among the top candidates. It is however possible that these did in fact cooccur, but at a percentage below the applied cut-off threshold, or that these were more frequent in the uninduced as compared to the induced library. The multiple synonymous substitutions may indicate that the receptor sequence might not be optimal for expression in *S. cerevisiae*, although the sequence has been codon optimized for this purpose (1). As such, it is also possible that this is an artifact of the strict filtering applied, in which case further analysis of the cooccurring mutations is required. An interesting approach could be analysis of reads based on the mutational load, as investigating these separately may elucidate the phylogeny of mutations contributing towards increased sensitivity and constitutive activation.

What we have learned

With this, we have isolated and evaluated a total of nine *Cau*Ste2 variants that exhibited improved response metrics to the cognate ligand in **Paper II**. We find that the majority of substitutions are located in parts of the receptor likely to affect dimer formation and Gpa1 interaction. As the receptor is expressed in a heterologous host, it is likely that differences in the lipid composition of the yeast cell membrane affect the receptor structure (155). Moreover, while we showed that the replacement of the Gpa1 C-terminus with that of *C. auris* Gpa1 may aid in G-protein coupling for the fungal GPCR, the interaction may not be the same as in the native host of *Cau*Ste2. As such, the majority of observed substitutions in related areas of the receptor may simply improve the receptor function in the heterologous host. We also identified one substitution likely to directly impact the interaction with the α mating factor of *C. auris*. This remains to be further explored through site saturation mutagenesis or similar strategies. Moreover, we demonstrated the applicability of long-read high-throughput sequencing towards identification of both single and cooccurring mutations contributing towards increased receptor sensitivity. Simultaneous sequencing of sub-libraries containing false-positive and all positive variants, respectively, enabled identification of substitutions conferring increased sensitivity without baseline expression, with identified variants aligning with those previously identified in experimental screenings. To summarize, these findings contribute towards the understanding of the importance of specific residues of *Cau*Ste2 on the function of the receptor when expressed in the heterologous host *S. cerevisiae.* Additional investigation could allow for

further improvement of the response upon activation, with potential applications in biosensor development. While previous work towards development of YBBs for detection of fungal pathogens have focused on optimization of the signaling pathway, we demonstrate the applicability of receptor engineering to improve the sensitivity and response curve dynamics.

Evaluation of a designed *Saccharomyces cerevisiae* Ste2 mutant library

*Sc*Ste2 is the most extensively studied class D GPCR, largely as a result of this yeast being commonly applied as a model organism for basic eukaryotic biology (156–158). Moreover, the structure of the receptor in its active homodimer state, bound to both its ligand and Gpa1, has been determined (140,142). Extensive mutagenic studies have been applied to Ste2, uncovering mutations resulting in altered function and ligand specificity (144,159–165). In total, 29 out of the 31 amino acids interacting with the *Sc* mating peptide α have been substituted, with substitutions in 23 of these positions resulting in major effects on receptor signaling, including loss of function, constitutive activity, altered ligand specificity, and altered ligand sensitivity (Paper III, Figure S1)(118). However, no study has simultaneously targeted the majority of the orthosteric site of the receptor for mutagenesis.

Here, we generated a designed library with substitutions in 22 ligand-binding and two non-ligand binding positions (**Figure 19**). Additionally, one of the targeted positions was highly conserved (>65 %) within Ste2 the fungal kingdom (118). By screening the library in the absence and presence of the *Sc* α mating factor and isolating functional, non-functional, and constitutively active variants, we hoped to gain further insight into the plasticity of the orthosteric site of this class D1 GPCR.

In the library (ARlib), the fraction of the WT residue in each position was set to 0.8, resulting in 0.37 % of library variants being predicted as the WT receptor. For the remaining substitution fraction of 0.2 in each position, 2-7 possible substitutions were selected to limit the total magnitude of possible library variants (**Figure 19**). The relative abundance of substitutions was based in part on the abundance of amino acids in each position in known Ste2 sequences across the fungal kingdom (118) and in part to include amino acids from different amino acid groups to introduce variability (Paper III, Supplementary file 2).

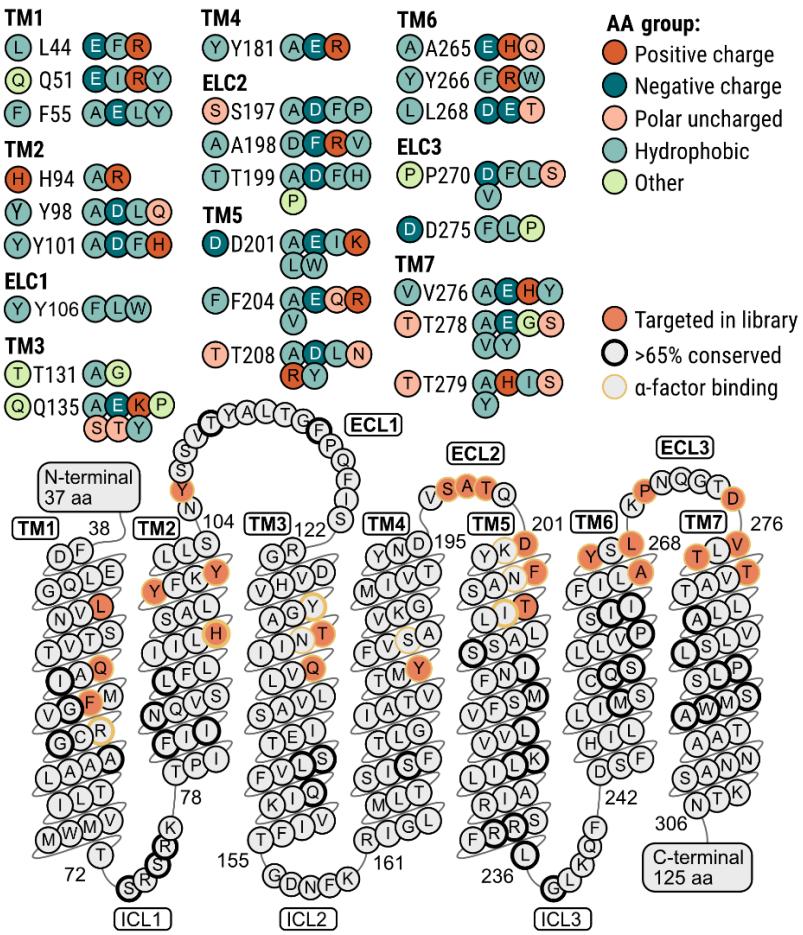

Figure 19. Library design overview for ARlib. The snakeplot displays the *Sc*Ste2 structure (118) and amino acid positions targeted in the library design in addition to the possible substitutions for each targeted position, as well as the amino acid group. Amino acids interacting with the α mating factor, highly conserved amino acid positions within class D1 GPCRs, and the location of positions targeted in the library are marked in the snakeplot. AA, amino acid; TM1-7, transmembrane helix 1-7; ICL1-3, intracellular loop 1-3; ECL1-3, extracellular loop 1-3; aa, amino acid.

The library was screened by FACS in the presence and absence of 1 μM *Sc* α mating factor, isolating cells with high GFP fluoresce intensity from both an uninduced (NA_p) and induced (Sc_p) culture, in addition to cells with the top 5% GFP fluoresce intensity in the induced population (Sc_t5p) and cells without fluorescence in the induced population (Sc_n; **Figure 15**). In total, 96 cells were sorted from each sub-library (NA_p, Sc_p, Sc_t5p, and Sc_n), from here on out referred to as individual libraries. After regrowth, a total of 190 variants were sequenced by Sanger sequencing (**Table 1**). However, due to the colony recovery after sorting being lower for library Sc_n, this library included fewer variants. The final number of variants analyzed from each library was further reduced in initial filtering of reads based on sequence quality (**Table 1**).

Table 1. Overview of sequenced reads and average amino acid substitutions. The number of amino acid substitutions per read (not including silent mutations) was evaluated, and the average per sub-library summarized in the table.

Library	Sequenced reads	Reads after trimming	Average substitutions/read
NA_p	59	51	4.9 ± 1.4
Sc_n	33	26	3.4 ± 1.4
Sc_p	50	41	4.4 ± 2.3
Sc_t5p	48	39	4.1 ± 1.7

Upon initial sequence analysis, we realized one mistake in library design, being that while the fraction of the WT amino acid in each position was indeed 0.8, the original codon in the DNA was in some cases substituted for a different codon encoding the same amino acid (silent mutation). As this could interfere with data analysis owing to the high mutational load when including these, we opted to instead compare sequences in terms of amino acid substitutions. Moreover, as all codon substitutions were made in regard to expression in *S. cerevisiae,* it is unlikely the silent mutations would have a major effect on expression levels of the receptor in the presently evaluated conditions of uninduced versus strongly induced. Even so, the average amino acid substitutions per read ranged between 3.4-4.9 (**Table 1**) with the majority of reads containing over two substitutions (Paper III, Figure S2).

Investigating reads with 1-2 substitutions in terms of their relative occurrence and enrichment in the respective isolated libraries, six substitutions and their hypothesized effect were identified (**Figure 20A**). One of these substitutions, A265E, hypothesized to cause constitutive activity when co-occurring with mutation Y106F, was further identified as significantly enriched in library NA_p in the subsequent enrichment analysis ($p<0.0001$, Fishers exact test; FDR<0.0001; **Figure 20B**). However, as the enrichment analysis does not take into consideration the co-occurring substitutions in reads, it is uncertain whether substitution A265E alone has this effect or solely in combination with other substitutions. For the remaining libraries, no significant enrichment or depletion was found after multiple testing correction (**Figure 20C-E**).

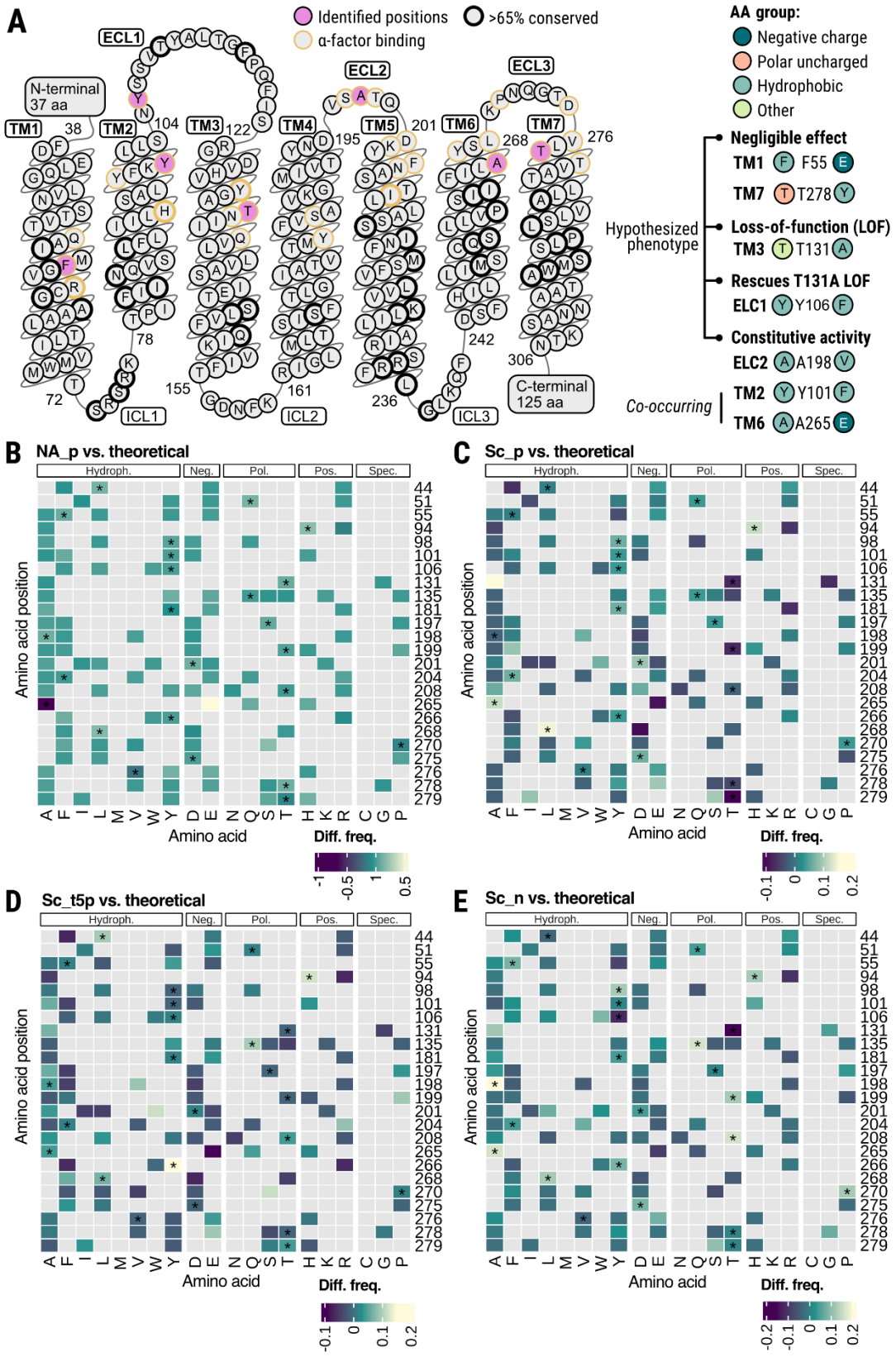

Figure 20. Identified *Sc*Ste2 substitutions and enrichment analysis. (A) Locations, amino acid group substitutions, and hypothesized phenotypes of identified substitutions from the evaluation of reads with 1-2 substitutions. AA, amino acid; TM1-7, transmembrane helix 1-7; ICL1-3, intracellular loop 1-3;

ECL1-3, extracellular loop 1-3; aa, amino acid. The heatmaps display the difference between the calculated frequency (Diff. freq.) of specific substitutions in the (B) NA_p, (C) Sc_p, (D) Sc_t5p, and (E) Sc_n libraries respectively, compared to the theoretical frequency of specific substitutions in the designed library. Amino acids are grouped by type, including hydrophobic (Hydroph.), negatively charged (Neg.), polar uncharged (Pol.), positively charged (Pos.), negatively charged (Neg.), and grey boxes signify amino acid substitutions not included in the designed library. Stars signify the wild-type amino acid in each position.

Upon investigation of whether the side chain exchange of substitutions resulted in new interactions within protein residues based on the AlphaFold2-predicted receptor structure (154), we found potential for altered interactions for all but substitution A198V (see paper II for details). Residue A265 has previously been identified as being important for receptor-ligand selectivity, conveying increased sensitivity towards the *Kluyveromyces lactis* α mating factor when substituted by the polar uncharged amino acid threonine (166). Located in the extracellular region of TM6, the WT alanine residue is known to directly interact with mating factor α (118). Substitution A265E replaces a small hydrophobic residue with a negatively charged and large one, introducing the possibility of hydrogen and ionic bond formation, with the possibility of stabilizing the receptor. Our results further establish residue A265 as important for receptor structure and function. Several other residues were found to be enriched prior to, but not after, multiple testing correction. Substitution Y106F was found to co-occur with A265E in several variants isolated with constitutive activity, present on the opposite side of the binding pocket. However, whether this has an impact on the receptor structure in the absence of the α mating factor is unclear as the structural difference between sidechains of phenylalanine and tyrosine is minor. Substitution Y106F was also found to co-occur with loss-of-function substitution T131A, resulting in two hydrogen bonds with V127 and Y128 in the *Sc*Ste2 receptor being abolished, possibly explaining the phenotype through resulting structural alterations. Here, Y106F appeared to rescue the receptor function, while the mechanism for this is unclear. Instead investigating residue substitutions without apparent effect on receptor signaling, F55E and T278Y (and TM7), these were somewhat surprising due to the change in side chain group. F55 is located in TM1 and is known to contribute towards α mating factor binding via Van der Waals interactions. Based on the ligand-bound model (118), introduction of a glutamic acid in place of a phenylalanine will remove this interaction, but introduce a hydrogen bond with residues R58 and S95. Substitution T278Y resulted in replacement of a small polar residue with a large hydrophobic one, but due to the side chain being located at the surface of the protein and being oriented outwards when bound to the α mating factor, it likely limits the effect on signaling. While these substitutions have limited effect on receptor activation, they contribute insight into the structural plasticity of *Sc*Ste2. Lastly, the substitution A198V was also found as a single mutation in a constitutively active variant. However, as the change in the side chain is small and is placed on the protein surface facing outwards, this substitution is likely to have little effect on the receptor structure. As such, this indicates the need for further experimental validation of the phenotype produced by the isolated variants.

What we have learned

In **Paper III**, we generated and screened mutant variant libraries of the class D1 GPCR *Sc*Ste2 towards uncovering substitutions in the orthosteric site of the receptor resulting in constitutive activity, loss-of-function, or improved receptor sensitivity. We identified substitutions associated with the respective phenotypes via enrichment analysis and investigation of variants with low substitution numbers. Moreover, the potential effect of substitutions on the protein structure was investigated based on the active structure of *Sc*Ste2. While the presented results require further experimental validation, they contribute towards elucidation of the plasticity and structure-function relationship of residues in this class D1 GPCR.

A limitation in the analysis performed is the number of samples sequenced from each, considering the probability of occurrence of residues in the theoretical library, which was especially the case for the smaller library of inactive variants. For some substitutions, this meant that only one or fewer occurrences were theoretically expected, as such not allowing for analysis of depletion, and only allowing for detection of substantial enrichment. Including 100 samples in each group would have increased the minimum theoretical frequency to two, with the same issue remaining. Here, enrichment prior to screening may have assisted in the amplification of substitutions of interest. However, it would also have made direct comparison with the frequency of substitutions in the theoretical library difficult, as the enriched library would technically be a separate library. Again, the risk of enriching false positives may have skewed the results as well, which is why we decided to follow the presented approach.

Evaluation and engineering of a YBB platform for free fatty acid 2 receptor (FFA2R)

Lastly, we attempted improvement of a yeast biosensor based on the platform design, namely for the human free fatty acid 2 receptor (FFA2R, also known as FFAR2, FFA2, GPR43), towards applications in ligand screening in **Paper IV**. FFA2R is expressed in cells of the adipose tissue, pancreatic β-cells, endocrine cells, and in several immune cell types, activating specific transcriptional responses in the presence of short-chain fatty acids (SCFAs) such as acetate, propionate, and butyrate (**Figure 21**A)(167–170). However, much is still unknown regarding the complex signaling mechanisms of this receptor, with this being an active field of study (171,172). As such, we started this project as a collaboration with the Dahlgren group at Gothenburg University, a group focusing on the investigation of the activity of this receptor in neutrophils. While the initial project aim was application of the yeast sensor for screening of fractionated ligand libraries towards identification of allosteric modulators, i.e. ligands binding outside the orthosteric site and affecting the activation response, it was limited to yeast sensor strain improvement due to time constraints.

The first mating pathway-based sensor in yeast for FFA2R was developed in the early 2000s, utilizing chimeric Gpa1-Gα substitutions for improved coupling between the human GPCR and the yeast mating pathway (40). Since then, this yeast-based sensor has been applied towards screening of ligands of FFA2R and their mode of action, including ligands binding the orthosteric or allosteric sites of the receptor, with either agonistic (activating) or antagonistic (inactivating) activity (40,115). The outputs of these sensor systems allowed detection by colorimetry (β-galactosidase) or growth (uracil or histidine auxotroph), determined after 24 h incubation (40,115). Moreover, the yeast platform strain applied utilized a minimally engineered yeast mating pathway, in which *GPA1*, *FAR1*, *SST2,* and *STE2* were deleted and the output genes were expressed from the mating pathway responsive promoter *FUS1p* (112). However, expression levels of genes were not tuned, while the GPCRs were often overexpressed from a plasmid or the genome. As such, we set out to investigate if the sensitivity and response intensity of a FFA2R platform strain could be improved by applying a minimized and tuned mating pathway in yeast (**Figure 21B**)(83).

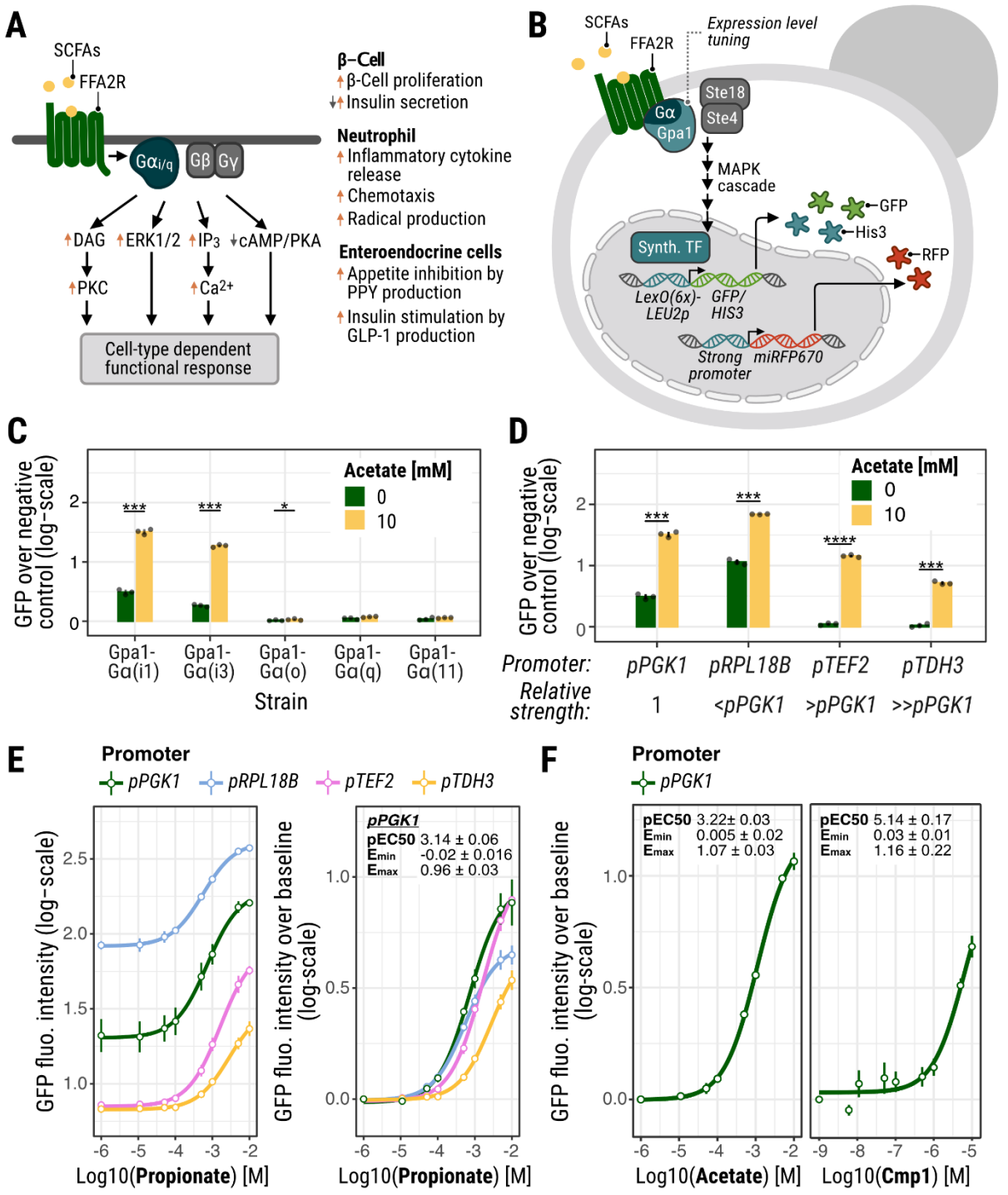

Figure 21. Overview of isolated variants from library L4N0. (A) General overview of the Gα and Gβγ-mediated signaling in human cell types (170,173) (B) Minimized mating overview with chimeric Gpa1 coupled to the heterologous GPCR FFA2R, in which expression levels of key components (shown in blue/green) have been tuned. The expression level of the chimeric Gpa1 was further tuned. (C) Bar plot displaying the mean GFP fluorescence intensity over baseline for different Gpa1-Gα chimeras, evaluated by flow-cytometry. Dots display the data from replicates (n=3) and vertical lines the s.d. (D) Bar plot displaying the mean GFP fluorescence intensity over baseline for different promoters applied

for expression of Gpa1-Gα_{i1}, evaluated by flow-cytometry. Dots display the data from replicates (n=3) and vertical lines the s.d. (E) Response curve of strains with different promoters for Gpa1-Gα_{i1} expression, induced by propionate as determined by flow-cytometry, either shown as unadjusted fold-change mean log10 GFP fluorescence (fluo.) intensity or fold-change mean log10 GFP fluorescence intensity over baseline. Curve parameters are shown for strain with promoter *pPGK1*. (D) Response curve of strain with promoter *pPGK1* when induced with acetate and synthetic ligand Cmp1 as determined by flow-cytometry. Data is presented as fold-change mean log10 GFP fluorescence intensity over baseline. All response curves were estimated via fitting of a three-parameter sigmoid curve, with the slope fixed (Hill slope =1), to the data. Dots display the mean and vertical lines the s.d. of three biological replicates. All response evaluations were carried out in media of pH 6.8. E_{min}, the effect at baseline; E_{max} the maximal effect; pEC50, -log10(concentration at 50 % of the maximal effect). *p<0.05, **p<0.01, ***p<0.001, ****p<0.0001, one-sided unpaired t-test.

In humans, FFA2R couples to more than one of the twelve Gα subunits, including Gα_{i1}, Gα_{i3}, and Gα_o of the G$\alpha_{i/o}$ subunit family and Gα_q and Gα_{11} of the G$\alpha_{q/11}$ subunit family. In yeast, functional coupling of FFA2R to chimeric Gpa1-Gα_{i1} and Gpa1-Gα_{i3} has been demonstrated, but not for the remaining groups. To identify the best chimeric Gpa1-Gα candidate in our platform, we implemented Gpa1-G$\alpha_{i1/i3/o/q/11}$ together with FFA2R in the engineered platform strain previously applied for library evaluation. Activation was found in strains with Gpa1-G$\alpha_{i1/i3}$, but not Gpa1-G$\alpha_{q/11}$ (**Figure 21C**). Moreover, there was very slight, but significant, activation in Gpa1-Gα_o. Additionally, a significant baseline expression was found for strains with Gpa1-G$\alpha_{q/11}$ compared to a negative control strain with Gpa1.

As Gpa1-Gα_{i1} produced the highest intensity response, we proceeded with this chimeric subunit for expression level tuning, applicable for tuning of the baseline expression of the output, to evaluate if the response intensity could be increased and the baseline expression adjusted (83). Three alternative promoters were applied, of which one weaker and two stronger relative to the initially applied *pPGK1* (**Figure 21D-E**)(128). We found that the baseline expression could indeed be diminished with promoter *pTEF2* and *pTDH3*, at the cost of sensitivity. If a slightly weaker promoter than *pTEF2* had been evaluated, it is possible that we could have achieved a strain without baseline expression and without loss of sensitivity. The weaker promoter, *pRPL18B,* demonstrated the saturation point of pathway activation. Even with the reduced Gpa1-Gα_{i1} mediated inhibition of pathway signaling, the increase in E_{max} was not proportional to the increase in baseline expression, resulting in a decreased dynamic range. As such, we chose to proceed with the originally applied promoter *pPGK1* for Gpa1-Gα_{i1} expression, as a baseline expression also allows for evaluation of antagonistic activity. Interestingly, we found the pEC50 of propionate induction of our strain to be slightly lower compared to than that of the previous FFA2R yeast strain, which utilized a growth-based output (115). While the reason for this remains unclear, it is possible that the high metabolic burden caused by constitutive RFP expression in our platform strain contributes to this result. Moreover, while induction assays in human cell lines are time consuming, the pEC50s reported for acetate and propionate induction in stable human cell lines with both G$\alpha_{i/o}$ and G$\alpha_{q/11}$

subunit families are higher ($pEC50_{Ac}$ = 3.94-4.43 and $pEC50_{Pr}$ = 3.99-4.66, depending on the assay) (174).

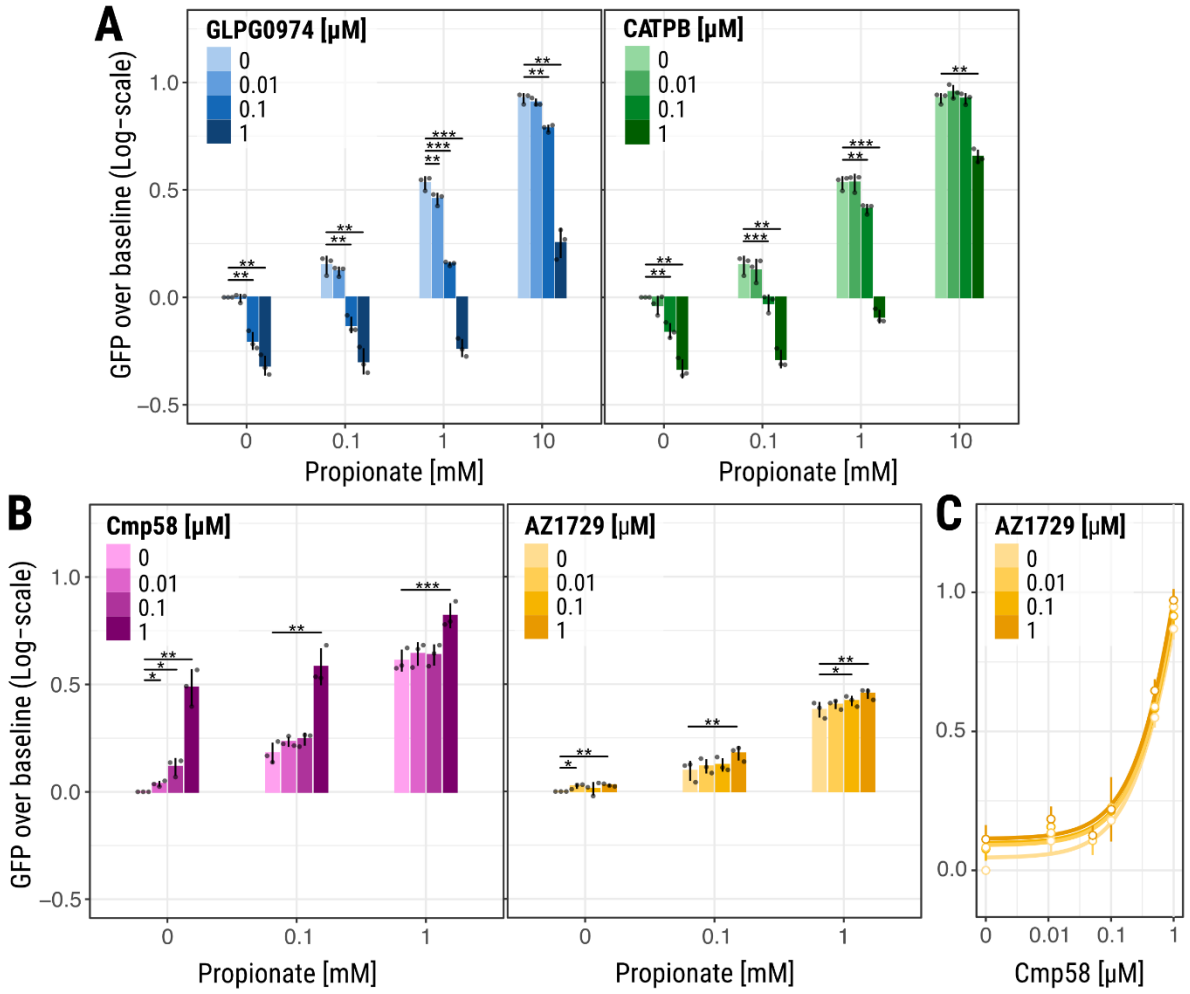

Figure 22. Evaluation of effect synthetic ligands applied alongside propionate. Bar plot displaying the mean GFP fluorescence intensity over baseline, evaluated by flow-cytometry. Dots display the data from replicates (n=3) and vertical lines the s.d. (A) The signal repression by synthetic orthosteric antagonists GLPG0974 and CATPB were evaluated when incubated with orthosteric agonist propionate. (B) The signal amplification by synthetic allosteric agonists Cmp58 and AZ1729 when incubated together with orthosteric agonis propionate. (C) The signal amplification by allosteric agonist AZ1728 when added together with allosteric agonist Cmp58. *p<0.05, **p<0.01, ***p<0.001, one-sided paired t-test.

Multiple synthetic ligands - including Cmp1 (orthosteric agonist), GLPG0974 (orthosteric antagonist), CATPB (orthosteric antagonist), Cmp58 (allosteric positive modulator), and AZ1729 (allosteric positive modulator) - were evaluated in the yeast platform based on their recent application in human neutrophil research (171,172,175–177). These ligands were all developed for potential therapeutic applications targeting FFA2R originally (178–182), in some cases with Gα subunit bias in signaling (182), and have not been previously evaluated in yeast. We found that, in accordance with the literature, Cmp1 produces a higher pEC50 compared to

acetate and propionate and has a lower LOD compared to acetate and propionate (**Figure 21**). Next, the synthetic antagonists GLPG0974 and CATPB were evaluated alongside propionate (**Figure 22A**), with both producing significant inhibition at concentrations from 0.1 μM and higher. Interestingly, both compounds repressed the baseline activation also in the absence of propionate, indicating these compounds as inverse agonists able to affect the receptor structure. While this has been suggested in the literature, the mode of signal repression of these ligands is currently unclear (167,183,184). This finding also aligns with recent findings in human neutrophils, where both GLPG0974 and CATPB were shown to inhibit transactivation of FFA2R by other receptors in addition to inhibiting the allosteric activity by Cmp58 and AZ1729, respectively (Lind et al. 2023). Interestingly, GLPG0974 has also been indicated as a positive modulator for co-activation by allosteric modulators AZ1729 and Cmp58 in these cells (Lind et al. 2022).

Lastly, allosteric modulators AZ1729 and Cmp58 were evaluated alongside propionate (**Figure 22B**), with both adding to the activation produced by the orthosteric ligand. Interestingly, both compounds produced activation also in the absence of propionate, indicating these functioning as allosteric agonists and not just modulators. However, the activation by AZ1729 was comparatively weak in relation to that of Cmp58 and propionate respectively, while in line with the response recorded in certain human cell lines (182). Moreover, the cooperative activation of Cmp58 and AZ1729 was evaluated, as these compounds have been shown to produce an amplifying effect in human neutrophils when added together (175,176). While the activation by both compounds was found to be additive (**Figure 22C**), the observed activation did not extend past that of the activation by the individual compounds combined. While this is in contrast with the reported cooperative activation in human neutrophils, the mechanisms of this activation are still unclear (175,176). As such, the absence of such an effect in the yeast may indicate that this effect occurs via an $G\alpha_{i1}$-independent signaling route (175,176).

What we have learned

In **Paper IV**, a platform strain for evaluation of ligands of the human FFA2R receptor was constructed in a minimal mating pathway platform already optimized for high sensitivity and a potent activation upon induction. We learned that in this platform, chimeric Gpa1-$G\alpha_{i1}$ and Gpa1-$G\alpha_{q}$ exhibited a significant but slight expression over a Gpa1-negative strain, indicating some interaction between the receptor and these chimeric Gpa1-Gα subunits not previously demonstrated in yeast. Upon further optimization of signaling in the strains with Gpa1-$G\alpha_{i1}$, by tuning of the Gα expression levels, we learned that the expression levels of the already applied *pPGK1* promoter allowed for expression with a full dynamic and operational range, with a higher baseline expression allowing for evaluation of antagonists. Instead applying the stronger promoter *pTEF2* removed the baseline expression, with minimal effects on dynamic and operational range. For screenings using induction of colorimetric outputs, this strain may be applicable as an alternative. We did however not succeed in engineering the sensitivity of the sensor strain by simple pathway engineering. Here, alternative strategies could be applied, such as further engineering of the pathway response by introduction positive feedback loops or

the use of yeast co-cultures to enable detection at lower concentrations (83,136). However, the sensor platform did demonstrate a decreased time-of-detection compared to previously applied platforms.

In terms of applicability for screening of allosteric modulators, it appears these may act somewhat differently in yeast as compared to in human cell lines, even when considering readouts in human cells that should be specific to Gα and Gβγ-mediated signaling. While this limits the applicability towards description of the effects, the demonstrated response induced in the strain by allosteric modulators and antagonists respectively does show that candidates can be identified via the yeast system. Moreover, the absence of the expected activation via $G\alpha_{i1}$ in yeast may also contribute towards the understanding of signaling mechanisms, indicating that the observed phenotype in human cells may be due to alternative signaling pathways (175,176).

Chapter 3: Final conclusions

GPCR-based YBBs constitute valuable platforms that can aid our understanding of GPCR-mediated diseases, GPCR structure, and GPCR-ligand interactions (40,118,166). Moreover, they have shown potential towards applications as low-cost sensors in point-of-use industrial and biomedical settings (39,91,136). As such, the work presented in this thesis was carried out with the overarching goal of further developing GPCR-based YBBs towards biomedical applications, focusing on three essential parts of yeast biosensor design, i.e. outputs, sensing element, and signaling pathway.

For the output, we investigated the violacein pathway side products prodeoxyviolacein and proviolacein for applications in screening on agar plates, in liquid media, and on paper slips in **Paper I**. Benchmarking these outputs against the already established lycopene (39), we found that while the pigments performed equally well on agar plates, lycopene outperformed prodeoxyviolacein and proviolacein in the other settings. Moreover, different media complexities were evaluated on agar plates which resulted in different levels of baseline expression in the absence of the inducer, demonstrating the importance of pathway optimization towards the specific media used in the target application setting.

Next, we focused towards expanding the current understanding of fungal mating GPCR structure and function upon expression in yeast, by constructing and screening mutant libraries of Ste2 from fungal pathogen *C. auris* in **Paper II** and from *S. cerevisiae* in **Paper III**. For *Cau*Ste2, an untargeted library was generated and screened towards increased sensitivity towards the cognate ligand, resulting in identification of ICL1 as a mutational hotspot likely affecting the interaction with the Gα and TM1 as a mutational hotspot likely affecting dimer formation. Moreover, a single substitution mutant, with L262S in ECL3, was found with improved LOD and response curve metrics, indicating this position as potentially important for ligand interaction, aligning with previous findings the heterologous *Sc*STE2 receptor (118). For *Sc*Ste2, a designed library targeting the majority of the orthosteric site residues was constructed, with substitutions selected based on the occurrence of these in heterologous Ste2 of the fungal kingdom. Mutant variants from this library were sorted into bins based on phenotype, followed by sequencing and sequence analysis. Based on the presence of mutations in single and dual substitution variants, we identified substitutions conferring constitutive activity (A265E, A198V), potential loss-of-function (T131A), and neutral effects on signaling (F55E, T278Y). Investigating the enrichment of substitutions within subgroups, A265E was further found to be highly enriched in constitutively active variants. Taken together, these findings contribute towards a better understanding of the structure-function relationship and plasticity of fungal GPCRs.

Lastly, we attempted to engineer the mating pathway signaling towards increased sensitivity and improved response curve metrics for detection of FFA2R ligands in **Paper IV**. While we found limited improvements upon pathway tuning, we investigated the activation mechanisms of several ligands not previously evaluated in yeast. As such, we found that GLPG0974 and

CATPB act as inverse agonists rather than antagonists, and that the collaborative activation by allosteric modulators AZ1729 and Cmp58 is likely to occur via mechanisms separate from $G\alpha_{i1}$-mediated signaling.

In summary, this work contributed towards the development of GPCR-based YBBs for biomedical applications by systematically benchmarking colorimetric outputs, identifying key receptor regions in fungal mating GPCRs, and optimizing signaling for FFA2R-mediated ligand evaluation. Although challenges remain, these findings highlight both the potential and current limitations of GPCR-based YBBs, setting a clear direction for future research.

Chapter 4: Future perspectives

As research in synthetic biology and protein engineering continues to advance, the potential applications of GPCR-based YBBs are rapidly expanding beyond the laboratory. In this thesis, I have largely focused on development of YBBs towards potential applications outside a research environment. This chapter aims to explore this possibility further by highlighting key areas of innovation relevant to the future of YBBs and biosensors as a whole - from the engineering of custom GPCRs and ligands, to the development of biosensors suited for deployment in diverse environments, and finally to speculative future scenarios where the technological boundaries of today may no longer apply.

Designing GPCR-based YBBs viable for point-of-use applications

While YBBs are already applied in pharmaceutical and industrial research, both for screening of ligands binding GPCRs of interest (185) and for acceleration of production host screening (186), their application beyond a research environment is limited or even nonexistent. However, with the recent development of a proof-of-concept sensor for broad-range point-of-use detection of cannabinoids by Miettinen and colleagues (91), we are moving closer to such a scenario. The authors leverage the modularity of YBBs to develop a GPCR-based sensor strain, applicable with colorimetric output and luminescent output respectively. To enable quantitative readouts, concept designs were developed which utilized the camera of a phone for image-based analysis, with a readout within 30 minutes depending on the output. This may indeed be the future for GPCR-based YBB applications, offering advantages over traditionally applied antibody-based tests in terms of being quantitative and having increased sensitivity. Moreover, depending on the GPCR applied, these YBBs can be developed with varying levels of selectivity, from being highly selective towards a single molecule to being selective towards a group of similar molecules (91).

Another demonstration of a proof-of-concept GPCR-based YBB design includes that of Ostrov and colleagues towards detection of fungal pathogen *C. albicans* (39). Utilizing a lateral flow assay (LFA) design often applied for antibody tests, the authors demonstrated detection with colorimetric outputs within 3 h of incubation. In a later study by Fan and colleagues (136), the sensitivity of detection was drastically increased towards the detection in the picomolar range of mating peptides of *C. albicans* by engineering of mating pathway signaling. However, even in the case of infection the units of fungi present in human samples are low (39), and the concentrations of mating peptides expected in a sample are unknown. As such, enrichment by cultivation may be needed prior to evaluation, while the time of detection would still exceed those of traditionally applied methods in such as agar plate-based cultivations in theory (39). Here, one can imagine alternative designs that enable evaluation alongside the enrichment of pathogenic fungi present in these patient samples, such as hydrogel-encapsulated YBBs that change color if the target peptide is present. With hydrogels having been shown to provide an extensive shelf-life of yeast while enabling separation of the yeast from a liquid culture (187,188), these may indeed be applicable. However, the production cost may be increased and

scalability decreased, as 3D bioprinting would theoretically be required for even distribution of cells within the hydrogel and to create a large surface area.

Beyond the development of YBBs for detection of single target ligands, one could postulate whether the use of mixed consortia of YBB strains would be applicable to allow for distinction between separate targets of interest in one single test. Indeed, this could be theoretically possible utilizing strains with distinct GPCRs and colorimetric outputs, with the potential for application in large-scale screenings to decrease the number of distinct tests to be performed. However, the mixed yeast strains may result in a decreased intensity of readout as well as issues with interpretation in the case that multiple strains are activated at once.

Altogether, these examples highlight the potential of GPCR-based yeast biosensors for diverse detection scenarios – ranging from detection of distinct chemical compound groups and detection of pathogenic fungi to a possible future of multiplexed screening in a single tube. Moreover, they also underscore the challenges of developing such tests towards large-scale applications, including consideration of the cost and ease of manufacturing, as well as the ease-of-use of tests. Addressing these factors in YBB design requires thoughtful engineering of the biosensor strains towards applications in tests that allow for specific, sensitive, and robust detection. With continued innovation, GPCR-based YBBs could ultimately transition from their use in research to widely adopted tools, bridging the gap between research and real-life applications.

Towards custom proteins for sensing applications

In GPCR-based YBBs, the GPCR itself constitutes the core detection unit. With GCPRs being able to detect diverse ligands – including photons, ions, lipids, hormones, peptides, and odorants (113) – these receptors show potential for sensing if we can engineer them accordingly. However, at present the availability of GPCRs able to detect a target of interest imposes a limitation of the possible application areas of GPCR-based YBBs. While research into the altering the ligand specificity of GPCRs has been conducted (166,189), we still lack a wider understanding of how to engineer GPCRs towards detection of novel targets. This may however be enabled soon, though the application of AI to elucidate the structure-function relationship of GPCRs and their ligand interactions (154,190–194).

We are presently amidst the boom of AI technology, applied towards diverse applications in our everyday lives in addition to applications to accelerate research. Deep learning models have already been trained towards deciphering and prediction of protein structures (154,194), prediction of protein-ligand interactions (195), design of synthetic proteins able to carry out novel functions (23,25), and prediction of proteins with a conserved function but altered properties (196). As such, the emergence of AI has already rapidly accelerated diverse areas of protein structure research, shifting the focus from “can we model this protein structure” to “how do we model protein ligand interactions” (197).

Despite this success in protein structure prediction, challenges still remain. The availability of structural data is key to model training, and for GPCRs fewer than 500 GPCR-ligand complexes were available as of 2024, in which several classes of GPCRs have little or no coverage (198). Here, the availability of data is largely limited by experimental constraints, as GPCRs are one of most challenging protein families in regards to structure determination, often requiring overexpression in a heterologous host in addition to protein engineering for increased structure stability (199). Even so, it has been shown that the application of AlphaFold allowed for modelling of GPCR-ligand interactions with reasonable accuracy (200). In cases where these predictions fail, model refinement such as via physics-based tools has been demonstrated to result in accuracy comparable to an experimental structure (201).

Beyond structure prediction lies the possibility of leveraging machine learning for the custom design of GPCRs that respond to user-designated ligands. Classic examples include receptors activated solely by a synthetic ligand (RASSL) and designer receptors exclusively activated by designer drugs (DREADDs) (189). These are developed via iterative mutagenesis of residues in the binding pocket of GPCRs, followed by screening towards isolation of variants inert to natural stimuli while responsive to a synthetic drug (189). Similar methods have also been applied in fungal GPCRs, where the ligand specificity of *Sc*Ste2 was altered towards the ligand of *Kluyveromyces lactis* Ste2 (166). While these methods ultimately allow for reprogramming of receptor specificity, they are labor intensive, as each receptor-ligand pair is evolved individually (189). More importantly, this approach is also limited in programmability, with the chance of successfully implementing larger modifications in receptor structure being low.

As such, predictive modelling offers a new avenue of possibilities via the option of *in silico* protein design. In fact, such an approach was recently implemented by Di Renzo and colleagues for the prediction of structural changes in *Sc*Ste2 required to change the ligand specificity of the receptor from the α mating factor peptide to epinephrine (202). While these results were solely confirmed via simulations of molecular docking, and not *in vivo*, they demonstrate a future avenue for development of GPCR-based YBBs towards detection of an expanded array of ligands.

Beyond the engineering of the GPCR-ligand interaction, a recent breakthrough called programmable antigen-GPCR chimeras (PAGERs) by Kalogriopoulos and colleagues demonstrates the use of chimeric receptor designs to fuse antigen-sensing domains to a GPCR scaffold (203). Applying the antibody as a conditional inhibitory domain, blocking GPCR-ligand binding in the absence of the antigen, enabled detection of dozens of new ligands (large protein antigens) without engineering the GPCR binding pocket (203). With this, GPCR-based sensors can theoretically be designed towards detection of a vastly expanded range of ligands. Moreover, the authors demonstrated the use of SPARK (specific protein association tool giving transcriptional readout with rapid kinetics) to enable transcriptional activation simply based on the GPCR and β-arrestin interaction (separate Gαβγ-mediated signaling), towards a rapid transcriptional response (203). As such, it may be possible to develop GPCR-based YBBs independent of mating pathway signaling, in which the signal amplification produced by

transcription is retained, and even to utilize multiple GPCRs for sensing per strain with distinct transcriptional outputs.

Beyond GPCR-based sensing

While GPCR-based YBB sensing offers detection of versatile targets, many emerging biosensing technologies bypass living cells entirely, such as the engineering of proteins and enzymes to act as molecular switches. Utilizing *de novo* protein design and protein engineering, biosensor proteins designed to directly detect a target molecule and produce a measurable signal have been developed (24). An example of this is the utilization of *de novo* protein design to produce a "luciferase cage" (LucCage) containing split luciferase fragments (24). While remaining in an off-state in the absence of a target protein, the luciferase is activated upon binding of a target protein ligand, enabled by structural changes in the protein (24). These biosensors have been demonstrated to be applicable for detection of an array of medically relevant proteins with a high sensitivity (24), and have already been developed towards commercial use (204). Moreover, engineered enzyme switches, such as split-protein sensors, have been developed which allow detection of small molecules (24). Thus far this technology is limited in terms of the types of ligands detectable, but with the advances in AI-guided protein structure modelling it is possible that we will see diversification in this area (23,25). Note, however, that as opposed to cell-based systems relying on a transcriptional output, these systems lack signal amplification, which may limit sensitivity of detection.

For alternatives in point-of-care detection of DNA and RNA, CRISPR-based diagnostic tools based on Cas12a and Cas13a respectively have been developed, demonstrating high specificity and sensitivity (205). These technologies allow detection in samples containing few target molecules, triggering nondiscriminatory cleavage of reporter-tagged DNA/RNA in tests, resulting in a visual readout (205). Outputs such as fluorescence in liquid or colorimetric readouts on a lateral flow assay strip has been demonstrated, making these technologies applicable in both medical and point-of-care settings (205). Because Cas enzymes can be programmed to detect virtually any DNA or RNA sequence, the possible applications are extensive. These enzymes are, however, limited to the detection of DNA/RNA, indicating the presence of a target organism or virus, but cannot be applied for detection of byproducts of active metabolism.

Beyond these technologies, circuit-based tests utilizing biological components in a cell-free system have been developed towards detection of environmental contaminants by Jung and colleagues (206). Utilizing programmable components including RNA polymerases, transcription factors, and DNA templates, the detection of varying target molecules was enabled via transcription of a fluorescence-activating RNA aptamer (206). The authors demonstrated detection of tetracyclines, large and small molecules, and metal ions, showing the applicability of this method towards detection of different ligand targets, while it is limited by the availability of transcription factors.

While storage of these cell-free sensing systems can be sensitive to changes in temperature or require low temperatures for a prolonged shelf-life, efforts have been made towards improving the stability of these. For example, lyophilization followed by freeze-drying has been demonstrated to preserve the function of both cell-free circuits and CRISPR-based proteins (206,207).

In summary, biosensing technologies are rapidly reaching maturity towards deployment, improving our ability to detect and monitor disease and the environment. Allowing for applications towards detection of a wide range of ligands, the applicability of these sensors is wide. By moving surveillance from the lab to the field, we are entering a new era of diagnostic and environmental monitoring, hopefully enabling improved possibilities for early intervention in the event of disease outbreaks or environmental contamination.

Implications of early detection in the propagation of infectious disease

Growing and aging human populations, increasing population density, and increased accessibility of travel in the last decades has contributed towards the development and rapid spread of infectious disease (208–210). These largely include diseases caused by viral, fungal, parasitic, and bacterial infection, as well as disease caused by prions (infectious misfolded proteins) (209). While we have been able to treat and manage the spread of both bacterial, fungal, and parasitic infections to some degree, the current rise in resistance against antibiotic, antimycotic, and antiparasitic treatments is limiting our capacity for intervention (211,212). Of course, research is ongoing towards finding novel solutions for treatment and prevention (213,214), but this process is slow and we cannot be sure when – or if – we will find comparatively effective solutions.

In the meantime, it is paramount that we shift our focus towards limiting the spread and impact of infectious disease through other means. Here, early detection is crucial to enable early preventative interventions, such as preparation of healthcare facilities to limit spread and to enable effective treatment (210,215,216). By isolating outbreaks, we also decrease the need for treatment, which is likely to have beneficial effects beyond fewer people suffering from the disease. For example, in the case of antibiotic and antimycotic resistance, limiting the spread of infection will likely limit the continued selection for resistance in pathogenic bacteria and fungi (217), thus making these continuously applicable in the case of emergency.

For this to be possible, we need tests that enable effective screening and surveillance of the spread of infectious disease, even beyond medical facilities. While blanket lockdowns are indeed the most effective way of hindering the spread of disease for which we have no countermeasures, these have also been shown to result in grave effects on the economy and mental health of populations (218). In the case of a pandemic, the availability of at-home tests at an earlier stage than for the recent Sars-CoV-2 pandemic may have limited the need for such widespread lockdowns, allowing only those that were sick and those at risk to stay at home. In

a future dream scenario where we are able to rapidly develop biosensing devices for accurate detection, we might be able to do so by implementing widespread population screenings. Even so, there would be hurdles to overcome for widespread point-of-care application of tests, such as how to handle cost, distribution logistics, and false positives/negatives. Moreover, compliance with the implementation of such testing regimes remains another challenge, as not all members of a population may be willing to participate.

Ultimately, more than just scientific innovation will be needed to realize the full potential of widespread and rapid biosensing for early detection. It will demand robust policy frameworks, global collaboration, and effective public education to address the issues of cost, logistics, and application (217,219). While the challenges are significant, the potential rewards – including healthier communities, reduced healthcare burdens, and slower emergence of drug resistance – underscore why continued investment and research in this field is critical. Through continued efforts, we can move closer to a future in which we can apply rapid and targeted interventions to curb the spread of infectious diseases before they become crises.

A future of smart biomaterials

Currently, we are entering a time and age where the development of wearable materials with incorporated biosensing abilities has become a possibility (220). At present, this includes materials in which cell-free sensor systems have been incorporated in a matrix or scaffold, to generate functionalized textiles and substrates as demonstrated by Nguyen and colleagues (207). Utilizing lyophilized and freeze-dried biosensor systems, these are activated upon hydration and generate colorimetric or fluorescent outputs in response to viral or bacterial nucleic acid signatures (207). Suggested applications included in textiles and in face masks, allowing for rapid detection in real time with a high sensitivity without the need for incorporation of electronic devices (207).

Beyond the use of cell-free circuits incorporated in wearable material, there is potential for development of living materials, which are responsive to environmental stimuli (220). Examples include skin patches containing live organisms engineered towards biosensing or drug delivery, enabling active detection and treatment (220). Challenges remain in terms of material design, as it needs to allow organisms to retain metabolic function and allow for diffusion of relevant molecules, while confining the organisms within the material.

Perhaps, in a not too distance future, we could go even further to produce living materials with self-healing properties, allowing for extended wear and tear (221), in which these biosensing modalities are incorporated (222). In fact, leather-like materials produced by bacteria are already being developed, with potential for further functionalization (223). As synthetic biology continues to push the boundaries of material engineering, smart biomaterials may evolve from passive sensing platforms into dynamic, multifunctional systems - capable of environmental adaptation, therapeutic delivery, and even self-regeneration - ultimately blurring the line between biological and synthetic matter. In this scenario, future biomaterials would not simply mimic life-like properties, but could behave as hybrid living systems, combining the

programmability of synthetic constructs with the adaptability and complexity of living cells. Who knows, we might even engineer these to emit pleasant, tailored fragrances, such a flowery aroma or perhaps even the smell of freshly baked bread.

Acknowledgements

These last five years have been a journey, during which - as is the case for any journey - there have been moments of joy and moments of struggle, allowing me to grow into the person I am today. I think it is fantastic however, that even though I know there have been some really tough times, what I remember looking back is mostly moments of warmth, happiness, curiosity, and – most of all – a feeling of being lucky. Because amidst everything that is life, I have been blessed with wonderful, kind, and brilliant people in my surroundings, and for me this the greatest blessing I could get.

I especially want to thank my supervisors Verena and Florian for always supporting me, through ups and downs. I have always felt encouraged by both of you and have always come out of any meeting or discussion more excited than I was going in, with new perspectives and ideas to try out. I feel super lucky to have had both of you with me on this journey, and I am thankful for all the things you have taught me.

I also want to thank all the people that have helped me, taught me, or worked with me along the way. Raphael, Doris, Linnea, John, and Michi when I was just a baby in the lab a long time ago, Louis, Max, Dany, Sara, Ric, Xiang, Mauro, and Olof for discussions on FACS-based screenings (the eternal thorn in the side), library transformations, and other experimental setups. Thank you to my collaborators at SINTEF - Francesca, Son, Simone, and Ingvild - as well as my collaborators at GU – Jonas, Huamei, Martina, and Claes – for teaching me things beyond my field and about methods I did not know prior, I learned a lot from you. I also want to thank the research engineers – Emelie, Angelica, Yili, Pun, and Vijay – for keeping the ship running and for truly caring about environment we work in.

A special thanks to my long-term office mates – Ela, Simone, Xiang, Mauro, Ric, Marta, Xiaozhi, Ivan, and Junko - while we've had some rotation over the years it has always been such a good time and many fun discussions, as well as never-ending support and encouragement. Thanks for all the laughs and hugs over the years, I will forever remember this as the best office!

To all the other people I have had the pleasure of getting to know at SysBio (and IndBio) over this time, I want to say that you have made working so much more fun! I think it's amazing that a work environment can be so warm and welcoming, and I know that (as a Swede that was originally even more Swedish) I have really appreciated this – you are ALL amazing. Special callouts to Tom, Sophia, Kamesh, Simone, Louisa, Veronica(s), Doris, Mauro, Raphael, Dany, Philip, Xiang, Ric, Sara, Chaeho, Cecilia, Iván, Andrea, Fabio, Mauri, Xiaozhi, Oliver, Marta, Ela, Yuika, Max, Emil, Mirjam, Andres, Leon, Jorge, and Jerry (I'm for sure forgetting people) with whom I share many fond memories of dance, music, games, and adventures beyond work hours – I'm happy to have gotten to know you all during these years and I hope that we stay in touch!

Lastly, I want to thank my near and dear, who have been my biggest supporters over the past five years. My mom and dad who have always been there for me and have encouraged and challenged me in turn to help me grow. My grandma who always listened and offered encouraging words. My dearest friends and my brother – Sara, Madelene, and Johan – who made sure that I had fun even in the most intense of periods of PhD and life, and lastly Angelo for always supporting me, turning every frown into a smile. Thank you for all the cozy dinners, talks, game nights, party times, and adventures alike, I could not have done this without you! These have been some banger years with you all, and I feel truly blessed to have you in my life.

References

1. Cho IH, Peterson DG. Chemistry of bread aroma: A review. Food Sci Biotechnol. 2010 Jun;19(3):575–82.
2. Morquecho-Campos P, Bikker FJ, Nazmi K, de Graaf K, Laine ML, Boesveldt S. Impact of food odors signaling specific taste qualities and macronutrient content on saliva secretion and composition. Appetite. 2019 Dec 1;143:104399.
3. Koshland Jr. DE. The Seven Pillars of Life. Science. 2002;295:2215–6.
4. Buccitelli C, Selbach M. mRNAs, proteins and the emerging principles of gene expression control. Nat Rev Genet. 2020 Oct;21(10):630–44.
5. Briscoe J, Small S. Morphogen rules: design principles of gradient-mediated embryo patterning. Development. 2015 Dec 1;142(23):3996–4009.
6. Kravchenko P, Tachibana K. Rise and SINE: roles of transcription factors and retrotransposons in zygotic genome activation. Nat Rev Mol Cell Biol. 2024 Oct 2;1–12.
7. Nüsslein-Volhard C. Gradients that organize embryo development. Sci Am. 1996;275(2):54–61.
8. Lewontin RC. The units of selection. Annu Rev Ecol. 1970;1:1–18.
9. McBride CS. Genes and odors underlying the recent evolution of mosquito preference for humans. Curr Biol. 2016 Jan 11;26(1):R41–6.
10. Bar-Peled L, Kory N. Principles and functions of metabolic compartmentalization. Nat Metab. 2022 Oct;4(10):1232–44.
11. Perera RM, Zoncu R. The lysosome as a regulatory hub. Annu Rev Cell Dev Biol. 2016 Oct 6;32(1):223–53.
12. Ballabio A, Bonifacino JS. Lysosomes as dynamic regulators of cell and organismal homeostasis. Nat Rev Mol Cell Biol. 2020 Feb;21(2):101–18.
13. Savini M, Zhao Q, Wang MC. Lysosomes: Signaling hubs for metabolic sensing and longevity. Trends Cell Biol. 2019 Nov 1;29(11):876–87.
14. Otterstedt K, Larsson C, Bill RM, Ståhlberg A, Boles E, Hohmann S, et al. Switching the mode of metabolism in the yeast *Saccharomyces cerevisiae*. EMBO Reports. 2004 May;5(5):532–7.
15. Wang H, Guo M, Wei H, Chen Y. Targeting p53 pathways: mechanisms, structures and advances in therapy. Sig Transduct Target Ther. 2023 Mar 1;8(1):1–35.
16. Gustafsson ÅB, Gottlieb RA. Recycle or die: The role of autophagy in cardioprotection. JMCC. 2008 Apr 1;44(4):654–61.
17. Pearson AM. Muscle growth and exercise. Crit Rev Food Sci Nutr. 1990 Jan;29(3):167–96.
18. Pathak MA, Jimbow K, Szabo G, Fitzpatrick TB. Sunlight and melanin pigmentation. In: Smith KC, editor. Photochemical and Photobiological Reviews. Boston, MA: Springer US; 1976. p. 211–39.
19. Bardwell L. A walk-through of the yeast mating pheromone response pathway. Peptides. 2005 Feb;26(2):339–50.
20. Chard T. REVIEW: Pregnancy tests: a review. Hum Reprod. 1992 May 1;7(5):701–10.
21. Filchakova O, Dossym D, Ilyas A, Kuanysheva T, Abdizhamil A, Bukasov R. Review of COVID-19 testing and diagnostic methods. Talanta. 2022 Jul 1;244:123409.
22. Pfeiffer EF. The glucose sensor: the missing link in diabetes therapy. Horm Metab Res Suppl. 1990;24:154–64.
23. Watson JL, Juergens D, Bennett NR, Trippe BL, Yim J, Eisenach HE, et al. De novo design of protein structure and function with RFdiffusion. Nat. 2023 Aug;620(7976):1089–100.
24. Quijano-Rubio A, Yeh HW, Park J, Lee H, Langan RA, Boyken SE, et al. De novo design of modular and tunable protein biosensors. Nat. 2021 Mar;591(7850):482–7.

25. Johnson SR, Fu X, Viknander S, Goldin C, Monaco S, Zelezniak A, et al. Computational scoring and experimental evaluation of enzymes generated by neural networks. Nat Biotechnol. 2024 Apr 23;

26. Bian SQ, Wang ZK, Gong JS, Su C, Li H, Xu ZH, et al. Protein engineering of substrate specificity toward nitrilases: Strategies and challenges. J Agric Food Chem. 2025 Jan 22;73(3):1775–89.

27. Harteveld Z, Bonet J, Rosset S, Yang C, Sesterhenn F, Correia BE. A generic framework for hierarchical de novo protein design. PNAS. 2022 Oct 25;119(43):e2206111119.

28. Repecka D, Jauniskis V, Karpus L, Rembeza E, Rokaitis I, Zrimec J, et al. Expanding functional protein sequence spaces using generative adversarial networks. Nat Mach Intell. 2021 Apr;3(4):324–33.

29. Ferruz N, Heinzinger M, Akdel M, Goncearenco A, Naef L, Dallago C. From sequence to function through structure: Deep learning for protein design. CSBJ. 2023 Jan 1;21:238–50.

30. Benner SA, Sismour AM. Synthetic biology. Nat Rev Genet. 2005 Jul;6(7):533–43.

31. Hobom B. Gene surgery: on the threshold of synthetic biology. Med Klin. 1980 Nov 21;75(24):834–41.

32. Cohen SN, Chang ACY, Boyer HW, Helling RB. Construction of biologically functional bacterial plasmids in vitro. PNAS. 1973 Nov;70(11):3240–4.

33. Carlson R. The changing economics of DNA synthesis. Nat Biotechnol. 2009 Dec;27(12):1091–4.

34. Carlson RH. Biology is technology: The promise, peril, and new business of engineering life. Harvard University Press; 2010. 290 p.

35. Aljabali AAA, El-Tanani M, Tambuwala MM. Principles of CRISPR-Cas9 technology: Advancements in genome editing and emerging trends in drug delivery. J Drug Deliv Sci Technol. 2024 Feb 1;92:105338.

36. Berman HM, Gierasch LM. How the Protein Data Bank changed biology: An introduction to the JBC Reviews thematic series, part 1. J Biol Chem. 2021 Mar 27;296:100608.

37. Derat E, Kamerlin SCL. Computational Advances in Protein Engineering and Enzyme Design. J Phys Chem B. 2022 Apr 7;126(13):2449–51.

38. Ma T, Shi B, Ye Z, Li X, Liu M, Chen Y, et al. Lipid engineering combined with systematic metabolic engineering of *Saccharomyces cerevisiae* for high-yield production of lycopene. Metab Eng. 2019 Mar 1;52:134–42.

39. Ostrov N, Jimenez M, Billerbeck S, Brisbois J, Matragrano J, Ager A, et al. A modular yeast biosensor for low-cost point-of-care pathogen detection. Sci Adv. 2017 Jun 1;3(6):e1603221.

40. Brown AJ, Goldsworthy SM, Barnes AA, Eilert MM, Tcheang L, Daniels D, et al. The orphan G protein-coupled receptors GPR41 and GPR43 are activated by propionate and other short chain carboxylic acids. JBC. 2003 Mar 28;278(13):11312–9.

41. Synthetic Biology in Australia: an outlook to 2030. [Internet]. Australian Council of Learned Academies Expert Working Group Horizon Scanning Project.; 2018 [cited 2025 Apr 25]. Available from: https://acola.org/hs3-synthetic-biology-australia/

42. Jackson DA, Symons RH, Berg P. Biochemical Method for Inserting New Genetic Information into DNA of Simian Virus 40: Circular SV40 DNA Molecules Containing Lambda Phage Genes and the Galactose Operon of *Escherichia coli*. Proc Natl Acad Sci USA. 1972 Oct;69(10):2904–9.

43. Sekiya T, Brown EL, Belagaje R, Fritz HJ, Gait MJ, Lees RG, et al. Total synthesis of a tyrosine suppressor tRNA gene. XV. Synthesis of the promoter region. Journal of Biological Chemistry. 1979 Aug;254(13):5781–6.

44. Watson JD, Crick FHC. The Structure of Dna. Cold Spring Harb Symp Quant Biol. 1953 Jan 1;18:123–31.

45. Nirenberg M, Caskey T, Marshall R, Brimacombe R, Kellogg D, Doctor B, et al. The RNA code and protein synthesis. Cold Spring Harb Symp Quant Biol. 1966 Jan 1;31:11–24.

46. Sanger F, Nicklen S, Coulson AR. DNA sequencing with chain-terminating inhibitors. Proceedings of the National Academy of Sciences. 1977 Dec;74(12):5463–7.

47. Caruthers MH. The chemical synthesis of DNA/RNA: Our gift to science. Journal of Biological Chemistry. 2013 Jan 11;288(2):1420–7.

48. Kell DB. From code to mode for orphan genes. Trends in Biotechnology. 1998 Dec 1;16(12):491–3.

49. Cello J, Paul AV, Wimmer E. Chemical synthesis of poliovirus cDNA: Generation of infectious virus in the absence of natural template. Science. 2002 Aug 9;297(5583):1016–8.

50. Guet CC, Elowitz MB, Hsing W, Leibler S. Combinatorial synthesis of genetic networks. Science. 2002 May 24;296(5572):1466–70.

51. Goffeau A, Barrell BG, Bussey H, Davis RW, Dujon B, Feldmann H, et al. Life with 6000 genes. Sci. 1996 Oct 25;274(5287):546–67.

52. Blattner FR, Plunkett G, Bloch CA, Perna NT, Burland V, Riley M, et al. The complete genome sequence of *Escherichia coli* K-12. Science. 1997 Sep 5;277(5331):1453–62.

53. Venter JC, Adams MD, Myers EW, Li PW, Mural RJ, Sutton GG, et al. The Sequence of the Human Genome. Science. 2001 Feb 16;291(5507):1304–51.

54. Isaacs FJ, Dwyer DJ, Ding C, Pervouchine DD, Cantor CR, Collins JJ. Engineered riboregulators enable post-transcriptional control of gene expression. Nat Biotechnol. 2004 Jul;22(7):841–7.

55. Martin VJJ, Pitera DJ, Withers ST, Newman JD, Keasling JD. Engineering a mevalonate pathway in Escherichia coli for production of terpenoids. Nat Biotechnol. 2003 Jul;21(7):796–802.

56. Zhang J, Hansen LG, Gudich O, Viehrig K, Lassen LMM, Schrübbers L, et al. A microbial supply chain for production of the anti-cancer drug vinblastine. Nature. 2022 Sep;609(7926):341–7.

57. Fan C, Deng Q, Zhu TF. Bioorthogonal information storage in l-DNA with a high-fidelity mirror-image Pfu DNA polymerase. Nat Biotechnol. 2021 Dec;39(12):1548–55.

58. Gibson DG, Benders GA, Andrews-Pfannkoch C, Denisova EA, Baden-Tillson H, Zaveri J, et al. Complete chemical synthesis, assembly, and cloning of a *Mycoplasma genitalium* genome. Science. 2008 Feb 29;319(5867):1215–20.

59. Watson JL, Juergens D, Bennett NR, Trippe BL, Yim J, Eisenach HE, et al. De novo design of protein structure and function with RFdiffusion. Nature. 2023 Aug;620(7976):1089–100.

60. Lu TK, Collins JJ. Dispersing biofilms with engineered enzymatic bacteriophage. Proceedings of the National Academy of Sciences. 2007 Jul 3;104(27):11197–202.

61. Anderson JC, Clarke EJ, Arkin AP, Voigt CA. Environmentally controlled invasion of cancer cells by engineered bacteria. Journal of Molecular Biology. 2006 Jan 27;355(4):619–27.

62. Lartigue C, Glass JI, Alperovich N, Pieper R, Parmar PP, Hutchison CA, et al. Genome transplantation in bacteria: Changing one species to another. Science. 2007 Aug 3;317(5838):632–8.

63. Chemla Y, Levin I, Fan Y, Johnson AA, Coley CW, Voigt CA. Hyperspectral reporters for long-distance and wide-area detection of gene expression in living bacteria. Nat Biotechnol. 2025 Apr 11;1–11.

64. Gassler T, Sauer M, Gasser B, Egermeier M, Troyer C, Causon T, et al. The industrial yeast Pichia pastoris is converted from a heterotroph into an autotroph capable of growth on CO2. Nat Biotechnol. 2020 Feb;38(2):210–6.

65. Annaluru N, Muller H, Mitchell LA, Ramalingam S, Stracquadanio G, Richardson SM, et al. Total synthesis of a functional designer eukaryotic chromosome. Science. 2014 Apr 4;344(6179):55–8.

66. Pretorius IS, Boeke JD. Yeast 2.0—connecting the dots in the construction of the world's first functional synthetic eukaryotic genome. FEMS Yeast Res. 2018 Mar 16;18(4):foy032.

67. Jinek M, Chylinski K, Fonfara I, Hauer M, Doudna JA, Charpentier E. A Programmable Dual-RNA–Guided DNA Endonuclease in Adaptive Bacterial Immunity. Science. 2012 Aug 17;337(6096):816–21.

68. Basu S, Gerchman Y, Collins CH, Arnold FH, Weiss R. A synthetic multicellular system for programmed pattern formation. Nature. 2005 Apr;434(7037):1130–4.

69. Hutchison CA, Chuang RY, Noskov VN, Assad-Garcia N, Deerinck TJ, Ellisman MH, et al. Design and synthesis of a minimal bacterial genome. Science. 2016 Mar 25;351(6280):aad6253.

70. Statello L, Guo CJ, Chen LL, Huarte M. Gene regulation by long non-coding RNAs and its biological functions. Nat Rev Mol Cell Biol. 2021 Feb;22(2):96–118.

71. Salzberg SL. Open questions: How many genes do we have? BMC Biology. 2018 Aug 20;16(1):94.

72. Lin D, Yin X, Wang X, Zhou P, Guo FB. Re-annotation of protein-coding genes in the genome of *Saccharomyces cerevisiae* based on support vector machines. PLOS ONE. 2013 Jul 10;8(7):e64477.

73. Schlitt T, Brazma A. Current approaches to gene regulatory network modelling. BMC Bioinform. 2007 Sep 27;8(6):S9.

74. Heinemann M, Panke S. Synthetic biology—putting engineering into biology. Bioinform. 2006 Nov 15;22(22):2790–9.

75. Chen Y, Xiao W, Wang Y, Liu H, Li X, Yuan Y. Lycopene overproduction in *Saccharomyces cerevisiae* through combining pathway engineering with host engineering. Microb cell fact. 2016 Jun 21;15(1):113.

76. Bhalla N, Jolly P, Formisano N, Estrela P. Introduction to biosensors. Essays Biochem. 2016 Jun 30;60(1):1–8.

77. Nayak S, Blumenfeld NR, Laksanasopin T, Sia SK. Point-of-care diagnostics: Recent developments in a connected age. Anal Chem. 2017 Jan 3;89(1):102–23.

78. Piorino F, Patterson AT, Styczynski MP. Low-cost, point-of-care biomarker quantification. Curr Opin Biotechnol. 2022 Aug;76:102738.

79. Das S, Frank KM. Strategies for scaling up SARS-CoV-2 molecular testing capacity. Clin Lab Med. 2022 Jun 1;42(2):261–82.

80. Gibson TD. Biosensors : the stabilité problem. Analusis. 1999 Sep;27(7):630–8.

81. Motulsky H, Christopoulos A. Fitting models to biological data using linear and nonlinear regression: A practical guide to curve fitting. Oxford University PressNew York, NY; 2004.

82. Moulahoum H, Ghorbanizamani F. The LOD paradox: When lower isn't always better in biosensor research and development. Biosens Bioelectron. 2024 Nov 15;264:116670.

83. Shaw WM, Yamauchi H, Mead J, Gowers GOF, Bell DJ, Öling D, et al. Engineering a model cell for rational tuning of GPCR signaling. Cell. 2019 Apr 18;177(3):782-796.e27.

84. de Araujo WR, Lukas H, Torres MDT, Gao W, de la Fuente-Nunez C. Low-cost biosensor technologies for rapid detection of COVID-19 and future pandemics. ACS Nano. 2024 Jan 23;18(3):1757–77.

85. Lalkhen AG, McCluskey A. Clinical tests: sensitivity and specificity. BJA Education. 2008 Dec 1;8(6):221–3.

86. Lee JM, Lowry KP, Cott Chubiz JE, Swan JS, Motazedi T, Halpern EF, et al. Breast cancer risk, worry, and anxiety: Effect on patient perceptions of false-positive screening results. Breast. 2020 Feb 13;50:104–12.

87. Nielsen J. Yeast systems biology: Model organism and cell factory. Biotechnol J. 2019;14(9):1800421.

88. Botstein D. Why yeast? Hosp Pract. 1991 Oct 15;26(10):157–64.

89. Malcı K, Watts E, Roberts TM, Auxillos JY, Nowrouzi B, Boll HO, et al. Standardization of synthetic biology tools and assembly methods for *Saccharomyces cerevisiae* and emerging yeast species. ACS Synth Biol. 2022 Aug 19;11(8):2527–47.

90. Kapolka NJ, Taghon GJ, Rowe JB, Morgan WM, Enten JF, Lambert NA, et al. DCyFIR: a high-throughput CRISPR platform for multiplexed G protein-coupled receptor profiling and ligand discovery. Proc Natl Acad Sci U S A. 2020 Jun 9;117(23):13117–26.

91. Miettinen K, Leelahakorn N, Almeida A, Zhao Y, Hansen LR, Nikolajsen IE, et al. A GPCR-based yeast biosensor for biomedical, biotechnological, and point-of-use cannabinoid determination. Nat Commun. 2022 Jun 27;13(1):3664.

92. Mendes F, Miranda E, Amaral L, Carvalho C, Castro BB, Sousa MJ, et al. Novel yeast-based biosensor for environmental monitoring of tebuconazole. Appl Microbiol Biotechnol. 2024 Jan 3;108(1):10.

93. Adeniran A, Sherer M, Tyo KEJ. Yeast-based biosensors: design and applications. FEMS Yeast Res. 2015 Feb 1;15(1):1–15.

94. Jarque S, Bittner M, Hilscherová K. Freeze-drying as suitable method to achieve ready-to-use yeast biosensors for androgenic and estrogenic compounds. Chemosphere. 2016 Apr 1;148:204–10.

95. Wahid E, Ocheja OB, Marsili E, Guaragnella C, Guaragnella N. Biological and technical challenges for implementation of yeast-based biosensors. Microb Biotechnol. 2023;16(1):54–66.

96. Yasi EA, Eisen SL, Wang H, Sugianto W, Minniefield AR, Hoover KA, et al. Rapid deorphanization of human olfactory receptors in yeast. Biochemistry. 2019 Apr 23;58(16):2160–6.

97. Reiländer H, Weiβ HM. Production of G-protein-coupled receptors in yeast. COBIOT. 1998 Oct 1;9(5):510–7.

98. Liu Y, Huang Y, Lu R, Xin F, Liu G. Synthetic biology applications of the yeast mating signal pathway. Trends Biotechnol. 2022 May 1;40(5):620–31.

99. McClure AW, Jacobs KC, Zyla TR, Lew DJ. Mating in wild yeast: delayed interest in sex after spore germination. Mol Biol Cell. 2018 Dec 15;29(26):3119–27.

100. Sprague GF. [5] Assay of yeast mating reaction. In: Methods in Enzymology. Academic Press; 1991. p. 77–93. (Guide to Yeast Genetics and Molecular Biology; vol. 194).

101. Wang Y, Lo WC, Chou CS. A modeling study of budding yeast colony formation and its relationship to budding pattern and aging. PLoS Comput Biol. 2017 Nov 9;13(11):e1005843.

102. Haber JE. Mating-type gene switching in *Saccharomyces cerevisiae*. Annu Rev Genet. 1998 Dec;32(1):561–99.

103. Herskowitz I, Jensen RE. [8] Putting the *HO* gene to work: Practical uses for mating-type switching. In: Methods in Enzymology. Academic Press; 1991. p. 132–46. (Guide to Yeast Genetics and Molecular Biology; vol. 194).

104. Weng G, Bhalla US, Iyengar R. Complexity in biological signaling systems. Science. 1999 Apr 2;284(5411):92–6.

105. Graves JD, Krebs EG. Protein phosphorylation and signal transduction. Pharmacol Ther. 1999 May 1;82(2):111–21.

106. Howell SL, Jones PM, Persaud SJ. Regulation of insulin secretion: the role of second messengers. Diabetologia. 1994 Sep 1;37(2):S30–5.

107. Alvaro CG, Thorner J. Heterotrimeric G protein-coupled receptor signaling in yeast mating pheromone response. JBC. 2016 Apr 8;291(15):7788–95.

108. Garrison TR, Zhang Y, Pausch M, Apanovitch D, Aebersold R, Dohlman HG. Feedback phosphorylation of an RGS protein by MAP kinase in yeast. JBC. 1999 Dec 17;274(51):36387–91.

109. Chang F, Herskowitz I. Identification of a gene necessary for cell cycle arrest by a negative growth factor of yeast: FAR1 is an inhibitor of a G1 cyclin, CLN2. Cell. 1990 Nov 30;63(5):999–1011.

110. Ammerer G, Sprague GF, Bender A. Control of yeast alpha-specific genes: evidence for two blocks to expression in MATa/MAT alpha diploids. Proc Natl Acad Sci U S A. 1985 Sep;82(17):5855–9.

111. Moore TI, Chou CS, Nie Q, Jeon NL, Yi TM. Robust spatial sensing of mating pheromone gradients by yeast cells. PLOS ONE. 2008 Dec 4;3(12):e3865.

112. Brown AJ, Dyos SL, Whiteway MS, White JHM, Watson MAEA, Marzioch M, et al. Functional coupling of mammalian receptors to the yeast mating pathway using novel yeast/mammalian G protein α-subunit chimeras. Yeast. 2000;16(1):11–22.

113. Zhang M, Chen T, Lu X, Lan X, Chen Z, Lu S. G protein-coupled receptors (GPCRs): advances in structures, mechanisms and drug discovery. Sig Transduct Target Ther. 2024 Apr 10;9(1):1–43.

114. Billerbeck S, Brisbois J, Agmon N, Jimenez M, Temple J, Shen M, et al. A scalable peptide-GPCR language for engineering multicellular communication. Nat Commun. 2018 Nov 29;9(1):1–12.

115. Brown AJ, Tsoulou C, Ward E, Gower E, Bhudia N, Chowdhury F, et al. Pharmacological properties of acid *N* -thiazolylamide FFA2 agonists. Pharmacology Res & Perspec. 2015 Jun;3(3):e00141.

116. Latorraca NR, Venkatakrishnan AJ, Dror RO. GPCR Dynamics: Structures in Motion. Chem Rev. 2017 Jan 11;117(1):139–55.

117. Yang D, Zhou Q, Labroska V, Qin S, Darbalaei S, Wu Y, et al. G protein-coupled receptors: structure- and function-based drug discovery. Sig Transduct Target Ther. 2021 Jan 8;6(1):1–27.

118. Velazhahan V, Ma N, Pándy-Szekeres G, Kooistra AJ, Lee Y, Gloriam DE, et al. Structure of the class D GPCR Ste2 dimer coupled to two G proteins. Nature. 2021 Jan;589(7840):148–53.

119. Adeniran A, Sherer M, Tyo KEJ. Yeast-based biosensors: design and applications. FEMS Yeast Res. 2015 Feb 1;15(1):1–15.

120. Shaw WM, Zhang Y, Lu X, Khalil AS, Ladds G, Luo X, et al. Screening microbially produced Δ9-tetrahydrocannabinol using a yeast biosensor workflow. Nat Commun. 2022 Sep 20;13(1):5509.

121. Leskinen P, Virta M, Karp M. One-step measurement of firefly luciferase activity in yeast. Yeast. 2003 Oct 15;20(13):1109–13.

122. Rajasärkkä J, Hakkila K, Virta M. Developing a compound-specific receptor for bisphenol a by directed evolution of human estrogen receptor α. Biotechnol Bioeng. 2011;108(11):2526–34.

123. Roy L, Buragohain P, Borse V. Strategies for sensitivity enhancement of point-of-care devices. Biosens Bioelectron: X. 2022 May 1;10:100098.

124. DeLoache WC, Russ ZN, Dueber JE. Towards repurposing the yeast peroxisome for compartmentalizing heterologous metabolic pathways. Nat Commun. 2016 Mar 30;7(1):11152.

125. Rantasalo A, Kuivanen J, Penttilä M, Jäntti J, Mojzita D. Synthetic toolkit for complex genetic circuit engineering in *Saccharomyces cerevisiae*. ACS Synth Biol. 2018 Jun 15;7(6):1573–87.

126. Sanford A, Kiriakov S, Khalil AS. A toolkit for precise, multigene control in *Saccharomyces cerevisiae*. ACS Synth Biol. 2022 Dec 16;11(12):3912–20.

127. Mans R, van Rossum HM, Wijsman M, Backx A, Kuijpers NGA, van den Broek M, et al. CRISPR/Cas9: a molecular Swiss army knife for simultaneous introduction of multiple genetic modifications in *Saccharomyces cerevisiae*. FEMS Yeast Res. 2015 Mar;15(2):fov004.

128. Lee ME, DeLoache WC, Cervantes B, Dueber JE. A highly characterized yeast toolkit for modular, multipart assembly. ACS Synth Biol. 2015 Sep 18;4(9):975–86.

129. Otto M, Skrekas C, Gossing M, Gustafsson J, Siewers V, David F. Expansion of the yeast modular cloning toolkit for CRISPR-based applications, genomic integrations and combinatorial libraries. ACS Synth Biol. 2021 Dec 17;10(12):3461–74.

130. Jessop-Fabre MM, Jakočiūnas T, Stovicek V, Dai Z, Jensen MK, Keasling JD, et al. EasyClone-MarkerFree: A vector toolkit for marker-less integration of genes into *Saccharomyces cerevisiae* via CRISPR-Cas9. Biotechnol J. 2016 Aug;11(8):1110–7.

131. Li Y, Sun J, Fu Z, He Y, Chen X, Wang S, et al. Engineering the L-tryptophan metabolism for efficient de novo biosynthesis of tryptophol in Saccharomyces cerevisiae. Biotechnol biofuels bioprod. 2024 Oct 16;17(1):130.

132. Zhang T, Bu P, Zeng J, Vancura A. Increased heme synthesis in yeast induces a metabolic switch from fermentation to respiration even under conditions of glucose repression. J Biol Chem. 2017 Oct 13;292(41):16942–54.

133. Lee ME, Aswani A, Han AS, Tomlin CJ, Dueber JE. Expression-level optimization of a multi-enzyme pathway in the absence of a high-throughput assay. Nucleic Acids Res. 2013 Dec 1;41(22):10668–78.

134. Li T, Chen X, Cai Y, Dai J. Artificial Protein Scaffold System (AProSS): An efficient method to optimize exogenous metabolic pathways in *Saccharomyces cerevisiae*. Metabolic Engineering. 2018 Sep 1;49:13–20.

135. Zhou Y, Li G, Dong J, Xing X hui, Dai J, Zhang C. MiYA, an efficient machine-learning workflow in conjunction with the YeastFab assembly strategy for combinatorial optimization of heterologous metabolic pathways in *Saccharomyces cerevisiae*. Metab Eng. 2018 May 1;47:294–302.

136. Fan C, He N, Yuan J. Cascaded amplifying circuit enables sensitive detection of fungal pathogens. Biosens Bioelectron. 2024 Apr 15;250:116058.

137. Brown NA, Schrevens S, van Dijck P, Goldman GH. Fungal G-protein-coupled receptors: mediators of pathogenesis and targets for disease control. Nat Microbiol. 2018 Apr;3(4):402–14.

138. Gao J, Xu X, Huang K, Liang Z. Fungal G-protein-coupled receptors: A promising mediator of the impact of extracellular signals on biosynthesis of ochratoxin A. Front Microbiol. 2021 Feb 12;12.

139. Massic L, Gorzalski A, Siao DD, Dykema P, Hua C, Schneider E, et al. Detection of five instances of dual-clade infections of *Candida auris* with opposite mating types in southern Nevada, USA. Lancet Infect Dis. 2023 Sep 1;23(9):e328–9.

140. Velazhahan V, McCann BL, Bignell E, Tate CG. Developing novel antifungals: lessons from G protein-coupled receptors. TIPS. 2023 Mar 1;44(3):162–74.

141. Muñoz JF, Gade L, Chow NA, Loparev VN, Juieng P, Berkow EL, et al. Genomic insights into multidrug-resistance, mating and virulence in Candida auris and related emerging species. Nat Commun. 2018 Dec 17;9(1):5346.

142. Velazhahan V, Ma N, Vaidehi N, Tate CG. Activation mechanism of the class D fungal GPCR dimer Ste2. Nature. 2022 Mar;603(7902):743–8.

143. Meng EC, Goddard TD, Pettersen EF, Couch GS, Pearson ZJ, Morris JH, et al. UCSF ChimeraX: Tools for structure building and analysis. Protein Science. 2023 Nov;32(11):e4792.

144. Di Roberto RB, Chang B, Trusina A, Peisajovich SG. Evolution of a G protein-coupled receptor response by mutations in regulatory network interactions. Nat Commun. 2016 Nov;7(1):12344.

145. Hu KKY, Suri A, Dumsday G, Haritos VS. Cross-feeding promotes heterogeneity within yeast cell populations. Nat Commun. 2024 Jan 10;15(1):418.

146. McCullum EO, Williams BAR, Zhang J, Chaput JC. Random mutagenesis by error-prone PCR. In: Braman J, editor. In Vitro Mutagenesis Protocols: Third Edition. Totowa, NJ: Humana Press; 2010. p. 103–9.

147. Geva A, Lassere TB, Lichtarge O, Pollitt SK, Baranski TJ. Genetic mapping of the human C5a receptor: Identification of transmembrane amino acids critical for receptor function. JBC. 2000 Nov 10;275(45):35393–401.

148. Keighley C, Garnham K, Harch SAJ, Robertson M, Chaw K, Teng JC, et al. *Candida auris*: Diagnostic challenges and emerging opportunities for the clinical microbiology laboratory. Curr Fungal Infect Rep. 2021;15(3):116–26.

149. Mishra SK, Yasir M, Willcox M. *Candida auris*: an emerging antimicrobial-resistant organism with the highest level of concern. The Lancet Microbe. 2023 Apr;S2666524723001143.

150. WHO. WHO fungal priority pathogens list to guide research, development and public health action [Internet]. 2022 [cited 2023 Feb 21]. Available from: https://www.who.int/publications-detail-redirect/9789240060241

151. CDC. *C. auris* identification. 2024 [cited 2025 Mar 2]. *C. auris* identification. Available from: https://www.cdc.gov/candida-auris/hcp/laboratories/identification-of-c-auris.html

152. Brown NA, Schrevens S, van Dijck P, Goldman GH. Fungal G-protein-coupled receptors: mediators of pathogenesis and targets for disease control. Nat Microbiol. 2018 Apr;3(4):402–14.

153. Yi S, Sahni N, Pujol C, Daniels KJ, Srikantha T, Ma N, et al. A *Candida albicans*-specific region of the α-pheromone receptor plays a selective role in the white cell pheromone response. Mol Microbiol. 2009;71(4):925–47.

154. Varadi M, Bertoni D, Magana P, Paramval U, Pidruchna I, Radhakrishnan M, et al. AlphaFold Protein Structure Database in 2024: providing structure coverage for over 214 million protein sequences. Nucleic Acids Res. 2024 Jan 5;52(D1):D368–75.

155. Bean BDM, Mulvihill CJ, Garge RK, Boutz DR, Rousseau O, Floyd BM, et al. Functional expression of opioid receptors and other human GPCRs in yeast engineered to produce human sterols. Nat Commun. 2022 May 24;13(1):2882.

156. Stefan CJ, Overton MC, Blumer KJ. Mechanisms Governing the Activation and Trafficking of Yeast G Protein-coupled Receptors. MBoC. 1998 Apr;9(4):885–99.

157. Naider F, Becker JM. The α-factor mating pheromone of *Saccharomyces cerevisiae*: a model for studying the interaction of peptide hormones and G protein-coupled receptors. Peptides. 2004 Sep 1;25(9):1441–63.

158. Altmann K, Dürr M, Westermann B. *Saccharomyces cerevisiae* as a model organism to study mitochondrial biology. In: Leister D, Herrmann JM, editors. Mitochondria: Practical protocols. Totowa, NJ: Humana Press; 2007. p. 81–90.

159. Weiner JL, Guttierez-Steil C, Blumer KJ. Disruption of receptor-G protein coupling in yeast promotes the function of an SST2-dependent adaptation pathway. JBC. 1993 Apr;268(11):8070–7.

160. Abel MG, Lee BK, Naider F, Becker JM. Mutations affecting ligand specificity of the G-protein-coupled receptor for the *Saccharomyces cerevisiae* tridecapeptide pheromone. Biochim Biophys Acta, Mol Cell Res. 1998 Nov 19;1448(1):12–26.

161. Son CD, Sargsyan H, Naider F, Becker JM. Identification of ligand binding regions of the Saccharomyces cerevisiae α-factor pheromone receptor by photoaffinity cross-linking. Biochemistry. 2004 Oct 1;43(41):13193–203.

162. Lin JC, Duell K, Saracino M, Konopka JB. Identification of residues that contribute to receptor activation through the analysis of compensatory mutations in the G protein-coupled α-factor receptor. Biochemistry. 2005 Feb 1;44(4):1278–87.

163. Huang LY, Umanah G, Hauser M, Son C, Arshava B, Naider F, et al. Unnatural amino acid replacement in a yeast G protein-coupled receptor in its native environment. Biochemistry. 2008 May 1;47(20):5638–48.

164. Mathew E, Bajaj A, Connelly SM, Sargsyan H, Ding FX, Hajduczok AG, et al. Differential interactions of fluorescent agonists and antagonists with the yeast G protein coupled receptor Ste2p. J Mol Biol. 2011 Jun 17;409(4):513–28.

165. Zuber J, Danial SA, Connelly SM, Naider F, Dumont ME. Identification of destabilizing and stabilizing mutations of Ste2p, a G protein-coupled receptor in *Saccharomyces cerevisiae*. Biochemistry. 2015 Mar 10;54(9):1787–806.

166. Di Roberto RB, Chang B, Peisajovich SG. The directed evolution of ligand specificity in a GPCR and the unequal contributions of efficacy and affinity. Scientific Reports. 2017 Nov 22;7(1):16012.

167. Namour F, Galien R, Van Kaem T, Van der Aa A, Vanhoutte F, Beetens J, et al. Safety, pharmacokinetics and pharmacodynamics of GLPG0974, a potent and selective FFA2 antagonist, in healthy male subjects. Br J Clin Pharmacol. 2016;82(1):139–48.

168. Sergeev E, Hansen AH, Bolognini D, Kawakami K, Kishi T, Aoki J, et al. A single extracellular amino acid in Free Fatty Acid Receptor 2 defines antagonist species selectivity and G protein selection bias. Sci Rep. 2017 Oct 23;7:13741.

169. Chun E, Lavoie S, Fonseca-Pereira D, Bae S, Michaud M, Hoveyda HR, et al. Metabolite-sensing receptor Ffar2 regulates colonic group 3 innate lymphoid cells and gut immunity. Immunity. 2019 Nov;51(5):871-884.e6.

170. Secor JD, Fligor SC, Tsikis ST, Yu LJ, Puder M. Free fatty acid receptors as mediators and therapeutic targets in liver disease. Front Physiol. 2021 Apr 7;12.

171. Lind S, Holdfeldt A, Mårtensson J, Granberg KL, Forsman H, Dahlgren C. Multiple ligand recognition sites in free fatty acid receptor 2 (FFA2R) direct distinct neutrophil activation patterns. Biochemical Pharmacology. 2021 Nov 1;193:114762.

172. Lind S, Granberg KL, Forsman H, Dahlgren C. The allosterically modulated FFAR2 is transactivated by signals generated by other neutrophil GPCRs. PLOS ONE. 2023 Apr 6;18(4):e0268363.

173. Teyani R, Moniri NH. Gut feelings in the islets: The role of the gut microbiome and the FFA2 and FFA3 receptors for short chain fatty acids on β-cell function and metabolic regulation. Br J Clin Pharmacol. 2023;180(24):3113–29.

174. Schmidt J, Smith NJ, Christiansen E, Tikhonova IG, Grundmann M, Hudson BD, et al. Selective orthosteric free fatty acid receptor 2 (FFA2) agonists: identification of the structural and chemical requirements for selective activation of FFA2 versus FFA3. JBC. 2011 Mar;286(12):10628–40.

175. Lind S, Holdfeldt A, Mårtensson J, Sundqvist M, Kenakin TP, Björkman L, et al. Interdependent allosteric free fatty acid receptor 2 modulators synergistically induce functional selective activation and desensitization in neutrophils. Biochim Biophys Acta, Mol Cell Res. 2020 Jun 1;1867(6):118689.

176. Lind S, Hoffmann DO, Forsman H, Dahlgren C. Allosteric receptor modulation uncovers an FFA2R antagonist as a positive orthosteric modulator/agonist in disguise. Cell Signal. 2022 Feb 1;90:110208.

177. Dahlgren C, Lind S, Mårtensson J, Björkman L, Wu Y, Sundqvist M, et al. G protein coupled pattern recognition receptors expressed in neutrophils: Recognition, activation/modulation, signaling and receptor regulated functions. Immunol Rev. 2023;314(1):69–92.

178. Hudson BD, Due-Hansen ME, Christiansen E, Hansen AM, Mackenzie AE, Murdoch H, et al. Defining the molecular basis for the first potent and selective orthosteric agonists of the FFA2 free fatty acid receptor. J Biol Chem. 2013 Jun 14;288(24):17296–312.

179. Wang Y, Jiao X, Kayser F, Liu J, Wang Z, Wanska M, et al. The first synthetic agonists of FFA2: Discovery and SAR of phenylacetamides as allosteric modulators. BMCL. 2010 Jan 15;20(2):493–8.

180. Park BO, Kim SH, Kong GY, Kim DH, Kwon MS, Lee SU, et al. Selective novel inverse agonists for human GPR43 augment GLP-1 secretion. Eur J Pharmacol. 2016 Jan 15;771:1–9.

181. Milligan G. G protein-coupled receptors not currently in the spotlight: free fatty acid receptor 2 and GPR35. Br J Pharmacol. 2018 Jul;175(13):2543–53.

182. Bolognini D, Moss CE, Nilsson K, Petersson AU, Donnelly I, Sergeev E, et al. A novel allosteric activator of free fatty acid 2 receptor displays unique Gi-functional bias. JBC. 2016 Sep 2;291(36):18915–31.

183. Sergeev E, Hansen AH, Pandey SK, MacKenzie AE, Hudson BD, Ulven T, et al. Non-equivalence of key positively charged residues of the Free Fatty Acid 2 Receptor in the recognition and function of agonist versus antagonist ligands. JBC. 2016 Jan;291(1):303–17.

184. Miyasato S, Iwata K, Mura R, Nakamura S, Yanagida K, Shindou H, et al. Constitutively active GPR43 is crucial for proper leukocyte differentiation. FASEB J. 2023;37(1):e22676.

185. Scott BM, Wybenga-Groot LE, McGlade CJ, Heon E, Peisajovich SG, Chang BSW. Screening of Chemical Libraries Using a Yeast Model of Retinal Disease. SLAS Discovery. 2019 Dec 1;24(10):969–77.

186. Shaw WM, Zhang Y, Lu X, Khalil AS, Ladds G, Luo X, et al. Screening microbially produced Δ9-tetrahydrocannabinol using a yeast biosensor workflow. Nat Commun. 2022 Sep 20;13(1):5509.

187. Johnston TG, Yuan SF, Wagner JM, Yi X, Saha A, Smith P, et al. Compartmentalized microbes and co-cultures in hydrogels for on-demand bioproduction and preservation. Nat Commun. 2020 Feb 4;11(1):563.

188. Brooks SM, Reed KB, Yuan SF, Altin-Yavuzarslan G, Shafranek R, Nelson A, et al. Enhancing long-term storage and stability of engineered living materials through desiccant storage and trehalose treatment. Biotechnol Bioeng. 2023;120(2):572–82.

189. Teng F, Cui T, Zhou L, Gao Q, Zhou Q, Li W. Programmable synthetic receptors: the next-generation of cell and gene therapies. Signal Transduct Target Ther. 2024 Jan 3;9:7.

190. Kim S, Mollaei P, Antony A, Magar R, Barati Farimani A. GPCR-BERT: Interpreting sequential design of G protein-coupled receptors using protein language models. J Chem Inf Model. 2024 Feb 26;64(4):1134–44.

191. Brahma R, Moon S, Shin JM, Cho KH. AiGPro: a multi-tasks model for profiling of GPCRs for agonist and antagonist. J Cheminform. 2025 Jan 29;17(1):12.

192. Buyanov I, Popov P. Characterizing conformational states in GPCR structures using machine learning. Sci Rep. 2024 Jan 11;14(1):1098.

193. Nguyen ATN, Nguyen DTN, Koh HY, Toskov J, MacLean W, Xu A, et al. The application of artificial intelligence to accelerate G protein-coupled receptor drug discovery. Br J Pharmacol. 2024;181(14):2371–84.

194. Varadi M, Anyango S, Deshpande M, Nair S, Natassia C, Yordanova G, et al. AlphaFold Protein Structure Database: massively expanding the structural coverage of protein-sequence space with high-accuracy models. Nucleic Acids Res. 2022 Jan 7;50(D1):D439–44.

195. Dhakal A, McKay C, Tanner JJ, Cheng J. Artificial intelligence in the prediction of protein–ligand interactions: recent advances and future directions. Brief Bioinform. 2022 Jan 17;23(1):bbab476.

196. Li G, Buric F, Zrimec J, Viknander S, Nielsen J, Zelezniak A, et al. Learning deep representations of enzyme thermal adaptation. Protein Sci. 2022;31(12):e4480.

197. Lee S, Kim S, Lee GR, Kwon S, Woo H, Seok C, et al. Evaluating GPCR modeling and docking strategies in the era of deep learning-based protein structure prediction. Comput Struct Biotechnol J. 2022 Dec 1;21:158–67.

198. Zhang H, Fan H, Wang J, Hou T, Saravanan KM, Xia W, et al. Revolutionizing GPCR–ligand predictions: DeepGPCR with experimental validation for high-precision drug discovery. Brief Bioinform. 2024 Jun 12;25(4):bbae281.

199. Bill RM, Hedfalk K. Aquaporins – Expression, purification and characterization. Biochim Biophys Acta, Biomembr. 2021 Sep 1;1863(9):183650.

200. Lee S, Kim S, Lee GR, Kwon S, Woo H, Seok C, et al. Evaluating GPCR modeling and docking strategies in the era of deep learning-based protein structure prediction. Comput Struct Biotechnol J. 2022 Dec 1;21:158–67.

201. Stampelou M, Ladds G, Kolocouris A. Computational workflow for refining AlphaFold models in drug design using kinetic and thermodynamic binding calculations: A case study for the unresolved inactive human adenosine A3 receptor. J Phys Chem B. 2024 Feb 1;128(4):914–36.

202. Rienzo LD, Miotto M, Milanetti E, Ruocco G. Computational structural-based GPCR optimization for user-defined ligand: Implications for the development of biosensors. CSBJ. 2023 Jan 1;21:3002–9.

203. Kalogriopoulos NA, Tei R, Yan Y, Klein PM, Ravalin M, Cai B, et al. Synthetic GPCRs for programmable sensing and control of cell behaviour. Nature. 2025 Jan;637(8044):230–9.

204. Monod Bio - AI-Powered Protein Design [Internet]. 2024 [cited 2025 Apr 10]. Available from: https://monod.bio/

205. Hassan YM, Mohamed AS, Hassan YM, El-Sayed WM. Recent developments and future directions in point-of-care next-generation CRISPR-based rapid diagnosis. Clin Exp Med. 2025;25(1):33.

206. Jung JK, Alam KK, Verosloff MS, Capdevila DA, Desmau M, Clauer PR, et al. Cell-free biosensors for rapid detection of water contaminants. Nat Biotechnol. 2020 Dec;38(12):1451–9.

207. Nguyen PQ, Soenksen LR, Donghia NM, Angenent-Mari NM, de Puig H, Huang A, et al. Wearable materials with embedded synthetic biology sensors for biomolecule detection. Nat Biotechnol. 2021 Nov;39(11):1366–74.

208. Oeschger TM, McCloskey DS, Buchmann RM, Choubal AM, Boza JM, Mehta S, et al. Early warning diagnostics for emerging infectious diseases in developing into late-stage pandemics. Acc Chem Res. 2021 Oct 5;54(19):3656–66.

209. Jones KE, Patel NG, Levy MA, Storeygard A, Balk D, Gittleman JL, et al. Global trends in emerging infectious diseases. Nature. 2008 Feb;451(7181):990–3.

210. Semenza JC, Lindgren E, Balkanyi L, Espinosa L, Almqvist MS, Penttinen P, et al. Determinants and drivers of infectious disease threat events in Europe. Emerg Infect Dis. 2016 Apr;22(4):581–9.

211. Reardon S. Spread of antibiotic-resistance gene does not spell bacterial apocalypse — yet. Nature. 2015 Dec 21;

212. Fisher MC, Alastruey-Izquierdo A, Berman J, Bicanic T, Bignell EM, Bowyer P, et al. Tackling the emerging threat of antifungal resistance to human health. Nat Rev Microbiol. 2022 Sep;20(9):557–71.

213. Fernebro J. Fighting bacterial infections—Future treatment options. Drug Resist Updat. 2011 Apr;14(2):125–39.

214. Mota Fernandes C, Dasilva D, Haranahalli K, McCarthy JB, Mallamo J, Ojima I, et al. The future of antifungal drug therapy: novel compounds and targets. Antimicrob Agents Chemother. 2021 Jan 20;65(2):e01719-20.

215. Luo Z, Ang MJY, Chan SY, Yi Z, Goh YY, Yan S, et al. Combating the coronavirus pandemic: Early detection, medical treatment, and a concerted effort by the global community. SPJ. 2020 Jun 16;2020.

216. Steele L, Orefuwa E, Bino S, Singer SR, Lutwama J, Dickmann P. Earlier outbreak detection—A generic model and novel methodology to guide earlier detection supported by data from low- and mid-income countries. Front Public Health. 2020 Sep 11;8.

217. Allel K, Day L, Hamilton A, Lin L, Furuya-Kanamori L, Moore CE, et al. Global antimicrobial-resistance drivers: an ecological country-level study at the human–animal interface. Lancet Planet Health. 2023 Apr 1;7(4):e291–303.

218. Richter D, Riedel-Heller S, Zürcher SJ. Mental health problems in the general population during and after the first lockdown phase due to the SARS-Cov-2 pandemic: rapid review of multi-wave studies. EPS. 2021 Jan;30:e27.

219. Van Boeckel TP, Pires J, Silvester R, Zhao C, Song J, Criscuolo NG, et al. Global trends in antimicrobial resistance in animals in low- and middle-income countries. Science. 2019 Sep 20;365(6459):eaaw1944.

220. Rodrigo-Navarro A, Sankaran S, Dalby MJ, del Campo A, Salmeron-Sanchez M. Engineered living biomaterials. Nat Rev Mater. 2021 Dec;6(12):1175–90.

221. Caro-Astorga J, Ellis T. Self-healing through adhesion. Nat Chem Biol. 2022 Mar;18(3):239–40.

222. Gilbert C, Tang TC, Ott W, Dorr BA, Shaw WM, Sun GL, et al. Living materials with programmable functionalities grown from engineered microbial co-cultures. Nat Mater. 2021 May;20(5):691–700.

223. Walker KT, Li IS, Keane J, Goosens VJ, Song W, Lee KY, et al. Self-pigmenting textiles grown from cellulose-producing bacteria with engineered tyrosinase expression. Nat Biotechnol. 2025 Mar 1;43(3):345–54.